METHYLARSENIC SORPTION AND SPECIATION MECHANISMS IN NATURAL SYSTEMS

by

Masayuki Shimizu

A dissertation submitted to the Faculty of the University of Delaware in partial fulfillment of the requirements for the degree of Doctor of Philosophy in Plant and Soil Sciences

Summer 2010

METHYLARSENIC SORPTION AND SPECIATION MECHANISMS IN NATURAL SYSTEMS

by

Masayuki Shimizu

Approved: _____

Blake C. Meyers, Ph.D.
Interim Chair of the Department of Plant and Soil Sciences

Approved: _____

Robin W. Morgan, Ph.D.
Dean of the College of Agriculture and Natural Resources

Approved: _____

Debra Hess Norris, M.S.
Vice Provost for Graduate and Professional Education

I certify that I have read this dissertation and that in my opinion it meets the academic and professional standard required by the University as a dissertation for the degree of Doctor of Philosophy.

Signed: _____

Donald L. Sparks, Ph.D.
Professor in charge of dissertation

I certify that I have read this dissertation and that in my opinion it meets the academic and professional standard required by the University as a dissertation for the degree of Doctor of Philosophy.

Signed: _____

Yan Jin, Ph.D.
Member of dissertation committee

I certify that I have read this dissertation and that in my opinion it meets the academic and professional standard required by the University as a dissertation for the degree of Doctor of Philosophy.

Signed: _____

Thomas J. Sims, Ph.D.
Member of dissertation committee

I certify that I have read this dissertation and that in my opinion it meets the academic and professional standard required by the University as a dissertation for the degree of Doctor of Philosophy.

Signed: _____

Yuji Arai, Ph.D.
External Member of dissertation committee

ACKNOWLEDGMENTS

I would like to acknowledge my advisor Dr. Donald L. Sparks for all his support on me. Dr. Sparks is a great mentor, and I have learned a lot of things from Dr. Sparks. Without Dr. Sparks, I could not purse this research topic.

I also like to acknowledge my other Ph.D. committee members. I like to acknowledge Dr. Yan Jin for her advice on my research and sharing her laboratory equipments with me. I like to acknowledge Dr. Tom Sims for serving as my Ph. D. committee member, supporting graduate student vegetable garden, and providing me funding through ISEQ fellowship. I also like to acknowledge Dr. Yuji Arai for serving as my Ph. D. committee member even before we have met and providing advice on my research during several conferences.

I like to acknowledge Jerry Hendricks and my group mates for their supports and sharing fun time with me.

Finally, I like to acknowledge Adrienne Kleintop and my family for their support all the time.

TABLE OF CONTENTS

LIST OF TABLES

LIST OF FIGURES

ABSTRACT

Arsenic (As) originates in many rocks and minerals throughout the world. Natural phenomena, such as weathering and biological activities, along with industrial activities and agricultural activities are responsible for As introduction to the environment. The most predominate oxidation states for inorganic As species are arsenate As^{V} (H_3AsO_4) and arsenite As^{III} (H_3AsO_3). In addition to inorganic forms, organic forms of As also exist in nature, typically occurring in terrestrial environments as monomethylarsenate, MMA ($CH_3H_2AsO_3$) and dimethylarsenate, DMA ($(CH_3)_2HAsO_2$). MMA and DMA have historically been used as herbicides and pesticides. Because of their large application to agricultural fields and the toxicity of MMA and DMA, the behavior of methylarsenics in the soil environment requires investigation. Accordingly, the objectives of this study were 1) characterize MMA and DMA sorption to aluminum oxide, 2) characterize MMA and DMA sorption, speciation, and distribution to a soil, and 3) characterize MMA and DMA sorption and desorption to various types of soils.

MMA and DMA sorption on amorphous aluminum oxide (AAO) were investigated using both macroscopic batch sorption kinetics and molecular scale Extended X-ray Absorption Fine Structure (EXAFS) and Fourier Transform infrared (FTIR) spectroscopic techniques. Sorption isotherm studies revealed sorption maxima of 0.183, 0.145, and 0.056 mmol As / mmol Al for arsenate (As^{V}), MMA, and DMA, respectively. In the sorption kinetics studies, 100 % of added As^{V} was sorbed within 5 min, while 78 % and 15 % of added MMA and DMA were sorbed, respectively.

Desorption experiments, using phosphate as a desorbing agent, resulted in 30 % release of absorbed As^V, while 48 % and 62 % of absorbed MMA and DMA, respectively, were released. FTIR and EXAFS studies revealed that MMA and DMA formed mainly bidentate binuclear complexes with AAO. Based on these results, it is proposed that increasing methyl group substitution results in decreased As sorption and increased As desorption on AAO.

The distribution, speciation, and sorption of MMA and DMA to soils were also investigated. MMA and DMA were reacted with the Reybold soil (Typic Hapludults) for up to 1 year under aerobic and anaerobic conditions. Micro synchrotron X-ray fluorescence (μ-SXRF) mapping studies showed that MMA and DMA were heterogeneously distributed in the soil, and were mainly associated with the iron oxides, goethite and ferrihydrite, in the soil. Micro X-ray absorption near edge structure (μ-XANES) spectra collected from As hotspots showed MMA and DMA were demethylated to As^V over 1 year of incubation period under aerobic conditions. MMA was methylated to DMA which persisted over 3 months of incubation period under anaerobic conditions. Under both redox conditions, arsenic-iron precipitation, such as the formation of scorodite ($FeAsO_4 \cdot 2H_2O$), was not observed, indicating that MMA and DMA were associated with iron oxides as sorption complexes. Our results suggest that redox potential is one of the factors that influence As speciation in the environment.

MMA and DMA sorption and desorption were investigated in soils, varying in mineralogical and organic matter contents. Sorption studies showed that Al/Fe-oxides were the main sorbents in the soils, and the sorption capacity increased as Al/Fe concentration in the soils increased. MMA sorption was greater than DMA

sorption, and the rate of MMA sorption was also faster than DMA sorption rate. Other potential sorbents, such as clay minerals, quartz, and organic matter did not affect MMA and DMA sorption as much as Al/Fe content did. EXAFS studies showed that both MMA/DMA-Fe interatomic distances were around 3.3 Å, which was indicative of inner-sphere complex formation, particularly bidentate binuclear complex formation. Desorption studies showed that not all of the sorbed MMA or DMA was desorbed due to the strong binding between MMA and DMA and iron oxides in the surface via inner-sphere complex formation. The amount of the desorbed MMA and DMA decreased as the sorption residence time increased. For example, 77 % of sorbed MMA was desorbed from the Reybold sub soil after 1 day residence time, and 66 % of sorbed MMA were desorbed from the same soil after 6 months of residence time. The decreases in the desorption was likely due to As speciation changes over time. As residence time increased more MMA was demethylated to As^{V} which was more strongly bound to the surface. This study highlights that MMA and DMA behavior is not only determined by sorption/desorption but also by methylation/demethylation processes. The persistency of these compounds in the environment was longer than was previously expected.

Chapter 1

INTRODUCTION

Methylarsenic in the Environment

Arsenic (As) originates in many rocks and minerals. These arsenic bearing rocks and minerals encounter intensive weathering and release As into the environment as inorganic species. The most predominant oxidation states for the inorganic arsenic species are arsenate (As^{V}, H_3AsO_4) and arsenite (As^{III}, H_3AsO_3). pKa values for several As species are shown in Table 1.1. As^{V} is predominately negatively charged in environmentally relevant pH ranges because its first pKa is 2.20. As^{III} has the first pKa of 9.22 and is often a neutral species in the environment. Studies have shown that As^{V} is strongly bound to various metal oxides, mostly aluminum oxides and iron oxides, and As^{III} is less strongly bound to metal oxides compared to As^{V} [1-2]. As^{III} is also a more toxic compound than As^{V} [3]. In addition to inorganic forms, organic forms of arsenic exist in nature: monomethylarsenate, dimethylarsenate, trimethylarsenate, tetramethylarsonium ion, arsenobetaine, methylarsines, arsenosugars, and so on. Organic forms are derived from biological activities [4]. Some species are common in marine environments, and some are common in terrestrial environments. The most common organoarsenicals in terrestrial environments are monomethylarsenate (MMA, $CH_3H_2AsO_3$) and dimethylarsenate (DMA, $(CH_3)_2HAsO_2$), which are transformed from inorganic species either naturally or anthropogenically. There are associated oxidation state ^{III} species,

monomethylarsenite (MMA^{III}, $CH_3H_2AsO_2$) and dimethylarsenate (DMA^{III}, $(CH_3)_2HAsO$). Similar to the relationship between As^V and As^{III}, MMA^V and DMA^V are less mobile and less toxic [5-7]. MMA^{III} and DMA^{III} are highly unstable and easily oxidized to MMA^V and DMA^V, and therefore, MMA^{III} and DMA^{III} are extremely rare in the environment [8]. MMA^V and DMA^V are generally minor components of total As in the environment, but MMA^V or DMA^V can sometimes be 10-50 % of total As in sea water, ground water, river water, lake water, and soil [9-11]. A study showed 48 % of total As was DMA, and 14 % of As was MMA in a river [9]. In the water of Lake Biwa, researchers have found seasonal As species variation and a link between biological activities in the lake and As species. DMA becomes the dominant As species in the eutrophic zone during summer, while As^{III} is the dominant As species during the rest of the season. 0.2 μg / L DMA was found in rain water collected in Wolfsberg, Austria [12]. 88 ppb MMA and 69 ppb DMA were found in rice paddy soils in Japan [13].

Methylation Process

Arsenic methylation is defined as a process where one or more methyl groups substitute for the arsenic atom instead of oxygen atoms. The fate of methylarsenates in the environment relies heavily on microbes, since arsenic methylation is truly a biotic process [4]. The methylation mechanism, the Challenger Mechanism, was first proposed in 1945 based on the observation of trimethylarsine production from fungi [14]. Later studies have verified the proposed mechanism [4, 15]. The methylation scheme is presented in Figure 1.1. Briefly, the initial reaction starts from As^V reduction to As^{III}. The reduction processes in methylation are

considered enzyme catalyzed, and reduced glutathione is a reducing agent [16-17]. As^{III} goes through oxidation-methylation to become MMA^{V}. Methylation processes involve S-adenosyl-methionine as a methyl group donor [18]. MMA^{V} is reduced to MMA^{III} and goes through another oxidation-methylation to become DMA^{V}. This process continues until trimethylarsenate (TMA^{V}, $(CH_3)_3AsO$) is reduced to TMA^{III}, which is a highly toxic arsenic gas compound trimethylarsine ($(CH_3)_3As$). The demethylation process follows exactly the opposite steps of the methylation process. DMA^{V} can be demethylated to MMA^{III}, which is subsequently oxidized to MMA^{V}. Further demethylation leads to As^{III} production. Recently, an alternative As methylation pathway (Fig. 1.1) was proposed [19]. The main differences in the newly proposed the Hayakawa pathway are 1) reduced (3+) species are formed at first, and they are oxidized to the analogue (5+) species and 2) MMA and DMA production is not continuous and MMA is also the end product of the methylation pathway. This suggests that the Challenger pathway is not the only route for methylation/demethylation, and there can be multiple As methylation/demethylation pathways. Arsenic methylation has been considered as a detoxification mechanism until recently. Now, As methylation is considered a bioactivation process since the toxicity of intermediate products, MMA^{III} and DMA^{III} is much higher than MMA^{V} and DMA^{V} [7, 20].

Arsenic methylation is commonly seen in many organisms: mammals, including human beings, fungi, bacteria, plants, and other animals [5, 14, 21-22]. Both reduced and oxidized forms of MMA and DMA have been observed in human urine [21]. Extensive studies have been conducted to characterize the methylation of cultured microbes [18, 23-26]. Microbes, including *Bacillus* sp, *Pseudomonas* sp, and

methanogenic bacteria are capable of methylating arsenic to methylarsenates and volatile arsines or demethylating methylarsenates to arsenate and arsenite.

There are studies that have investigated arsenic methylation in soil, particularly volatile arsine production. Studies conducted earlier (~1980's) showed high volatile arsine production. In these studies, 30 to 60 percent of initial As was converted to arsine [27-28]. On the other hand, later studies (1980's ~) showed low or negligible volatile arsine production [29-32]. In these studies, volatile arsine production ranged between 0.001 and 1.4 %. The difference in volatile arsine production may be due to the different analytical techniques and experimental protocols used. Early studies employed an As mass balance equation, measuring As concentration before and after the experiments, assuming the As loss during the experiments was equivalent to volatile arsine production, while later studies actually measured the produced arsine species by GC-MS. In addition, based on a methylation scheme diagram, volatile arsine is the final product of the process. If the intermediate product of the methylation process, such as MMA or DMA, is detected at a low concentration, the volatile arsine product would be much smaller than the DMA or MMA concentration, indicating that As volatilization has a small contribution to overall global As cycling.

Other studies have investigated the methylation of As^{III} or As^{V} to MMA or DMA and demethylation MMA or DMA to As^{V}. There are studies that investigated methylation/demethylation of MMA. For example, under aerobic conditions, 43 % of MMA was demethylated to As^{V} in 70 days [30]. Another study showed that 16 % of MMA was demethylated to As^{V} in 30 days [33]. Under anaerobic conditions, up to 47 % of MMA^{V} was reduced to MMA^{III} and 2.5 % of MMA^{V} was methylated to DMA^{V}

[34]. Other studies investigated demethylation of DMA. For example, under aerobic conditions, 73 % and 0.8 % of DMA was demethylated to As^{V} and MMA, respectively in 70 days [30]. Another study showed 38 % and 8 % of DMA was demethylated to As^{V} and MMA, respectively [32]. Under anaerobic conditions, 65 % of DMA was demethylated to MMA [34].

Arsenic Toxicity

The main reason that arsenic has received great attention is its acute toxicity. Arsenic toxicity varies among species, and each species has different toxin mechanisms. Generally, arsenite species, As^{III}, MMA^{III}, or DMA^{III} are more toxic than arsenate species, As^{V}, MMA^{V}, or DMA^{V} [20]. LD_{50} values on As^{V}, As^{III}, MMA, and DMA are summarized in Table 1.2 [35-36]. LD_{50}, lethal dose, 50%, is defined as the dose required to kill half the members of a tested population after a specific duration. Briefly, As^{III} has the lowest LD_{50} of 0.0045 g/kg body mass, and MMA has the highest LD_{50} of 1.8 g/kg body mass, which means that As^{III} is the most acute and MMA is the least acute. Table 1.2 shows that organic arsenic species have much higher LD_{50} than inorganic species do.

MMA and DMA can be produced in many animals, including human beings via methylation. This methylation process is thought as a detoxification process [37]. Over time, there has been a shift from using inorganic arsenic herbicide and pesticide to organic herbicide and pesticide because it was thought that organic arsenic compounds were less toxic. However, during the methylation processes, MMA^{III} and DMA^{III} are produced as intermediate products. MMA^{III} and DMA^{III} are considered more toxic compounds than As^{V} or As^{III} [7, 20]. Although MMA and

DMA themselves possess lower toxicity than As^{V} or As^{III}, the reduction of MMA or DMA can produce very toxic MMA^{III} or DMA^{III}. The potential toxicities of MMA and DMA should be considered more carefully.

As^{V} is an analog to phosphate and can replace phosphate during the phosphorylation process [38-39]. Adenosine diphosphate (ADP) requires an additional phosphate molecule to become adenosine triphosphate (ATP) which supplies energy to living organisms. In the presence of arsenate, ATP cannot be synthesized from ADP, and therefore, organisms cannot gain energy. As^{III} toxicity comes from its binding to the thiol groups, particularly vicinal thiols, on various enzymes, which eventually leads to the inhibition of catalytic activities of more than 200 enzymes [40-41]. There are no studies explaining the mechanisms of toxicities of MMA and DMA. MMA is known to cause peripheral artery disease related to atherosclerosis [42]. DMA is known to be an urinary, bladder, kidney, liver, and thyroid gland cancer promoter [43-44]. DMA itself does not cause cancer at high rates. When a known carcinogen is applied to samples with the addition of DMA, the cancer incident rate increased dramatically compared to when the known carcinogen was applied without DMA.

Methylarsenate uses in Agriculture

The main anthropogenic point source of MMA and DMA in the environment is agricultural application. Ironically, As toxicity to organisms make As a useful agent as herbicides, pesticides, and fungicides. Historically, calcium arsenate was used for boll weevil control in cotton, and lead arsenate was used for insect control in tobacco and tree fruits. Sodium arsenite was use as a herbicide, a desiccant

in cotton, and a vine killer in potatoes [45]. For example, about 6.8 million kg of As was applied in New Jersey as lead arsenate and calcium arsenate. Inorganic arsenic species were eventually replaced with MMA and DMA. MMA and DMA are less phytotoxic than As^{V} and As^{III} [33]. Large amounts of MMA and DMA were applied particularly to cotton fields in the so-called cotton belt of the United States: Alabama, Arkansas, Texas, Louisiana, and Mississippi. The monosodium form of MMA (MSMA, $NaCH_3HAsO_3$) was applied throughout these cotton belt states due to its effectiveness on weedy grasses as well as cotton's tolerance to MMA. Cacodylic acid (DMA) was applied as a cotton defoliant at the same time. In the 1990's, more than 3000 metric tons per year of MMA and more than 30 metric tons per year of DMA were applied in cotton belt states [46]. The agricultural application of MMA and DMA often leads to MMA and DMA sorption to soil constituents. In a field experiment, MMA and DMA were detected 1.5 years after application, and the half life of MMA and DMA were 20 and 22 days, respectively [32]. Another study has shown that elevated amounts of MMA, DMA, As^{III}, and As^{V} were detected in surface water and groundwater nearby or beneath agricultural fields that had received MMA and DMA as herbicides and pesticides [10]. Also, MMA, DMA, As^{III}, and As^{V} were detected in a river where a pesticide plant was located upstream of sampling sites [47]. MMA has been used as a common pesticide at golf courses in Southern Florida and has been linked to the elevated concentration of As in the groundwater beneath the golf courses [48]. MSMA has been used as a pesticide against mountain pine beetle (*Dendroctonus ponderosae*) outbreaks in British Columbia, Canada [49]. Approximately 960 kg of MSMA are applied annually, and over 60,000 trees in the Cascades Forest District were treated with MSMA between 2000 and 2004 [50-51].

Another organoarsenical fungicide, ferric methanearsonate ($(CH_3AsO_3)_3Fe_2$) was used to control sheath blight of rice plants in Japan [52].

Arsenic in Plants

It is known that some plants can uptake As. MMA and DMA uptake by plants is much slower than As^V uptake [53-54]. As^V can move into plants through the phosphate transport system, since the molecular geometry is similar for As^V and phosphate [55]. As^{III} can move into plants via the silicic acid transport system [56]. Exact mechanisms of MMA and DMA uptake into plants are not understood [57]. A study on As uptake by non-crop plants revealed As accumulation [58]. This study showed that up to 0.5 ppm of accumulated As was MMA or DMA. For some cases, organoarsenicals are the main As species in plants. There are two arguments about whether plants uptake MMA and DMA or whether plants uptake As^V and methylate them internally. However, there are contradictions about both theories. MMA and DMA uptake are too slow, while there are only two cases of methylation by tomato plants and bent grass documented [58-61]. It is still uncertain which hypothesis is correct.

Arsenic is not an essential nutrient for plants and it seems that As is not involved in any specific metabolic reactions [62-63]. If a large amount of As is accumulated in plants, it can be also toxic to plants [64]. Arsenic accumulation can kill the plant itself. Arsenic accumulated plants can be toxic, if they are consumed by other organisms, but at the same time, As hyperaccumulators can remove As from the soil. Indian mustard and fern show great potential as hyperaccumulators [65-66]. However, in most cases, As accumulation in plants has negative impacts on humans.

As a result of long As application to farm lands where farmers alternate several crops or switch to other crops, As has accumulated in the following crop plants: spinach, corn, turnip, carrots, barley, and particularly rice [57, 61, 64, 67-69]. Rice is the main carbohydrate source in Asian people. As accumulation in rice plants is a serious concern that is receiving attention [53, 56, 61, 70-81]. Recent studies showed that rice grown in former cotton fields in the southern U. S. had elevated As concentrations in their grain [79]. Rice grown in Bangladesh contains an average of 0.13-0.15 mg As kg^{-1}, while rice grown in the southern U.S. contains an average of 0.26-0.30 mg As kg^{-1}. Rice from California contains an average of 0.13-0.17 mg As kg^{-1}. Southern U. S. rice has a higher arsenic concentration than rice from Bangladesh. Bangladesh is facing the most serious mass As ground water contamination in the world. Rice from the southern U. S. is unique in that it contains predominantly DMA, whereas rice from the rest of the world contains mostly As^{III}. There is a current debate as to why southern U. S. rice contains more As than Bangladesh rice and why DMA is the dominant species. Some researchers speculate that many rice paddy fields in the U. S. were once used as cotton fields. Arsenic residues from methylarsenic herbicide and defoliant applications to cotton fields could have caused the DMA accumulation. Others speculate that DMA uptake by plants is 10-20 times slower than As^{III}. Arsenic methylation inside rice plants causes DMA accumulation. Therefore, genetic variations in rice rather than geographical variations in As concentrations may have caused the results.

Mining sites in Peru have released As into river systems [82]. As a result, some plants grown along the rivers accumulated As, mostly As^{V} and As^{III} in their leaves, which can be eaten by cattle from the region. In this case, non-crop plants can

also potentially be toxic to humans if the cattle accumulate As, and people from the region consume the cattle.

X-Ray Absorption Spectroscopy (XAS) and μ-Synchrotron X-Ray Fluorescence (μSXRF) Microprobe Spectroscopy

XAS employs a synchrotron based X-Ray to investigate molecular scale interaction between a target element and its neighboring atoms [83]. Each element has specific set absorption edges (K, L, M) at the binding energies of electrons. XAS experiments apply an element specific wide energy range of X-Rays, approximately 200 eV below an absorption edge to approximately 1000 eV above the edge, to collect spectra. XAS spectra can be divided into two regions: X-Ray Absorption Near Edge Structure (XANES) and Extended X-Ray Absorption Fine Structure (EXAFS). The XANES part of the spectra, ± 50 eV of the absorption edge, can provide the binding geometry and oxidation state of the element. The EXAFS part of the spectra, 50 eV to 1000 eV above the edge, can provide the types and coordination numbers of neighboring atoms and their bonding distances.

XAS spectra data analysis involves several steps. For each sample, 3-12 scans are collected based on data quality (data vs. noise). Averaged spectra are normalized to eliminate variations between samples, which are caused by target element concentration, sample thickness, or the detector. The background of normalized spectra is subtracted, and spectra are transformed from energy space to wave number κ space. The spectra are Fourier transformed to distinguish shells at different distances. XANES analysis uses normalized spectra, comparing sample spectra and the standard spectra of known samples to determine oxidation states. For

EXAFS analysis, theoretical spectra and sample spectra are compared to determine coordination number, neighboring atoms, and interatomic distances.

μ-SXRF microprobe analysis employs the same synchrotron based X-Ray principle. Bright and intense X-Rays from the synchrotron enable the production of a small sub-micron size X-Ray beam. This beam is used to create two dimensional elemental distribution maps. In a map, each pixel is made of an XAS spectrum. The broad energy range of X-Rays is applied to each pixel. When electrons from a certain element are excited by the X-Ray and go back to ground states, they emit fluorescence at element specific energies. Such signals are detected and recorded. The higher concentration of the element produces a stronger signal. On maps, the higher concentration is displayed as a brighter color: white > black. The advantage of μXAS over XAS is the small X-Ray beam size. Typical XAS has a mm size X-Ray beam. In many environmental samples, including soil samples, elements are heterogeneously distributed. Even though the total As concentration is the same, As concentration per beam size is larger for μ-XAS. The sub-micron size X-Ray beam can pin point As hotspots and one can obtain the XANES region of the spectra from a sample while regular XAS suffers from large background noise.

XAS and μ-SXRF have been extensively used in environmental science research. XAS has been used to speciate or identify the oxidation state of As in natural samples [84-85]. Focusing only on sorption mechanism research, As^{V} forms an inner-sphere complex with iron oxides [86-93] and aluminum oxides [2, 94-97]. As^{III} forms an inner-sphere complex with goethite [98] and both inner-sphere and outer sphere complexes with aluminum oxide [2]. μ-SXRF analysis revealed As speciation, distribution, association with soil constituents and the formation of precipitate in the

environment [91, 95, 99-104]. μ-SXRF coupled with μ-XRD successfully identified As rich particles as possibly phaunouxite, a calcium arsenate like mineral [105]. Arsenic in poultry litter was always observed around needle-shaped micron scale particles and was associated with Ca, Cu and Fe [100].

Methylarsenate/Arsenate Sorption

Since methylarsenate structures are comparable to As^V and there are not many studies on methylarsenate sorption to mineral oxides, it is reasonable to compare methylarsenate sorption to As^V sorption and review arsenate sorption to metal oxides. There have been extensive studies on As^V sorption to soil constituents, especially iron and aluminum oxides [1-2, 86-89, 94-96, 106-113]. As^V is mainly sorbed to Fe/Al oxides in soil, and As^V sorption capacity on iron oxides and aluminum oxides is similarly high. There are several factors affecting the As^V sorption to these oxides. One of them is the surface area of oxide minerals. In general, As^V sorption to amorphous oxides, such as ferrihydrite or amorphous aluminum oxide, is higher than the sorption to crystallized oxides, such as goethite or gibbsite, because amorphous oxides have higher surface areas compared to well crystallized oxides. The larger surface areas create more available sites for As^V to be sorbed. Another factor that affects the As^V sorption to those oxides is the pH. As^V sorption is a function of pH. As^V sorption maxima on both metal oxides occur at low pHs, pH 4 or 5, and as the pH of the sorption reaction increases, As^V sorption decreases. This observation is mainly due to electrostatic attraction. At the low pH, Fe/Al oxide surface is positively charge, and As^V is negatively charge (Table 1.1). Fe/Al oxides have PZC above 7 in general [1-2]. As the pH increases, As^V increases negative charge, but the oxide surface

becomes negative as well. Negatively charged As^V and the negatively charged oxide surface repel each other, and therefore, As^V sorption decreases at high pH. Another factor that affects As^V sorption is the competition of available reactive sites with other anions. As^V sorption competes for the same surface sites with phosphate, due to their structural similarities. The addition of phosphate to the As^V sorption system leads to a substantial decrease in As^V sorption or As^V desorption from both iron and aluminum oxide surface sites [1, 114-115].

Molecular scale techniques, such as XAS and FTIR, have been employed to investigate molecular scale interactions between As and oxide surfaces. These studies have shown that the strong As^V sorption to the oxide surface is the result of inner-sphere complex formation [2, 87, 89, 110, 116]. Arsenate mainly forms inner-sphere complexes with iron or aluminum oxides, and the dominant complex form is a bidentate binuclear complex. Based on a XAS study, bidentate mononuclear complex formation has been reported at As-Fe interatomic distances around 2.85 Å, but some argue that this is not from an As-Fe interaction [87-88]. Instead, the distance corresponds to As-O-O multiple scattering. The multiple scattering is a kind of photoelectron wave scattering observed between more than 2 atoms in XAS spectra. Generally, single scatterings, such as As-O, As-Fe, or As-Al are the main photoelectron scatterings that largely affect XAS spectra. For single scattering, the photoelectron wave emitted by an As atom hits surrounding O, Fe, or Al atoms and bounces back to the As atom. For multiple scattering, the photoelectron wave emitted by an As atom hits an O atom and hits another neighboring O atom before it bounces back to the As atom. Such multiple scattering can affect final EXAFS fitting results when the multiple scattering paths are not included in the fitting [88, 117]. The actual

As-Fe bidentate binuclear peak signal is usually observed around 3.3 Å[87-89]. In addition, a peak around 3.5 Å is sometime reported which corresponds to monodentate mononuclear complexes [87]. In case of As sorption to aluminum oxides, the As-O-O multiple scattering is calculated around 3.1 Å by FEFF, which is very close to the As-Al interatomic distance. The addition of multiple scattering does not change the final EXAFS fitting dramatically. With or without multiple scattering, the bidentate binuclear complex formation for the As-Al system is reported around 3.15 Å [2, 94-95].

Many similarities are seen in methylarsenate sorption studies. MMA and DMA are mainly sorbed to Fe/Al oxides in soils [48, 118]. More MMA and DMA are sorbed to ferryhydride than to goethite [6, 119]. MMA and DMA sorption to iron oxides is a function of pH and the concentrations of sorbate and sorbent. MMA and DMA sorption maxima to iron oxides occur at lower pHs of 4 or 5. As pH increases, less MMA and DMA are sorbed to iron oxide surfaces. The sorption capacity of MMA and DMA to iron oxides is comparable at lower pH. The difference in sorption capacity is observed as pH increases. Less MMA is sorbed compared to As^V as the pH increases. DMA sorption to iron oxides is slightly different from As^V and MMA. DMA sorption dramatically drops above pH 6.5, and almost no sorption is observed above pH 7.5. Phosphate addition enhances MMA and DMA desorption from iron oxide surfaces at a greater extent than it does for As^V. Roughly 50 % of sorbed As^V is desorbed by phosphate, while roughly 80 % and almost 100 % of MMA and DMA, respectively, are desorbed by the same concentration of phosphate. There is only one study that has applied molecular scale XAS techniques to examine the surface complex formation of MMA and DMA. MMA and DMA also form inner-sphere

complexes with TiO_2 [120]. MMA forms a bidentate binuclear complex, and DMA forms a monodentate mononuclear complex.

Objectives.

There are limited studies on methylarsenates in the environment. Several new studies have emerged during the past few years, yet more studies are necessary to fully understand MMA and DMA behavior in the environment [6, 34, 119, 121-127]. Our goal is to investigate MMA and DMA reactivity, bioavailability, distribution, and interaction with other elements in the environment by conducting the following studies: 1) elucidate sorption mechanisms of MMA and DMA sorption on aluminum oxide using macroscopic and molecular scale techniques, 2) characterize the *in-situ* behavior of MMA and DMA speciation, localization, and association with soil components using μ-SXRF, μ-X-ray absorption spectroscopy (μ-XAS), and μ-X-ray diffraction (μ-XRD), and 3) elucidate the soil characteristics that affect MMA and DMA sorption, investigate the residence time effects on MMA and DMA desorption in soils, and identify sorption mechanisms between MMA and DMA and goethite, the major soil component responsible for MMA and DMA sorption.

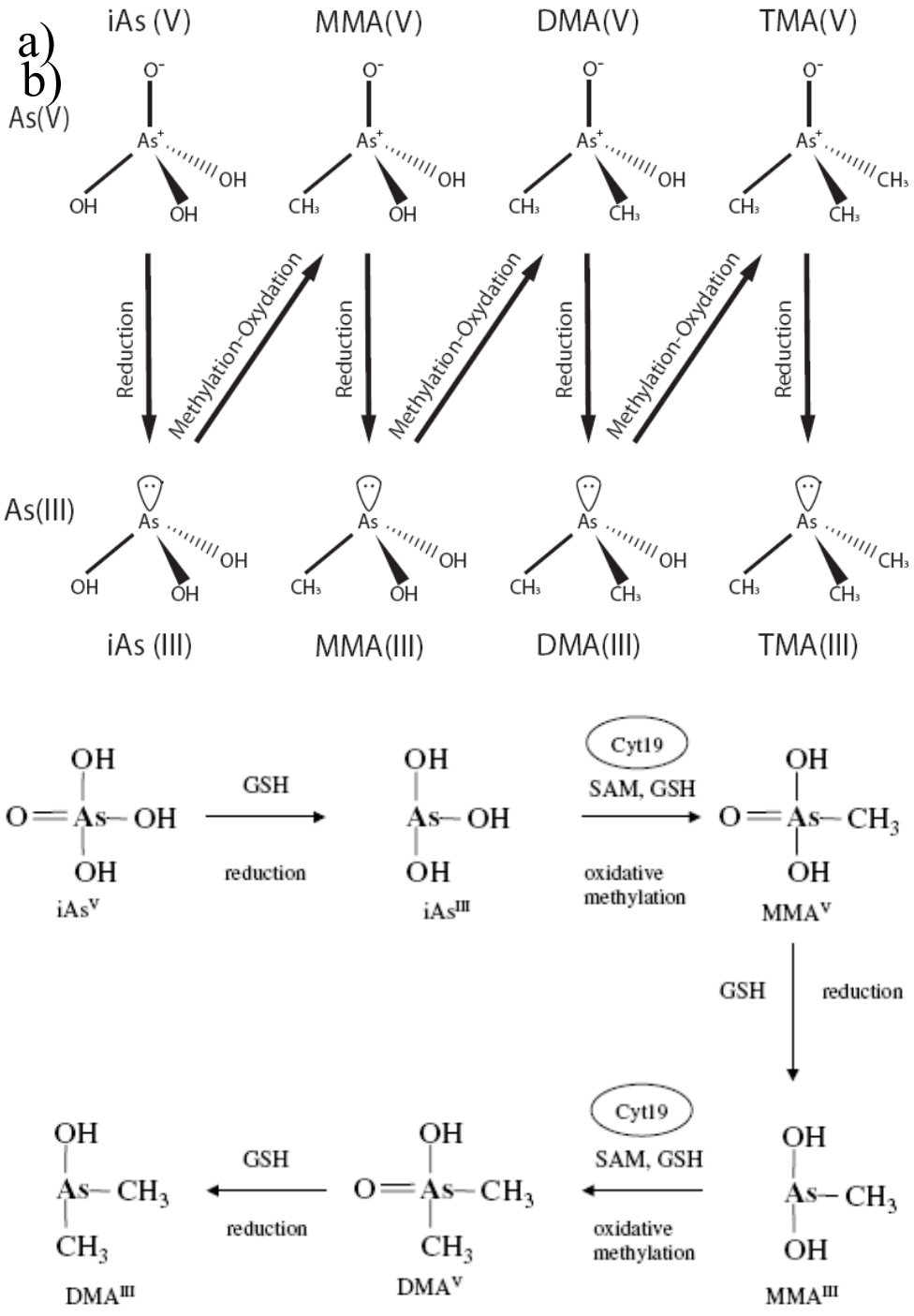

Figure 1.1 Arsenic methylation scheme diagram. a) Challenger Mechanism and b) Hayakawa Mechanism [19].

Table 1.1 pKa values for various As species**.**

Species / pKa	pKa_1	pKa_2	pKa_3
H_3AsO_4	2.20	6.97	11.53
$CH_3H_2AsO_4$	4.19	8.77	—
$(CH_3)_2HAsO_4$	6.14	—	—

Table 1.2 LD_{50} values for various arsenic species.

Arsenic Species	LD_{50} [g/kg body mass]	Animal	Mode of administration
As^{III}	0.0045	Rat	intraperitoneal
As^{V}	0.014-0.018	Rat	intraperitoneal
MMA	1.8	Mouse	Oral
DMA	1.2	Mouse	Oral
TMA	10.6	Mouse	Oral

REFERENCES

(1)Dixit, S.; Hering, J. G., Comparison of arsenic(V) and arsenic(III) sorption onto iron oxide minerals: Implications for arsenic mobility. *Environ. Sci. Technol.* **2003,** *37*, (18), 4182-4189.

(2)Arai, Y.; Elzinga, E. J.; Sparks, D. L., X-ray absorption spectroscopic investigation of arsenite and arsenate adsorption at the aluminum oxide-water interface. *J. Colloid Interface Sci.* **2001,** *235*, (1), 80-88.

(3)Knowles, F. C.; Benson, A. A., The Biochemistry of Arsenic. *Trends Biochem. Sci.* **1983,** *8*, (5), 178-180.

(4)Cullen, W. R.; Reimer, K. J., Arsenic speciation in the environment. *Chem. Rev.* **1989,** *89*, (4), 713-764.

(5)Styblo, M.; Serves, S. V.; Cullen, W. R.; Thomas, D. J., Comparative inhibition of yeast glutathione reductase by arsenicals and arsenothiols. *Chem. Res. Toxicol.* **1997,** *10*, (1), 27-33.

(6)Lafferty, B. J.; Loeppert, R. H., Methyl arsenic adsorption and desorption behavior on iron oxides. *Environ. Sci. Technol.* **2005,** *39*, (7), 2120-2127.

(7)Petrick, J. S.; Ayala-Fierro, F.; Cullen, W. R.; Carter, D. E.; Aposhian, H. V., Monomethylarsonous acid (MMA(III)) is more toxic than arsenite in Chang human hepatocytes. *Toxicol. Appl. Pharmacol.* **2000,** *163*, (2), 203-207.

(8)Gong, Z. L.; Lu, X. F.; Cullen, W. R.; Le, X. C., Unstable trivalent arsenic metabolites, monomethylarsonous acid and dimethylarsinous acid. *J. Ana. At. Spectrom.* **2001,** *16*, (12), 1409-1413.

(9)Braman, R. S.; Foreback, C. C., Methylated forms of arsenic in environment. *Science* **1973,** *182*, (4118), 1247-1249.

(10)Bednar, A. J.; Garbarino, J. R.; Ranville, J. F.; Wildeman, T. R., Presence of organoarsenicals used in cotton production in agricultural water and soil of the southern United States. *J. Agric. Food Chem.* **2002,** *50*, (25), 7340-7344.

(11)Marin, A. R.; Pezeshki, S. R.; Masschelen, P. H.; Choi, H. S., Effect of dimethylarsenic acid (DMAA) on growth, tissue arsenic, and photosynthesis of rice plants. *J. Plant Nutr.* **1993,** *16*, (5), 865-880.

(12)Pongratz, R., Arsenic speciation in environmental samples of contaminated soil. *Sci. Total Environ.* **1998,** *224*, (1-3), 133-141.

(13)Takamatsu, T.; Aoki, H.; Yoshida, T., Determination of Arsenate, Arsenite, Monomethylarsonate, and Dimethylarsinate in Soil Polluted with Arsenic. *Soil Sci.* **1982,** *133*, (4), 239-246.

(14)Challenger, F., Biological methylation. *Chem. Rev.* **1945,** *36*, (3), 315-361.

(15)Dombrowski, P. M.; Long, W.; Farley, K. J.; Mahony, J. D.; Capitani, J. F.; Di Toro, D. M., Thermodynamic analysis of arsenic methylation. *Environ. Sci. Technol.* **2005,** *39*, (7), 2169-2176.

(16)Buchet, J. P.; Lauwerys, R., Study of inorganic arsenic methylation by rat-liver invitro - Relevance for the interpretation of observations in man. *Arch. Toxicol.* **1985,** *57*, (2), 125-129.

(17)Buchet, J. P.; Lauwerys, R., Study of factors influencing the invivo methylation of inorganic arsenic in rats. *Toxicol. Appl. Pharmacol.* **1987,** *91*, (1), 65-74.

(18)Bentley, R.; Chasteen, T. G., Microbial methylation of metalloids: Arsenic, antimony, and bismuth. *Microbiol Mol Biol R* **2002,** *66*, (2), 250-+.

(19)Hayakawa, T.; Kobayashi, Y.; Cui, X.; Hirano, S., A new metabolic pathway of arsenite: Arsenic-glutathione complexes are substrates for human arsenic methyltransferase Cyt19. *Arch. Toxicol.* **2005,** *79*, (4), 183-191.

(20)Styblo, M.; Del Razo, L. M.; Vega, L.; Germolec, D. R.; LeCluyse, E. L.; Hamilton, G. A.; Reed, W.; Wang, C.; Cullen, W. R.; Thomas, D. J., Comparative toxicity of trivalent and pentavalent inorganic and methylated arsenicals in rat and human cells. *Arch. Toxicol.* **2000,** *74*, (6), 289-299.

(21)Aposhian, H. V.; Gurzau, E. S.; Le, X. C.; Gurzau, A.; Healy, S. M.; Lu, X. F.; Ma, M. S.; Yip, L.; Zakharyan, R. A.; Maiorino, R. M.; Dart, R. C.; Tircus, M. G.; Gonzalez-Ramirez, D.; Morgan, D. L.; Avram, D.; Aposhian, M. M., Occurrence of monomethylarsonous acid in urine of humans exposed to inorganic arsenic. *Chem. Res. Toxicol.* **2000,** *13*, (8), 693-697.

(22)Oremland, R. S.; Stolz, J. F., The ecology of arsenic. *Science* **2003,** *300*, (5621), 939-944.

(23)Hanaoka, K.; Hasegawa, S.; Kawabe, N.; Tagawa, S.; Kaise, T., Aerobic and anaerobic degradation of several arsenicals by sedimentary microorganisms. *Appl. Organomet. Chem.* **1990,** *4*, (3), 239-243.

(24)Hanaoka, K.; Araki, N.; Tagawa, S.; Kaise, T., Degradation of a tetramethylarsonium salt by microorganisms occurring in sediments and suspended substances under both aerobic and anaerobic conditions. *Appl. Organomet. Chem.* **1994,** *8*, (3), 201-206.

(25)Honschopp, S.; Brunken, N.; Nehrkorn, A.; Breunig, H. J., Isolation and characterization of a new arsenic methylating bacterium from soil. *Microbiol Res* **1996,** *151*, (1), 37-41.

(26)Lehr, C. R.; Polishchuk, E.; Radoja, U.; Cullen, W. R., Demethylation of methylarsenic species by Mycobacterium neoaurum. *Appl. Organomet. Chem.* **2003,** *17*, (11), 831-834.

(27)Woolson, E. A.; Kearney, P. C., Persistence and reactions of C-14-cacodylic acid in soils. *Environ. Sci. Technol.* **1973,** *7*, (1), 47-50.

(28)Braman, R. S., Arsenic in Environment. *Advances in Chemistry Series* **1975**, (7), 108-123.

(29)Turpeinen, R.; Pantsar-Kallio, M.; Haggblom, M.; Kairesalo, T., Influence of microbes on the mobilization, toxicity and biomethylation of arsenic in soil. *Sci. Total Environ.* **1999,** *236*, (1-3), 173-180.

(30)Gao, S.; Burau, R. G., Environmental factors affecting rates of arsine evolution from and mineralization of arsenicals in soil. *J. Environ. Qual.* **1997,** *26*, (3), 753-763.

(31)Huysmans, K. D.; Frankenberger, W. T., Evolution of trimethylarsine by a *Penicillium* Sp isolated from agricultural evaporation pond water. *Sci. Total Environ.* **1991,** *105*, 13-28.

(32)Woolson, E. A.; Aharonson, N.; Iadevaia, R., Application of the high-performance liquid-chromatography flameless atomic-absorption method to the study of alkyl arsenical herbicide metabolism in soil. *J. Agric. Food Chem.* **1982,** *30*, (3), 580-584.

(33)Dickens, R.; Hiltbold, A. E., Movement and persistence of methanearsonates in soil. *Weeds* **1967,** *15*, (4), 299-304.

(34)Sierra-Alvarez, R.; Yenal, U.; Field, J. A.; Kopplin, M.; Gandolfi, A. J.; Garbarino, J. R., Anaerobic biotransformation of organoarsenical pesticides monomethylarsonic acid and dimethylarsinic acid. *J. Agric. Food Chem.* **2006,** *54*, (11), 3959-3966.

(35)Franke, F. W.; Moxon, A. L., A comparsion of the minimun fatal doses of selenium, tellurium, arsenic and vanadium. *J. Pharmacol. Exp. Ther.* **1936,** *58*, (4), 454-459.

(36)Kaise, T.; Yamauchi, H.; Horiguchi, Y.; Tani, T.; Watanabe, S.; Hirayama, T.; Fukui, S., A comparative study on acute toxicity of methylarsonic acid, dimethylarsinic acid and trimethylarsine oxide in mice. *Appl. Organomet. Chem.* **1989,** *3*, (3), 273-277.

(37)Gebel, T. W., Arsenic methylation is a process of detoxification through accelerated excretion. *Int. J. Hyg. Environ. Health.* **2002,** *205*, (6), 505-508.

(38)Dixon, H. B. F., The biochemical action of arsonic acids especially as phosphate analogues. In *Advances in Inorganic Chemistry, Vol. 44*, Academic Press Inc: San Diego, 1997; Vol. 44, pp 191-227.

(39)Crane, R. K.; Lipmann, F., The effect of arsenate on aerobic phosphorylation. *J. Biol. Chem.* **1953,** *201*, (1), 235-243.

(40)Peters, R. A.; Sinclair, H. M.; Thompson, R. H. S., An analysis of the inhibition of pyruvate oxidation by arsenicals in relation to the enzyme theory of vesication. *Biochem. J.* **1946,** *40*, (4), 516-524.

(41)Abernathy, C. O.; Liu, Y. P.; Longfellow, D.; Aposhian, H. V.; Beck, B.; Fowler, B.; Goyer, R.; Menzer, R.; Rossman, T.; Thompson, C.; Waalkes, M., Arsenic: Health effects, mechanisms of actions, and research issues. *Environ. Health Perspect.* **1999,** *107*, (7), 593-597.

(42)Tseng, C. H.; Huang, Y. K.; Huang, Y. L.; Chung, C. J.; Yang, M. H.; Chen, C. J.; Hsueh, Y. M., Arsenic exposure, urinary arsenic speciation, and peripheral vascular disease in blackfoot disease-hyperendemic villages in Taiwan *Toxicol. Appl. Pharmacol.* **2006,** *211*, (2), 175-175.

(43)Arnold, L. L.; Cano, M.; St John, M.; Eldan, M.; van Gemert, M.; Cohen, S. M., Effects of dietary dimethylarsinic acid on the urine and urothelium of rats. *Carcinogenesis* **1999,** *20*, (11), 2171-2179.

(44)Yamanaka, K.; Ohtsubo, K.; Hasegawa, A.; Hayashi, H.; Ohji, H.; Kanisawa, M.; Okada, S., Exposure to dimethylarsinic acid, a main metabolite of inorganic arsenics, strongly promotes tumorigenesis initiated by 4-nitroquinoline 1-oxide in the lungs of mice. *Carcinogenesis* **1996,** *17*, (4), 767-770.

(45)Johnson, L. R.; Hiltbold, A. E., Arsenic content of soil and crops following use of methanearsonate herbicides. *Soil Sci. Soc. Am. Proc.* **1969,** *33*, (2), 279-

(46)Perkins, H. H.; Brushwood, D. E., Effects of mechanical processing and wet treatments on arsenic acid desiccant residues in cotton. *Text. Chem. Color.* **1991,** *23*, (2), 26-28.

(47)Faust, S. D.; Winka, A. J.; Belton, T., An assessment of chemical and biological significance of arsenical species in the Maurice River Drainage Basin (N.J.). Part I. Distribution in water and river and lake sediments. *J. Environ. Sci. Health A* **1987,** *22*, (3), 209 - 237.

(48)Feng, M.; Schrlau, J. E.; Snyder, R.; Snyder, G. H.; Chen, M.; Cisar, J. L.; Cai, Y., Arsenic transport and transformation associated with MSMA application on a golf course green. *J. Agric. Food Chem.* **2005,** *53*, (9), 3556-3562.

(49)Albert, C. A.; Williams, T. D.; Morrissey, C. A.; Lai, V. W. M.; Cullen, W. R.; Elliott, J. E., Dose-dependent uptake, elimination, and toxicity of monosodium methanearsonate in adult zebra finches (*Taeniopygia guttata*). *Environ. Toxicol. Chem.* **2008,** *27*, (3), 605-611.

(50)Morrissey, C.; Elliot, J. E.; Dods, P.; A., A. C.; Wilson, L.; Lai, V.; Cullen, W. R. *Assessing forest bird exposure and effects from monosodium methanearsonate (MSMA) during the mountain pine beetle epidemic in British Columbia.*; Pacific and Yukon Region, Delta, BC. Canada: 2006.

(51)Dost, F. *Public health and environmental impacts of monosodium methanearsonate as used in bark beetle control in British Columbia*; FS 48 HIS 95/2 Ministry of Forests, Victroria, BC, Canada: 1995.

(52)Odanaka, Y.; Tsuchiya, N.; Matano, O.; Goto, S., Metabolic fate of the arsenical fungicide, ferric methanearsonate, in soil. *J. Pestic. Sci.* **1985,** *10*, (1), 31-39.

(53)Abedin, M. J.; Feldmann, J.; Meharg, A. A., Uptake kinetics of arsenic species in rice plants. *Plant Physiol.* **2002,** *128*, (3), 1120-1128.

(54)Odanaka, Y.; Tsuchiya, N.; Matano, O.; Goto, S., Absorption, translocation and metabolism of the arsenical fungicides, iron methanearsonate and ammonium iron methanearsonate, in rice plants. *J. Pestic. Sci.* **1987,** *12*, (2), 199-208.

(55)Bhumbla, D. K.; Keefer, R. F., Arsenic mobilization and bioavailability in soils. *Advances in environmental science and technology.* **1994,** *26*, 51.

(56)Ma, J. F.; Yamaji, N.; Mitani, N.; Xu, X. Y.; Su, Y. H.; McGrath, S. P.; Zhao, F. J., Transporters of arsenite in rice and their role in arsenic accumulation in rice grain. *PNAS* **2008,** *105*, (29), 9931-9935.

(57)Abbas, M. H. H.; Meharg, A. A., Arsenate, arsenite and dimethyl arsinic acid (DMA) uptake and tolerance in maize (Zea mays L.). *Plant Soil* **2008,** *304*, (1-2), 277-289.

(58)Ruiz-Chancho, M. J.; Lopez-Sanchez, J. F.; Schmeisser, E.; Goessler, W.; Francesconi, K. A.; Rubio, R., Arsenic speciation in plants growing in arsenic-contaminated sites. *Chemosphere.* **2008,** *71*, (8), 1522-1530.

(59)Nissen, P.; Benson, A. A., Arsenic Metabolism in Fresh-Water and Terrestrial Plants. *Physiol. Plant.* **1982,** *54*, (4), 446-450.

(60)Wu, J. H.; Zhang, R.; Lilley, R. M., Methylation of arsenic in vitro by cell extracts from bentgrass (*Agrostis tenuis*): Effect of acute exposure of plants to arsenate. *Funct. Plant Biol.* **2002,** *29*, (1), 73-80.

(61)Zavala, Y. J.; Duxbury, J. M., Arsenic in rice: I. Estimating normal levels of total arsenic in rice grain. *Environ. Sci. Technol.* **2008,** *42*, (10), 3856-3860.

(62)Chapman, H. D., *Diagnostic criteria for plants and soils*. University of California, Div. of Agricultural Sciences: Berkeley, 1966.

(63)Lepp, N. W., *Effects of heavy metal pollution on plants. Vol.1, Effects of trace metals on plant function*. Applied Science Publishers: London, 1981.

(64)Carbonell-Barrachina, A. A.; Burlo, F.; Valero, D.; Lopez, E.; Martinez-Romero, D.; Martinez-Sanchez, F., Arsenic toxicity and accumulation in turnip as affected by arsenic chemical speciation. *J. Agric. Food Chem.* **1999,** *47*, (6), 2288-2294.

(65)Pickering, I. J.; Prince, R. C.; George, M. J.; Smith, R. D.; George, G. N.; Salt, D. E., Reduction and coordination of arsenic in Indian mustard. *Plant Physiol.* **2000,** *122*, (4), 1171-1177.

(66)Francesconi, K.; Visoottiviseth, P.; Sridokchan, W.; Goessler, W., Arsenic species in an arsenic hyperaccumulating fern, Pityrogramma calomelanos: a potential phytoremediator of arsenic-contaminated soils. *Sci. Total Environ.* **2002,** *284*, (1-3), 27-35.

(67)Asher, C. J.; Reay, P. F., Arsenic uptake by barley seedlings. *Aust. J. Plant Physiol.* **1979,** *6*, (4), 459-466.

(68)Woolson, E. A., Arsenic phytotoxicity and uptake in 6 vegetable crops. *Weed Sci.* **1973,** *21*, (6), 524-527.

(69)Zandstra, B. H.; De Kryger, T. A., Arsenic and lead residues in carrots from foliar applications of monosodium methanearsonate (MSMA): A comparison between mineral and organic soils, or from soil residues. *Food Addit. Contam.* **2007,** *24*, (1), 34-42.

(70)Norton, G. J.; Duan, G.; Dasgupta, T.; Islam, M. R.; Lei, M.; Zhu, Y.; Deacon, C. M.; Moran, A. C.; Islam, S.; Zhao, F.-J.; Stroud, J. L.; McGrath, S. P.; Feldmann, J.; Price, A. H.; Meharg, A. A., Environmental and Genetic Control of Arsenic Accumulation and Speciation in Rice Grain: Comparing a Range of Common Cultivars Grown in Contaminated Sites Across Bangladesh, China, and India. *Environ. Sci. Technol.* **2009,** *43*, (21), 8381-8386.

(71)Norton, G. J.; Islam, M. R.; Deacon, C. M.; Zhao, F.-J.; Stroud, J. L.; McGrath, S. P.; Islam, S.; Jahiruddin, M.; Feldmann, J.; Price, A. H.; Meharg, A. A., Identification of Low Inorganic and Total Grain Arsenic Rice Cultivars from Bangladesh. *Environ. Sci. Technol.* **2009,** *43*, (15), 6070-6075.

(72)Norton, G. J.; Islam, M. R.; Duan, G.; Lei, M.; Zhu, Y.; Deacon, C. M.; Moran, A. C.; Islam, S.; Zhao, F.-J.; Stroud, J. L.; McGrath, S. P.; Feldmann, J.; Price, A. H.; Meharg, A. A., Arsenic Shoot-Grain Relationships in Field Grown Rice Cultivars. *Environ. Sci. Technol.* **2010,** *44*, (4), 1471-1477.

(73)Meharg, A. A.; Lombi, E.; Williams, P. N.; Scheckel, K. G.; Feldmann, J.; Raab, A.; Zhu, Y. G.; Islam, R., Speciation and localization of arsenic in white and brown rice grains. *Environ. Sci. Technol.* **2008,** *42*, (4), 1051-1057.

(74)Meharg, A. A.; Sun, G. X.; Williams, P. N.; Adomako, E.; Deacon, C.; Zhu, Y. G.; Feldmann, J.; Raab, A., Inorganic arsenic levels in baby rice are of concern. *Environmental Pollution* **2008,** *152*, (3), 746-749.

(75)Meharg, A. A.; Williams, P. N.; Adomako, E.; Lawgali, Y. Y.; Deacon, C.; Villada, A.; Cambell, R. C. J.; Sun, G.; Zhu, Y.-G.; Feldmann, J.; Raab, A.; Zhao, F.-J.; Islam, R.; Hossain, S.; Yanai, J., Geographical Variation in Total and Inorganic Arsenic Content of Polished (White) Rice. *Environ. Sci. Technol.* **2009,** *43*, (5), 1612-1617.

(76)Meharg, A. A.; Rahman, M., Arsenic contamination of Bangladesh paddy field soils: Implications for rice contribution to arsenic consumption. *Environ. Sci. Technol.* **2003,** *37*, (2), 229-234.

(77)Zavala, Y. J.; Gerads, R.; xfc; rley; xfc; k, H.; Duxbury, J. M., Arsenic in rice: II. Arsenic speciation in USA grain and implications for human health. *Environ. Sci. Technol.* **2008,** *42*, (10), 3861-3866.

(78)Williams, P. N.; Price, A. H.; Raab, A.; Hossain, S. A.; Feldmann, J.; Meharg, A. A., Variation in arsenic speciation and concentration in paddy rice related to dietary exposure. *Environ. Sci. Technol.* **2005,** *39*, (15), 5531-5540.

(79)Williams, P. N.; Raab, A.; Feldmann, J.; Meharg, A. A., Market basket survey shows elevated levels of as in South Central US processed rice compared to California: Consequences for human dietary exposure. *Environ. Sci. Technol.* **2007,** *41*, (7), 2178-2183.

(80)Meharg, A. A.; Deacon, C.; Campbell, R. C. J.; Carey, A. M.; Williams, P. N.; Feldmann, J.; Raab, A., Inorganic arsenic levels in rice milk exceed EU and US drinking water standards. *Journal of Environmental Monitoring* **2008,** *10*, (4), 428-431.

(81)Lombi, E.; Scheckel, K. G.; Pallon, J.; Carey, A. M.; Zhu, Y. G.; Meharg, A. A., Speciation and distribution of arsenic and localization of nutrients in rice grains. *New Phytol.* **2009,** *184*, (1), 193-201.

(82)Bech, J.; Poschenrieder, C.; Llugany, M.; Barcelo, J.; Tume, P.; Tobias, F. J.; Barranzuela, J. L.; Vasquez, E. R., Arsenic and heavy metal contamination of soil and vegetation around a copper mine in Northern Peru. *Sci. Total Environ.* **1997,** *203*, (1), 83-91.

(83)Sparks, D. L., *Environmental Soil Chemistry*. 2nd ed.; Academic Press: Boston, 2002.

(84)Weber, F. A.; Hofacker, A. F.; Voegelin, A.; Kretzschmar, R., Temperature dependence and coupling of iron and arsenic reduction and release during flooding of a contaminated soil. *Environ. Sci. Technol.* **2010,** *44*, (1), 116-122.

(85)Grafe, M.; Tappero, R. V.; Marcus, M. A.; Sparks, D. L., Arsenic speciation in multiple metal environments: I. Bulk-XAFS spectroscopy of model and mixed compounds. *J. Colloid Interface Sci.* **2008,** *320*, (2), 383-399.

(86)Foster, A. L.; Brown, G. E.; Tingle, T. N.; Parks, G. A., Quantitative arsenic speciation in mine tailings using X-ray absorption spectroscopy. *Am. Miner.* **1998,** *83*, (5-6), 553-568.

(87)Fendorf, S.; Eick, M. J.; Grossl, P.; Sparks, D. L., Arsenate and chromate retention mechanisms on goethite .1. Surface structure. *Environ. Sci. Technol.* **1997,** *31*, (2), 315-320.

(88)Sherman, D. M.; Randall, S. R., Surface complexation of arsenie(V) to iron(III) (hydr)oxides: Structural mechanism from ab initio molecular geometries and EXAFS spectroscopy. *Geochim. Cosmochim. Acta* **2003,** *67*, (22), 4223-4230.

(89)Waychunas, G. A.; Rea, B. A.; Fuller, C. C.; Davis, J. A., Surface-chemistry of ferrihydrite: Part 1. EXAFS studies of the geometry of coprecipitated and adsorbed arsenate. *Geochim. Cosmochim. Acta* **1993,** *57*, (10), 2251-2269.

(90)Arai, Y.; Sparks, D. L.; Davis, J. A., Effects of dissolved carbonate on arsenate adsorption and surface speciation at the hematite-water interface. *Environ. Sci. Technol.* **2004,** *38*, (3), 817-824.

(91)Cances, B.; Juillot, F.; Morin, G.; Laperche, V.; Alvarez, L.; Proux, O.; Hazemann, J. L.; Brown, G. E.; Calas, G., XAS evidence of As(V) association with iron oxyhydroxides in a contaminated soil at a former arsenical pesticide processing plant. *Environ. Sci. Technol.* **2005,** *39*, (24), 9398-9405.

(92)O'Reilly, S. E.; Strawn, D. G.; Sparks, D. L., Residence time effects on arsenate adsorption/desorption mechanisms on goethite. *Soil Sci. Soc. Am. J.* **2001,** *65*, (1), 67-77.

(93)Randall, S. R.; Sherman, D. M.; Ragnarsdottir, K. V., Sorption of As(V) on green rust (Fe-4(II)Fe-2(III)(OH)(12)SO4 center dot 3H(2)O) and lepidocrocite (gamma-FeOOH): Surface complexes from EXAFS spectroscopy. *Geochim. Cosmochim. Acta* **2001,** *65*, (7), 1015-1023.

(94)Ladeira, A. C. Q.; Ciminelli, V. S. T.; Duarte, H. A.; Alves, M. C. M.; Ramos, A. Y., Mechanism of anion retention from EXAFS and density functional calculations: Arsenic (V) adsorbed on gibbsite. *Geochim. Cosmochim. Acta* **2001,** *65*, (8), 1211-1217.

(95)Beaulieu, B. T.; Savage, K. S., Arsenate adsorption structures on aluminum oxide and phyllosilicate mineral sufaces in smelter-impacted soils. *Environ. Sci. Technol.* **2005,** *39*, (10), 3571-3579.

(96)Arai, Y.; Sparks, D. L., Residence time effects on arsenate surface speciation at the aluminum oxide-water interface. *Soil Sci.* **2002,** *167*, (5), 303-314.

(97)Arai, Y.; Sparks, D. L.; Davis, J. A., Arsenate adsorption mechanisms at the allophane - water interface. *Environ. Sci. Technol.* **2005,** *39*, (8), 2537-2544.

(98)Manning, B. A.; Fendorf, S. E.; Goldberg, S., Surface structures and stability of arsenic(III) on goethite: Spectroscopic evidence for inner-sphere complexes. *Environ. Sci. Technol.* **1998,** *32*, (16), 2383-2388.

(99)Grafe, M.; Tappero, R. V.; Marcus, M. A.; Sparks, D. L., Arsenic speciation in multiple metal environments - II. Micro-spectroscopic investigation of a CCA contaminated soil. *J. Colloid Interface Sci.* **2008,** *321*, (1), 1-20.

(100)Arai, Y.; Lanzirotti, A.; Sutton, S.; Davis, J. A.; Sparks, D. L., Arsenic speciation and reactivity in poultry litter. *Environ. Sci. Technol.* **2003,** *37*, (18), 4083-4090.

(101)Arai, Y.; Lanzirotti, A.; Sutton, S. R.; Newville, M.; Dyer, J.; Sparks, D. L., Spatial and temporal variability of arsenic solid-state speciation in historically lead arsenate contaminated soils. *Environ. Sci. Technol.* **2006,** *40*, (3), 673-679.

(102)Manning, B., Arsenic speciation in As(III)- and As(V)-treated soil using XANES spectroscopy. *Microchimica Acta* **2005,** *151*, (3-4), 181-188.

(103)Paktunc, D.; Foster, A.; Laflamme, G., Speciation and characterization of arsenic in Ketza River mine tailings using x-ray absorption spectroscopy. *Environ. Sci. Technol.* **2003,** *37*, (10), 2067-2074.

(104)Voegelin, A.; Weber, F. A.; Kretzschmar, R., Distribution and speciation of arsenic around roots in a contaminated riparian floodplain soil: Micro-XRF element mapping and EXAFS spectroscopy. *Geochim. Cosmochim. Acta* **2007,** *71*, 5804-5820.

(105)Yang, L.; Donahoe, R. J., The form, distribution and mobility of arsenic in soils contaminated by arsenic trioxide, at sites in southeast USA. *Appl. Geochem.* **2007,** *22*, (2), 320-341.

(106)Jain, A.; Loeppert, R. H., Effect of competing anions on the adsorption of arsenate and arsenite by ferrihydrite. *J. Environ. Qual.* **2000,** *29*, (5), 1422-1430.

(107)Manning, B. A.; Goldberg, S., Modeling competitive adsorption of arsenate with phosphate and molybdate on oxide minerals. *Soil Sci. Soc. Am. J.* **1996,** *60*, (1), 121-131.

(108)Catalano, J. G.; Park, C.; Fenter, P.; Zhang, Z., Simultaneous inner- and outer-sphere arsenate adsorption on corundum and hematite. *Geochim. Cosmochim. Acta* **2008,** *72*, (8), 1986-2004.

(109)Fukushi, K.; Sverjensky, D. A., A predictive model (ETLM) for arsenate adsorption and surface speciation on oxides consistent with spectroscopic and theoretical molecular evidence. *Geochim. Cosmochim. Acta* **2007,** *71*, (15), 3717-3745.

(110)Goldberg, S.; Johnston, C. T., Mechanisms of arsenic adsorption on amorphous oxides evaluated using macroscopic measurements, vibrational spectroscopy, and surface complexation modeling. *J. Colloid Interface Sci.* **2001,** *234*, (1), 204-216.

(111)Kubicki, J. D., Comparison of As(III) and As(V) Complexation onto Al- and Fe-Hydroxides. *ACS SYMPOSIUM SERIES* **2005**, (915), 104-117.

(112)Ladeira, A. C. Q.; Ciminelli, V. S. T., Adsorption and desorption of arsenic on an oxisol and its constituents. *Water Res.* **2004,** *38*, (8), 2087-2094.

(113)Violante, A.; Ricciardella, M.; Del Gaudio, S.; Pigna, M., Coprecipitation of arsenate with metal oxides: Nature, mineralogy, and reactivity of aluminum precipitates. *Environ. Sci. Technol.* **2006,** *40*, (16), 4961-4967.

(114)Cox, C. D.; Ghosh, M. M., Surface Complexation of Methylated Arsenates by Hydrous Oxides. *Water Res.* **1994,** *28*, (5), 1181-1188.

(115)Ghosh, M. M.; Yuan, J. R., Adsorption of inorganic arsenic and organoarsenicals on hydrous oxides. *Environ. Prog.* **1987,** *6*, (3), 150-157.

(116)Myneni, S. C. B.; Traina, S. J.; Waychunas, G. A.; Logan, T. J., Vibrational spectroscopy of functional group chemistry and arsenate coordination in ettringite. *Geochim. Cosmochim. Acta* **1998,** *62*, (21-22), 3499-3514.

(117)Pandya, K. I., Multiple-scattering effects in X-ray absorption fine structure: Chromium in a tetrahedral configuration. *Phy. Rev. B* **1994,** *50*, (21), 15509-15515.

(118)Datta, R.; Sarkar, D.; Sharma, S.; Sand, K., Arsenic biogeochemistry and human health risk assessment in organo-arsenical pesticide-applied acidic and alkaline soils: An incubation study. *Sci. Total Environ.* **2006,** *372*, (1), 39-48.

(119)Zhang, J. S.; Stanforth, R. S.; Pehkonen, S. O., Effect of replacing a hydroxyl group with a methyl group on arsenic (V) species adsorption on goethite (alpha-FeOOH). *J. Colloid Interface Sci.* **2007,** *306*, (1), 16-21.

(120)Jing, C. Y.; Meng, X. G.; Liu, S. Q.; Baidas, S.; Patraju, R.; Christodoulatos, C.; Korfiatis, G. P., Surface complexation of organic arsenic on nanocrystalline titanium oxide. *J. Colloid Interface Sci.* **2005,** *290*, (1), 14-21.

(121)Zhang, J. S.; Stanforth, R.; Pehkonen, S. O., Irreversible adsorption of methyl arsenic, arsenate, and phosphate onto goethite in arsenic and phosphate binary systems. *J. Colloid Interface Sci.* **2008,** *317*, (1), 35-43.

(122)Smith, P. G.; Koch, I.; Gordon, R. A.; Mandoli, D. F.; Chapman, B. D.; Reimer, K. J., X-ray absorption near-edge structure analysis of arsenic species for application to biological environmental samples. *Environ. Sci. Technol.* **2005,** *39*, (1), 248-254.

(123)Smith, P. G.; Koch, I.; Reimer, K. J., An investigation of arsenic compounds in fur and feathers using X-ray absorption spectroscopy speciation and imaging. *Sci. Total Environ.* **2008,** *390*, (1), 198-204.

(124)Adamescu, A.; Gray, H.; Stewart, K. M. E.; Hamilton, I. P.; Al-Abadleh, H. A., Trends in the frequencies of nu(AsOxHx-1) [x=2-4] in selected As(V)-containing compounds investigated using quantum chemical calculations. *Can. J. Chem.-Rev. Can. Chim.* **2009,** *88*, (1), 65-77.

(125)Chabot, M.; Hoang, T.; Al-Abadleh, H. A., ATR-FTIR studies on the nature of surface complexes and desorption efficiency of p-arsanilic acid on iron (oxyhydr)oxides. *Environ. Sci. Technol.* **2009,** *43*, (9), 3142-3147.

(126)Depalma, S.; Cowen, S.; Hoang, T.; Al-Abadleh, H. A., Adsorption thermodynamics of p-arsanilic acid on iron (oxyhydr)oxides: In-situ ATR-FTIR studies. *Environ. Sci. Technol.* **2008,** *42*, (6), 1922-1927.

(127)Cowen, S.; Duggal, M.; Hoang, T.; Al-Abadleh, H., Vibrational spectroscopic characterization of some environmentally important organoarsenicals - A guide for understanding the nature of their surface complexes. *Can. J. Chem.* **2008,** *86*, 942-950.

Chapter 2

MOLECULAR SCALE ASSESSMENT OF METHYLARSENIC SORPTION ON ALUMINUM OXIDE

Abstract

Methylated forms of arsenic (As), monomethylarsenate (MMA) and dimethylarsenate (DMA), have historically been used as herbicides and pesticides. Because of their large application to agriculture fields and the toxicity of MMA and DMA, the sorption of methylated As to soil constituents requires investigation. MMA and DMA sorption on amorphous aluminum oxide (AAO) was investigated using both macroscopic batch sorption kinetics and molecular scale Extended X-ray Absorption Fine Structure (EXAFS) and Fourier Transform infrared (FTIR) spectroscopic techniques. Sorption isotherm studies revealed sorption maxima of 0.183, 0.145, and 0.056 mmol As / mmol Al for arsenate (As^V), MMA, and DMA, respectively. In the sorption kinetics studies, 100 % of added As^V was sorbed within 5 min, while 78 % and 15 % of added MMA and DMA were sorbed, respectively. Desorption experiments, using phosphate as a desorbing agent, resulted in 30 % release of absorbed As^V, while 48 % and 62 % of absorbed MMA and DMA, respectively, were released. FTIR and EXAFS studies revealed that MMA and DMA formed mainly bidentate binuclear complexes with AAO. Based on these results, it is proposed that increasing methyl group substitution results in decreased As sorption and increased As desorption on AAO.

Introduction

Arsenic originates in many rocks and minerals throughout the world. The weathering of these rocks and minerals releases As into the environment as inorganic species. The predominant oxidation states for inorganic As species are As^{V} (H_3AsO_4) and arsenite (As^{III}, H_3AsO_3). In addition to inorganic forms, organic forms of As also exist in nature, typically occurring in terrestrial environments as MMA ($CH_3H_2AsO_3$) and DMA ($(CH_3)_2HAsO_2$). MMA and DMA have historically been used as herbicides and pesticides in agriculture [1]. Due to cotton's tolerance to MMA, it was applied particularly to fields in the "cotton belt" of the United States, including Alabama, Arkansas, Texas, Louisiana, and Mississippi, to control weedy grasses[1]. DMA was simultaneously applied as a defoliant. In the 1990's, more than 3000 metric tons per year of MMA and more than 30 metric tons per year of DMA were applied in cotton belt states [2]. Subsequent studies on the surface water from these cotton producing regions have shown elevated levels of methylarsenates [3]. MMA also has been used as a herbicide on golf courses, and it has been linked to elevated As concentrations in ground water in southern Florida [4]. Additionally, MMA has been used as a pesticide to control mountain pine beetle (*Dendroctonus ponderosae*) outbreaks in British Columbia, Canada [5]. Approximately 960 kg of MMA were applied annually, and over 60,000 trees in the Cascades Forest District were treated with MMA between 2000 and 2004 [6-7].

Arsenic has attracted large public interest due to its acute toxicity. Arsenic toxicity and the mode of toxin mechanisms depend on its speciation. Arsenite species, As^{III}, MMA^{III}, and DMA^{III} are generally more toxic than arsenate species, As^{V}, MMA^{V}, or DMA^{V} [8]. MMA and DMA are produced in many animals, including human beings via methylation. During the methylation processes, MMA^{III} and DMA^{III}

are produced as intermediate products and are considered more toxic compounds than As^{V} or As^{III} [8-9]. Although MMA^{V} and DMA^{V} themselves possess lower toxicity than As^{V} or As^{III}, their reduction can produce very toxic MMA^{III} or DMA^{III}.

Aluminum oxides are ubiquitous in the environment and are one of the most important mineral oxides in soil systems. Unlike iron oxides, Al oxides are stable over a range of redox conditions. Under a reduced environment, Al oxides can influence contaminant transport to a larger extent than iron oxides can. Due to their reactivity and high surface area, AAOs have high sorption capacities for a range of environmental contaminants, including MMA^{V} and DMA^{V}. Synthetic analogs for AAOs can be used as a surrogate since natural AAOs are difficult to isolate from natural soils [10]. To date, there has been no extensive investigation on methylarsenate sorption to Al oxides, including AAOs, employing molecular scale techniques. Accordingly, the goal of this study is to characterize MMA^{V} and DMA^{V} sorption to AAO, employing macroscopic and molecular scale techniques.

Materials and Methods

Arsenic compounds

Inorganic arsenate (As^{V}) was purchased from Fisher Scientific as Na_2HAsO_4, MMA was purchased from Chem Service as sodium salt monosodium acid methane-arsonate sesquihydrate ($NaCH_3AsO_3H$), and DMA was purchased from Fisher Scientific as cacodylic acid ($(CH_3)_2AsO_2H$).

Amorphous Aluminum Oxide Synthesis

AAO was synthesized by titrating an aluminum chloride solution with sodium hydroxide [10]. The suspension was centrifuged (15,000 G for 30 min) four

times with Barnstead nanopure water and stored at 4 °C. Aliquot was taken to determine solid concentration (g / L) by drying the suspension in an oven at 100 °C for 48 hr. The AAO suspension was used in experiments within three weeks from the time of synthesis. XRD analysis confirmed that the oxide was amorphous. Nitrogen BET analysis revealed that the average surface area was 140 m^2/g.

Sorption Kinetics

Sorption kinetics experiments were conducted using 0.5 g/L AAO, and 0.5 mM As^V, MMA, or DMA, in 0.01 M $NaNO_3$ at pH 6 with 1 mM MES buffer. The samples were reacted for various time periods (5 min, 15 min, 30 min, 1 h, 2 h, 6 h, 12 h, 24 h, 48 h, and 96 h) by placing them on rotating shakers at 30 RPM. Suspensions were filtered through 0.22 μm pore size filters. The arsenic concentrations were analyzed using inductively coupled plasma atomic emission spectroscopy (ICP-AES).

Sorption Isotherms

Sorption isotherms were determined via batch experiments at pH 5 and pH 7 with various arsenic concentrations, ranging from 50 μM to 1.5 mM. AAO suspensions (0.5 g/L) containing 0.01 M $NaNO_3$ were placed in 50 mL centrifuge tubes and equilibrated at pH 5 or pH 7 for 24 h by using rotating shakers (30 RPM) prior to arsenic addition. 20 mM and 1 mM As^V, MMA, and DMA stock solutions were also prepared at pH 5 and 7. Throughout the experiments, the pH of solutions and samples were adjusted with 0.1 M HNO_3 or 0.1 M NaOH. After the arsenic solution was added, the suspension was equilibrated for 48 hrs by using rotating shakers. The pH was measured and adjusted three times daily to maintain a pH of 5 or 7. The suspensions were centrifuged, and supernatants were sampled using Nylon

syringe filters, passing through 0.22 μm pore size. The arsenic concentrations were analyzed using ICP-AES.

Sorption Edges

Sorption edge experiments were conducted using a method similar to the sorption isotherm study. Briefly, AAO suspensions (0.5 g/L) in 50 mL centrifuge tubes were equilibrated at pH of 5.0, 5.5, 6.0, 6.5, 7.0, 7.5, 8.0, 8.5, 9.0, and 9.5 for 24 h by placing the tubes on rotating shakers (30 RPM) prior to arsenic addition. Arsenic stock solutions were added to AAO suspensions so that the final arsenic concentrations were 0.5 mM. The solutions were equilibrated for 48 h. During this period, the pH was measured and adjusted to maintain the initial AAO solution pH. Test tubes were centrifuged, the supernatants were filtered, and the solution pH was measured. The arsenic concentrations were analyzed using ICP-AES.

Desorption Studies

Desorption studies were conducted by using phosphate as a desorbing agent. At the end of the sorption edge experiments, 30 mL of solution were removed from each tube (10 mL remaining in each tube). An equivalent amount of phosphate (NaH_2PO_4) solution was added to achieve 0.05 M phosphate in each tube. The pH was adjusted and maintained so that the desorption pH was the same as the pH at the end of the sorption edge experiments. After a 48 h reaction period, the solutions were centrifuged, and the supernatants were filtered through 0.22 μm pore size filters. The arsenic concentrations were analyzed by ICP-AES.

Electrophoretic Mobility (EM)

Samples were prepared in a similar manner to those in the sorption kinetics experiment. Briefly, 0.5 g/L AAO suspension was equilibrated by placing on rotating shakers at 30 RPM with or without 0.5 mM MMA and DMA for 48 h at various pHs, ranging from 5 to 9.5. The EM of each sample was measured by using a Zetasizer Nano ZS (Malvern Instruments, Southborough, MA) instrument at 25 °C by placing aliquots of each sample in special sample holders purchased from the manufacturer.

Fourier Transform Infrared Spectroscopy (FTIR) Investigations

FTIR spectra were collected using a Thermo Nicolet Nexus spectrometer equipped with a singe bounce attenuated total reflectance (ATR) accessory with a diamond internal reflection element (SmartOrbit, Thermo) and MCT/A detector. An AAO suspension (25 g/L) was reacted with 0.025 M MMA or DMA for 48 hrs at pH 5 by placing on a rotating shaker at 30 RPM. A background electrolyte solution of 0.01 M NaCl was used instead of $NaNO_3$ to prevent any signal interference arising from NO_3^-. Aliquots of 100 µL each MMA or DMA were deposited on the crystal and 128 spectra were collected at 4 cm^{-1} resolution. Along with the reacted suspension spectra, spectra of 25 g/L AAO suspension without As at pH 5 and 0.1 M MMA and DMA solutions at pH 5 with 0.01 M NaCl background were collected at the same conditions and analyzed. Water, NaCl, and AAO background spectra are subtracted by using the OMNIC program Version 7.2. Aqueous phases of MMA and DMA were also subtracted from the spectra to account for unsorbed/solution phases.

X-Ray Absorption Spectroscopy (XAS) Investigations

All XAS samples were prepared using similar experimental methods as those for the sorption edge experiments with an initial arsenic concentration of 0.1 mM at pH 5 for all samples. After 48 hr of reaction, samples were centrifuged and washed with 0.01 M $NaNO_3$ three times to remove excess As compounds. After the third centrifugation, the wet paste was kept moist by sealing the tubes and saving them for analysis. Arsenic K-edge (11,867 eV) XAS spectra were collected at X11A beamline at the National Synchrotron Light Source (NSLS) at Brookhaven National Laboratory. Three spectra per sample were collected, and the SIXPack/IFEFFIT program package was used to analyze the data [11]. The inflection point of all studied samples did not change between the first and last scan. First, three spectra per sample were averaged. The averaged spectra were normalized with respect to E_0, and then the Autobk value was set at the half distance to neighboring atoms. Next, the data were converted from E space to κ space and weighted by κ^3 to compensate for dampening of the XAFS amplitude with increasing κ space. Fourier transformation was then performed over the k-space range from 3 to 12.5 $Å^{-1}$ to obtain the radial distribution functions (RDF). Final fitting of the spectra was conducted on Fourier transformed κ^3 weighted spectra in R space. The WebAtoms and FEFF7 code were utilized to calculate single scattering theoretical spectra for As–O and As–Al backscatters using an input file based on the structural refinement of mansfieldite ($AlAsO_4 \cdot 2H_2O$) minerals. During the fitting process, the coordination numbers for MMA and DMA, As-O and As-C, were fixed to reduce adjustable parameters. The molecular configurations of MMA and DMA sorbed to AAO based on XAS data analysis were created by using GaussView [12].

Results and Discussion

Sorption Kinetics Studies

Sorption kinetics experiments for As^V, MMA and DMA on AAO revealed biphasic sorption characteristics; fast initial sorption was followed by slow continuous sorption (Fig. 2.1a). As^V and MMA sorption were nearly complete by the end of the 96 h experimental periods, but DMA sorption was not. As^V sorption reached a maximum before the first sample was collected (5 min). The data showed that the MMA sorption rate was slightly lower than the As^V sorption rate. 78 % of added MMA was sorbed within the first 5 minutes, and rapid MMA sorption continued for 6 h at which time 92 % of the initially added MMA was sorbed. MMA sorption reached pseudo-equilibrium in 24 h. In contrast to As^V and MMA, only 15 % of the added DMA was sorbed in 5 min. Rapid DMA sorption occurred during the first 6 h, and 34 % of the initially added DMA was sorbed. DMA sorption reached pseudo-equilibrium in 48 h, but only 45 % of the added DMA was sorbed at the end of 96 h.

As^V, MMA, and DMA's molecular structural variations can explain the differences in sorption kinetics. The kinetics data showed As^V, with no methyl group substitution, had the highest sorption rate, while DMA, with two substituted methyl groups, had the lowest sorption rate. Increasing the methyl group substitution results in fewer hydroxyl groups being available for deprotonation and surface complex formation. Based on their pK_a values (Table 1.1) and the number of deprotonation sites, As^V has the largest quantity of negatively charged species, and DMA has the smallest quantity of negatively charged species at pH 5. Electrostatic attraction between positively charged AAO (Fig. 2.3) and negatively charged As species is the highest for As^V and the lowest for DMA. In addition, if MMA and DMA form outer-

sphere complexes similar to As^V, the electrostatic attraction can affect the complex formation and therefore impact the rate of sorption [13-14]. In the case of inner-sphere complex formation via sharing of oxygen, As^V can have six possible edge site, MMA can have only three possible edge sites, and DMA can have only one edge site to form bidentate binuclear complexes with AAO. In the case of monodentate mononuclear complex formation, As^V can have four possible sites, MMA can have three possible sites, and DMA can have two possible sites. Less reactive sites can result in a lower probability of forming any surface complexes and increased time for aligning to a favorable molecular orientation, which could decreases the rate of sorption on MMA and DMA.

Sorption Isotherm Studies

Sorption isotherms for As^V, MMA, and DMA showed increasing As sorption at decreasing As sorption rates as the initial As^V, MMA, and DMA concentration increased from 0.01 to 1 mM (Fig. 2.1b). As^V, MMA, and DMA sorption were higher at pH 5 than at pH 7. Similar trends were observed for ferrihydrite [15]. MMA sorption at pH 5 was as high as As^V sorption at the initial MMA concentrations below 0.75 mM. As the initial MMA concentration increased above 0.75 mM, a smaller percentage of the added MMA was sorbed to AAO compared to As^V sorption. At pH 7, almost 100 % of the added MMA was sorbed to AAO at the initial MMA concentrations below 0.5 mM, and above this concentration a smaller percentage of the added MMA was sorbed. DMA sorption was much less than As^V and MMA sorption to AAO. At pH 5, DMA sorption reached approximately 85 % of the initial DMA concentration (0.05 mM), and this sorption ratio decreased to 36 % at the initial DMA concentration of 1 mM. At pH 7, approximately 40 % of the

initial DMA concentration (0.05 mM) was sorbed, and this sorption ratio decreased to approximately 20 % at the initial DMA concentration of 1mM. Compared to the MMA and DMA sorption isotherm study on ferrihydrite, sorption maxima values (Table 2.2) for MMA and DMA are comparable between AAO and ferrihydrite.

MMA and DMA sorption was higher at pH 5 than at pH7 because the AAO surface was more positively charged at pH 5 than at pH 7 (Fig. 2.3), resulting in stronger electrostatic attraction at pH 5 than pH7. In addition, the charge differences between As species also influenced the higher sorption of As^V and lower sorption of DMA due to the larger quantity of negatively charged As^V and the smaller quantity of negatively charged DMA at any pH.

The differences in molecular structures also affected the sorption maximum. A methyl group substituted to an As atom makes the MMA molecule larger than As^V. For example, the average As-O distance is approximately 1.7 Å, and the average As-C distance is approximately 1.9 Å [16-17]. In addition, three hydrogen atoms are attached to the C atom with a typical H covalent bond distance of approximately 1 Å. This makes the As-O-H linear distance approximately 2.7 Å, and the As-C-H linear distance approximately 2.9 Å. The methyl groups also do not form hydrogen bonding within or with other molecules, while hydroxyl groups do. As a result, the number of MMA molecules that can cover and sorb to the AAO surface becomes smaller than for As^V. DMA has an additional methyl group and a total of two methyl groups substituted for the As atom. The DMA molecule size is much larger than As^V. It is also possible that the second methyl group substitution magnified the factors discussed above.

pH Sorption Edge Studies

The general trend in pH sorption edges showed higher sorption at lower pH, and as the reaction pH increased, the sorption decreased (Fig. 2.2a) similar to MMA and DMA sorption on ferrihydrite [15]. MMA sorption was almost 100% at a pH value below 6.5. Sorption gradually decreased as pH increased above pH 6.5. At pH 9.5, approximately 20 % of MMA was sorbed to AAO. MMA sorption was lower than As^V sorption above pH 6.5. DMA sorption behavior showed a parabolic sorption curve and was different from As^V and MMA with less DMA sorbed to AAO. DMA sorption increased from pH 5 to 5.5 where the maximum sorption occurred. Above pH 5.5, DMA sorption decreased as pH increased. At pH 5.5, approximately 60 % of DMA was sorbed to AAO. Above pH 8, only a small percentage of DMA was sorbed to AAO.

AAO has a point of zero charge at pH ≈ 9 (Fig. 2.3). Below this pH, electrostatic attraction enhanced sorption. As pH increased, the AAO surface became less positive. Decreases in electrostatic attraction diminished As^V, MMA, and DMA sorption, and less sorption at high pH was attributed to increasing repulsive potentials between the negatively charged As species and the negatively charged AAO surfaces [15]. The charge differences between As species also influenced the higher sorption of As^V and lower sorption of DMA. Electrostatic attraction also helps to explain the pH where maximum DMA sorption occurred. Typically, sorption maxima are observed at pH values near the pK_a values for oxyanions; however, the sorption maximum for DMA on AAO was observed at pH 5.5, which is lower than its pK_a of 6.14 [18]. The shift in sorption maximum pH is attributed to the AAO surface charge. At lower pH, the AAO surface is more positively charged (Figure S2) and can enhance electrostatic attraction between AAO and DMA. Similar trends were observed for DMA sorption

on goethite (sorption maximum at pH below 6) and As^{III} sorption on γ-aluminum oxide (sorption maximum at pH below $pK_a = 9.22$) [15-16].

Desorption Studies

Complete MMA and DMA desorption by phosphate was not observed over the pH ranges examined (Fig. 2.2b). The desorption ratio was calculated as desorbed As to sorbed As (desorbed As / sorbed As) %. As^V, MMA, and DMA desorption envelopes showed a similar trend. Arsenic desorption increased as pH increased until a particular pH, and further pH increases resulted in decreased desorption. As^V desorption increased as pH increased until pH 9. At pH 5 and 9, 31% and 70% of sorbed As^V was desorbed, respectively. Above pH 9, As^V desorption decreased as pH increased. MMA desorption increased until pH 8.5, and as pH increased above pH 8.5, desorption decreased. At pH 5, 47 % of sorbed MMA was desorbed, and the ratio increased up to 80% at pH 8.5. DMA desorption increased from pH 5 to 7 and decreased above pH 7. At pH 5 and 7, 61 % and 78 % of sorbed DMA were desorbed, respectively. Desorption decreased to 32 % at pH 9.5. Compared to the desorption study on ferrihydrite, the trend in desorption is similar with DMA desorbing the most and As^V the least [15].

The increases in desorption at lower pH indicated that sorption occurred partially via electrostatic attraction. As pH increased, the AAO surface became less positive, weakening the attraction, resulting in phosphate being able to replace sorbed As. The desorption decreased at higher pH because less As^V, MMA, and DMA were sorbed initially and less As was desorbed by phosphate due to its strong affinity to AAO. Similar to As^V desorption from γ-aluminum oxide, a portion of MMA and DMA sorption was irreversible [19]. The binding of MMA, DMA, and As^V to AAO is

fairly strong, as evidenced by the inability of phosphate to desorb the As species. This suggests that MMA, DMA, and As^V form similar surface complexes with AAO, such as inner-sphere complexes, since the inner-sphere complex formation leads to irreversible sorption [18].

FTIR Investigations

At pH 5, the dominant form of MMA ($pK_{a1} = 4.19$) is $CH_3AsO_2OH^{-1}$ and DMA ($pK_a = 6.14$) is $(CH_3)_2AsOOH$. The MMA aqueous solution spectrum had peaks at 877 cm^{-1} and 709 cm^{-1}, corresponding to $\nu_s(AsO_2)$ and ν(As-OH), respectively (Fig. 2.4a) [20-22]. Peaks from a methyl group, such as those observed in the DMA FTIR spectra, were not observed in the MMA spectra. This is likely due to the weak peak signal from a single methyl group being overshadowed by the intense $\nu_s(AsO_2)$ peak [22]. When MMA was sorbed to AAO, the peak at 877 cm^{-1} shifted down to 833 cm^{-1}, and the peak at 709 cm^{-1} disappeared. This could be due to an apparent increase in molecular symmetry upon the sorption or to the peak shifting to a lower wave number (< 650 cm^{-1}) below the wave number limit for the MCT/A detector. Due to decreased signal sensitivity, the DTGS detector was unable to provide good quality data for examination of lower wave numbers. The DMA aqueous spectrum contained two shoulders at 914 and 895 cm^{-1} and three peaks at 880, 833, and 729 cm^{-1} (Fig. 2.4b). These shoulders and peaks were assigned as $\rho(CH_3)$, $\rho(CH_3)$, ν(As-O), $\nu(As\text{-}O_2^-)$, and ν(As-OH), respectively [21-23]. When DMA was sorbed to AAO, the peak at 880 cm^{-1} shifted down to 830 cm^{-1} (overlapping the previous peak at 833 cm^{-1}), the peak at 729 cm^{-1} disappeared, and the shoulder at 914 cm^{-1} did not shift. This also could be due to an apparent increase in molecular symmetry upon the sorption or to the peak shifting to a lower wave number (< 650 cm^{-1}).

The observed peak shifts were likely caused by inner-sphere complex formation and changes in the vibrational freedom of MMA and DMA upon sorption to AAO. During this process, one or two of the As-O(H) groups from MMA or DMA may go through ligand exchange reactions with OH groups from the AAO surface, forming inner-sphere complexes. As^V sorption to ferrihydrite and AAO showed similar As-O peak shifts to lower wave numbers [24]. Similarly, As^V has been shown to form inner-sphere complexes with iron and aluminum oxides [16, 24-25]. During As^V sorption on AAO, the As-O peak (945 cm^{-1}) downshifts to 862 cm^{-1} as a result of inner-sphere complex formation at the mineral surface [24]. MMA's and DMA's As-O peak shifts were similar to the As^V peak shift, which suggested that MMA and DMA also formed inner-sphere complexes with AAO. In addition, the shoulder peak at 914 cm^{-1}, representing the methyl groups of DMA, did not shift upon the addition of AAO to the solution, indicating that the methyl groups were not involved in DMA-AAO surface complex formation.

XAS Investigations

Based on the fit for MMA sorption on AAO, the As-O bond distance was calculated to be 1.69 Å, while the As-C bond distance was 1.89 Å, and 2.1 aluminum atoms were located at an As-Al interatomic distance of 3.15 Å (Table 2.1). As-O and As-C bond distances from this study agreed with other experimental studies and XAS investigations [21, 26]. The coordination number and As-Al distances were indicative of a MMA-AAO bidentate binuclear complex (Fig. 2.5c) [16, 27-28]. Based on the coordination number and bond distance (Table 2.1), DMA also formed a bidentate binuclear complex with AAO (Fig. 2.5c). It should be mentioned that it is possible that MMA and DMA also form outer-sphere complexes with AAO, similar to As^V sorption

on aluminum and iron oxides; however, XAS and FTIR techniques used in this study cannot verify outer-sphere complex formation [13].

Our results showed that MMA and DMA formed bidentate binuclear complex on AAO, similar to As^V [16, 27-28]. This result partially agrees with another MMA and DMA XAS study where MMA formed a bidentate binuclear complex and DMA formed a monodentate mononuclear complex on nanocrystalline titanium oxide (TiO_2) [26]. One possible explanation for DMA bidentate binuclear complexation with AAO could be the surface charge differences between AAO and TiO_2. TiO_2 had a PZC of pH 5.8, and the XAS sample pH in the study of Jing et al. (2005) was 5, while in this study AAO had a PZC of pH 9 and the reaction pH was 5. At pH 5, the TiO_2 surface is more neutrally charged, and the AAO surface is more positively charged. There are many protonated $Al\text{-}OH_2^+$ functional groups on the AAO surface. The O atom in the $Al\text{-}OH_2^+$ group shares electrons with the second proton, and the electron density of the O atom is shifted toward protons. Because the O atom has high electron negativity, it tends to pull the electron density between Al and O closer to the O atom to fulfill its charge. This makes the Al atoms in $Al\text{-}OH_2^+$ more positively charged overall, compared to Al-OH. In addition, $Al\text{-}OH_2^+$ has a higher water exchange rate than a neutral Al-OH surface. As a result, $Al\text{-}OH_2^+$ functional groups can have a higher potential to trigger ligand exchange reactions with As-O or As-OH from the DMA to form a bidentate binuclear complex.

However, these observations do not explain differences in the sorption/desorption characteristics between As^V, MMA, and DMA. One can assume that if all three species formed the same type of surface complex, the sorption/desorption capacity would be similar, but this was not the case in this study.

This discrepancy seems to arise from differences in molecular structure, rather than different types of surface complex formation. As discussed earlier, more methyl groups attached to the As atom can lead to less affinity of the As species for the AAO surface. Another reason for the lower sorption affinity of DMA on the AAO surface is that the formation of bidentate binuclear complexes may put stress on the geometry of DMA. Such steric hindrances can make this type of surface complex formation more unstable.

In the DMA molecule, two oxygen atoms are attached to an As atom (Fig S1). One of the oxygen atoms forms a π bond with the As atom, As=O, and another oxygen atom is within a hydroxyl (OH) group bound to As, As-OH. The formation of a bidentate binuclear complex between DMA and the AAO surface requires that both As=O and As-OH bonds are involved in the complexation. The As=O bond becomes an As^{+}-O^{-} bond and another oxygen atom from the As-OH forms a complex with an Al atom on the oxide surface. Based on the XANES spectrum of DMA sorbed on AAO, the oxidation state of the As remains pentavalent (Fig. 2.6), and the inflection points of free DMA and sorbed DMA are consistent with other studies [26, 29]. To maintain the oxidation state, additional negative charge has to be supplied to the As atom. Methyl groups may provide a small amount of additional negative charge by being closer to the As atom. However, due to the size and the protons attached to the C atoms, two methyl groups are unlikely to move closer to the As atom to satisfy all the missing charge. Instead, O atoms, forming a bidentate binuclear complex, may move closer to the As atom to fulfill the remaining charge imbalance. This can make the Al-O complexation weaker than a typical bidentate binuclear complex and result in large DMA desorption when the complex is replenished by phosphate.

Environmental Significance

MMA and DMA are generally minor components of total As in the environment but can sometimes reach 10-50 % of total As [3, 30-31]. A better understanding of MMA and DMA sorption on AAO, an important soil component analog, is critical to predict the fate of these chemicals in the environment. Our study revealed that MMA and DMA sorption on AAO showed similar trends to As^{V} sorption on AAO with slightly lower MMA sorption and much lower DMA sorption than As^{V} sorption. FTIR and XAS studies revealed that MMA and DMA formed bidentate binuclear complexes, similarly to As^{V} sorption on aluminum oxides. These findings suggest that the more mobile MMA and DMA can easily percolate to ground water or be taken up by plants compared to As^{V}. More mobile, and therefore more bioavailable, MMA and DMA can be demethylated to As^{V} or As^{III}. Accordingly, MMA and DMA sorption can play an important role in total arsenic cycling in the environment. MMA and DMA sorption mechanisms, along with sorption envelope results, are also useful for establishing important parameters for surface complexation model development.

REFERENCES

(1)Dickens, R.; Hiltbold, A. E., Movement and persistence of methanearsonates in soil. *Weeds* **1967,** *15*, (4), 299-304.

(2)Perkins, H. H.; Brushwood, D. E., Effects of mechanical processing and wet treatments on arsenic acid desiccant residues in cotton. *Text. Chem. Color.* **1991,** *23*, (2), 26-28.

(3)Bednar, A. J.; Garbarino, J. R.; Ranville, J. F.; Wildeman, T. R., Presence of organoarsenicals used in cotton production in agricultural water and soil of the southern United States. *J. Agric. Food Chem.* **2002,** *50*, (25), 7340-7344.

(4)Feng, M.; Schrlau, J. E.; Snyder, R.; Snyder, G. H.; Chen, M.; Cisar, J. L.; Cai, Y., Arsenic transport and transformation associated with MSMA application on a golf course green. *J. Agric. Food Chem.* **2005,** *53*, (9), 3556-3562.

(5)Albert, C. A.; Williams, T. D.; Morrissey, C. A.; Lai, V. W. M.; Cullen, W. R.; Elliott, J. E., Dose-dependent uptake, elimination, and toxicity of monosodium methanearsonate in adult zebra finches (*Taeniopygia guttata*). *Environ. Toxicol. Chem.* **2008,** *27*, (3), 605-611.

(6)Morrissey, C.; Elliot, J. E.; Dods, P.; A., A. C.; Wilson, L.; Lai, V.; Cullen, W. R. *Assessing forest bird exposure and effects from monosodium methanearsonate (MSMA) during the mountain pine beetle epidemic in British Columbia.*; Pacific and Yukon Region, Delta, BC. Canada: 2006.

(7)Dost, F. *Public health and environmental impacts of monosodium methanearsonate as used in bark beetle control in British Columbia*; FS 48 HIS 95/2 Ministry of Forests, Victroria, BC, Canada: 1995.

(8)Styblo, M.; Del Razo, L. M.; Vega, L.; Germolec, D. R.; LeCluyse, E. L.; Hamilton, G. A.; Reed, W.; Wang, C.; Cullen, W. R.; Thomas, D. J., Comparative toxicity of trivalent and pentavalent inorganic and methylated arsenicals in rat and human cells. *Arch. Toxicol.* **2000,** *74*, (6), 289-299.

(9)Petrick, J. S.; Ayala-Fierro, F.; Cullen, W. R.; Carter, D. E.; Aposhian, H. V., Monomethylarsonous acid (MMA(III)) is more toxic than arsenite in Chang human hepatocytes. *Toxicol. Appl. Pharmacol.* **2000,** *163*, (2), 203-207.

(10)Goldberg, S.; Lebron, I.; Suarez, D. L.; Hinedi, Z. R., Surface characterization of amorphous aluminum oxides. *Soil Sci. Soc. Am. J.* **2001,** *65*, (1), 78-86.

(11)Webb, S. M., SIXpack: a graphical user interface for XAS analysis using IFEFFIT. *Phy. Scr.* **2005,** *T115*, 1011-1014.

(12)Dennington II, R.; Keith, T.; Millam, J.; Eppinnett, K.; Hovell, W. L.; Gilliland, R., GaussView, Version 3.09. *Semichem, Inc., Shawnee Mission, KS* **2003**.

(13)Catalano, J. G.; Park, C.; Fenter, P.; Zhang, Z., Simultaneous inner- and outer-sphere arsenate adsorption on corundum and hematite. *Geochim. Cosmochim. Acta* **2008,** *72*, (8), 1986-2004.

(14)Sposito, G., The operational definition of the zero-point of charge in soils. *Soil Sci. Soc. Am. J.* **1981,** *45*, (2), 292-297.

(15)Lafferty, B. J.; Loeppert, R. H., Methyl arsenic adsorption and desorption behavior on iron oxides. *Environ. Sci. Technol.* **2005,** *39*, (7), 2120-2127.

(16)Arai, Y.; Elzinga, E. J.; Sparks, D. L., X-ray absorption spectroscopic investigation of arsenite and arsenate adsorption at the aluminum oxide-water interface. *J. Colloid Interface Sci.* **2001,** *235*, (1), 80-88.

(17)Trotter, J.; Zobel, T., Stereochemistry of arsenic .16. Cacodylic acid. *J. Chem. Soc.* **1965**, (AUG), 4466-4471.

(18)Sparks, D. L., *Environmental Soil Chemistry*. 2nd ed.; Academic Press: Boston, 2002.

(19)Arai, Y.; Sparks, D. L., Residence time effects on arsenate surface speciation at the aluminum oxide-water interface. *Soil Sci.* **2002,** *167*, (5), 303-314.

(20)Vansant, F. K.; Vanderveken, B. J.; Herman, M. A., Vibrational analysis of methylarsonic acid, trideuteromethylarsonic acid and their anions. *J. Mol. Struct.* **1976,** *35*, (2), 191-200.

(21)Grundler, H. V.; Schumann, H. D.; Steger, E., Raman and infrared spectroscopic investigation of alkyl derivatives of arsenic acid .6. AsO bond - calculation of force constants and vibrational energy-distribution in compounds of type $RAsO_3X_2$ and R_2AsO_2X. *J. Mol. Struct.* **1974,** *21*, (1), 149-157.

(22)Cowen, S.; Duggal, M.; Hoang, T.; Al-Abadleh, H., Vibrational spectroscopic characterization of some environmentally important organoarsenicals - A guide for understanding the nature of their surface complexes. *Can. J. Chem.* **2008,** *86*, 942-950.

(23)Vansant, F. K.; Vanderve.Bj; Herman, M. A., Vibrational analysis of dimethylarsinic acid. *Spectrochim. Acta, Part A* **1974,** *A 30*, (1), 69-78.

(24)Goldberg, S.; Johnston, C. T., Mechanisms of arsenic adsorption on amorphous oxides evaluated using macroscopic measurements, vibrational spectroscopy, and surface complexation modeling. *J. Colloid Interface Sci.* **2001,** *234*, (1), 204-216.

(25)Waychunas, G. A.; Rea, B. A.; Fuller, C. C.; Davis, J. A., Surface-chemistry of ferrihydrite: Part 1. EXAFS studies of the geometry of coprecipitated and adsorbed arsenate. *Geochim. Cosmochim. Acta* **1993,** *57*, (10), 2251-2269.

(26)Jing, C. Y.; Meng, X. G.; Liu, S. Q.; Baidas, S.; Patraju, R.; Christodoulatos, C.; Korfiatis, G. P., Surface complexation of organic arsenic on nanocrystalline titanium oxide. *J. Colloid Interface Sci.* **2005,** *290*, (1), 14-21.

(27)Ladeira, A. C. Q.; Ciminelli, V. S. T.; Duarte, H. A.; Alves, M. C. M.; Ramos, A. Y., Mechanism of anion retention from EXAFS and density functional calculations: Arsenic (V) adsorbed on gibbsite. *Geochim. Cosmochim. Acta* **2001,** *65*, (8), 1211-1217.

(28)Beaulieu, B. T.; Savage, K. S., Arsenate adsorption structures on aluminum oxide and phyllosilicate mineral sufaces in smelter-impacted soils. *Environ. Sci. Technol.* **2005,** *39*, (10), 3571-3579.

(29)Smith, P. G.; Koch, I.; Gordon, R. A.; Mandoli, D. F.; Chapman, B. D.; Reimer, K. J., X-ray absorption near-edge structure analysis of arsenic species for application to biological environmental samples. *Environ. Sci. Technol.* **2005,** *39*, (1), 248-254.

(30)Braman, R. S.; Foreback, C. C., Methylated forms of arsenic in environment. *Science* **1973,** *182*, (4118), 1247-1249.

(31)Marin, A. R.; Pezeshki, S. R.; Masschelen, P. H.; Choi, H. S., Effect of dimethylarsenic acid (DMAA) on growth, tissue arsenic, and photosynthesis of rice plants. *J. Plant Nutr.* **1993,** *16*, (5), 865-880.

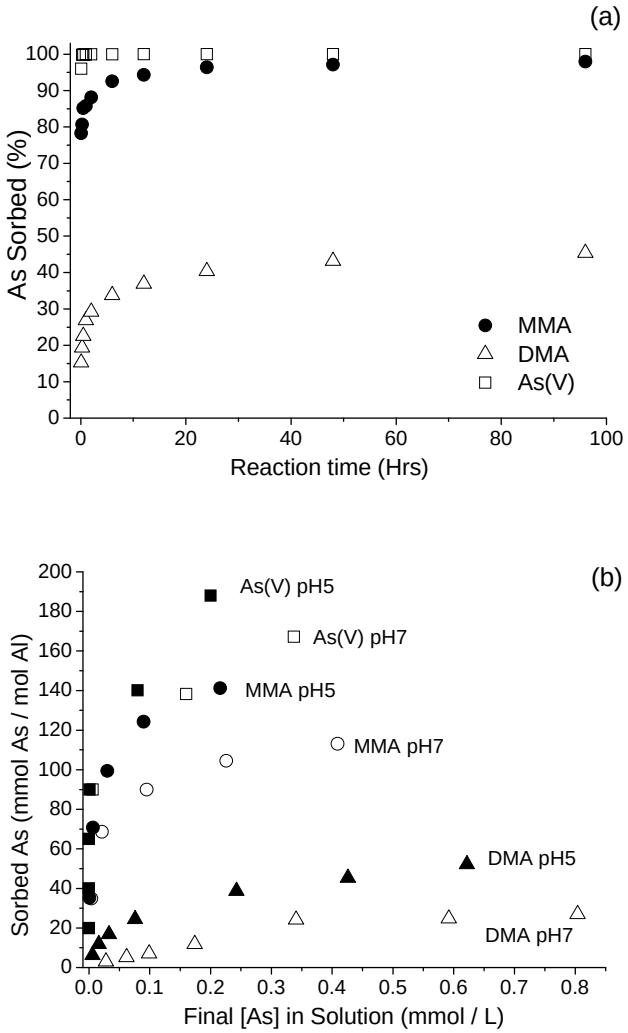

Figure 2.1 MMA, DMA and As(V) sorption kinetics (a) and isotherms (b) on AAO.

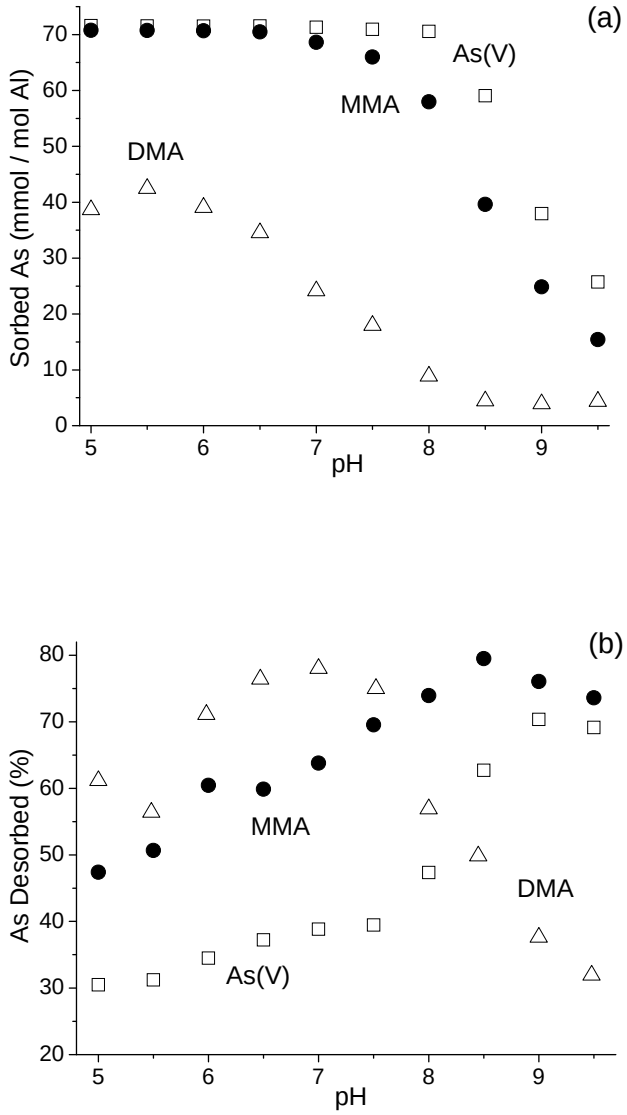

Figure 2.2 MMA, DMA, and As(V) sorption edges on AAO (a) and desorption from AAO (b).

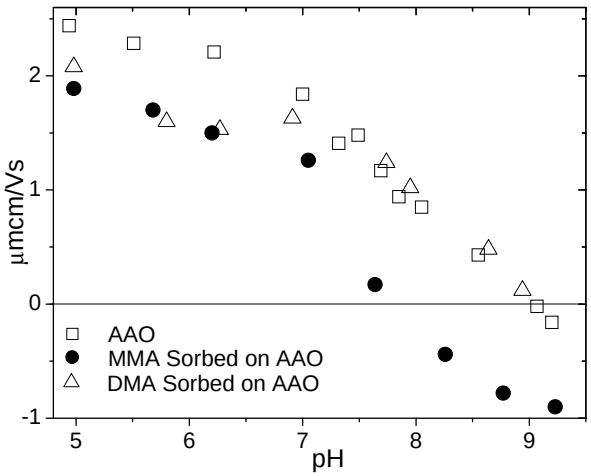

Figure 2.3 Electrophoretic mobility measurement for AAO with or without sorbed MMA and DMA.

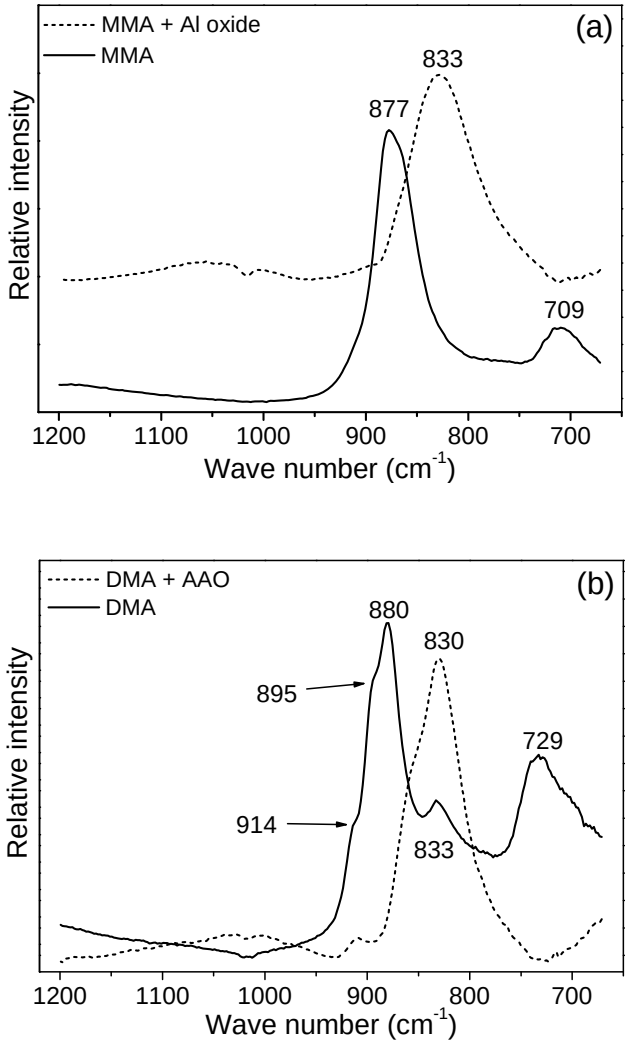

Figure 2.4 FTIR spectra for MMA and MMA sorbed on AAO (a) and DMA and DMA sorbed on AAO (b).

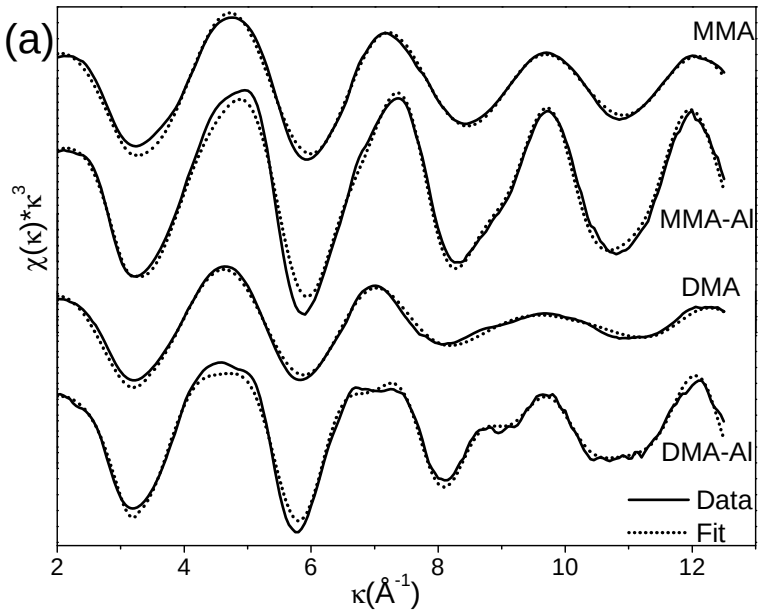
(a)
MMA
MMA-Al
DMA
DMA-Al
Data
Fit
χ(κ)*κ^3
2
4
6
8
10
12
κ(Å^-1)

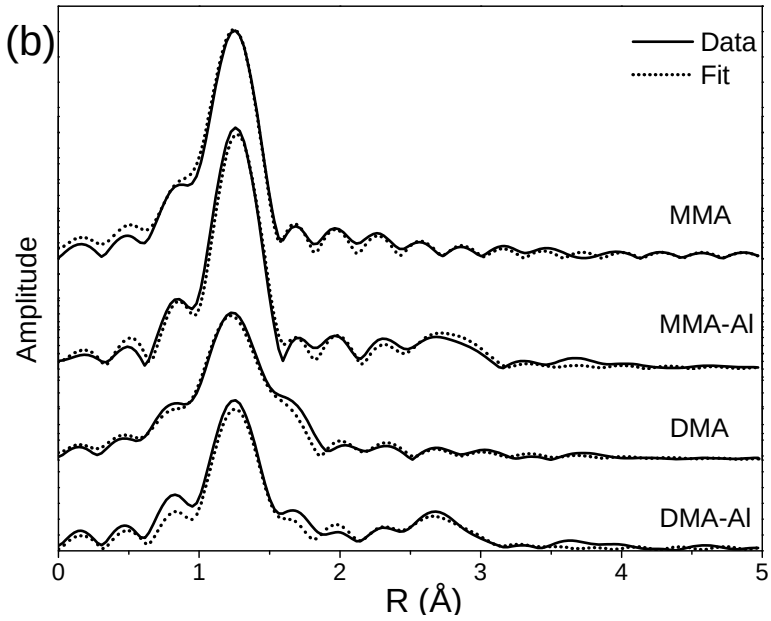
(b)
Data
Fit
MMA
MMA-Al
DMA
DMA-Al
Amplitude
0
1
2
3
4
5
R (Å)

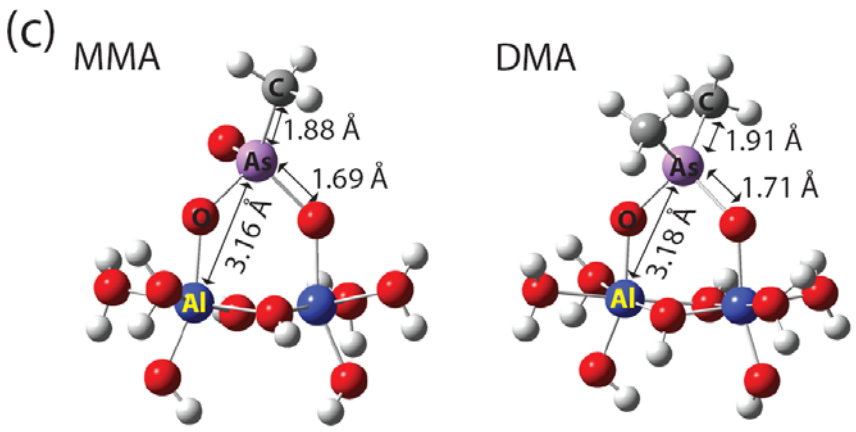

Figure 2.5 MMA and DMA XAS spectra in (a) κ space, (b) Fourier transformation of XAS spectra, and molecular configurations of MMA and DMA sorbed on AAO cluster (c).

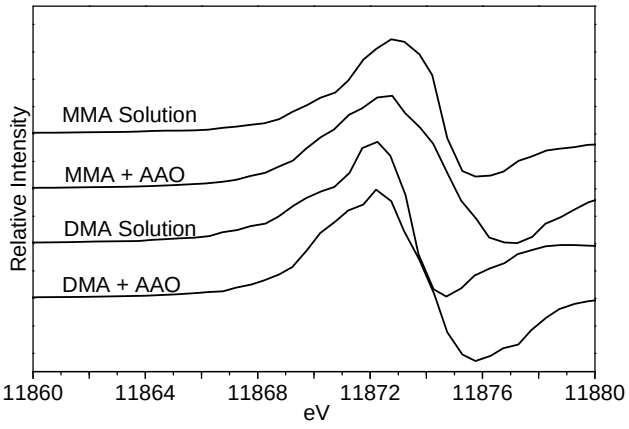

Figure 2.6 The first derivative of normalized MMA and DMA XANES spectra.

Table 2.1 Structural parameters for XAS analysis of MMA and DMA solutions and MMA and DMA sorbed on AAO.

		MMA	MMA-Al	DMA	DMA-Al	As^V-Al [g]
	CN [a] (Fixed)	3	3	2	2	
As-O	R [b] (Å)	1.69 ± 0.004 [f]	1.69 ± 0.007	1.69 ± 0.008	1.70 ± 0.01	
	Σ^2 [c] ($Å^2$)	0.0027 ± 0.0003	0.0012 ± 0.0006	0.0026 ± 0.0005	0.0011 ± 0.0004	
	CN (Fixed)	1	1	2	2	
As-C	R (Å)	1.88 ± 0.09	1.89 ± 0.008	1.90 ± 0.011	1.90 ± 0.01	
	Σ^2 ($Å^2$)	0.0015 ± 0.0008	0.0009 ± 0.0025	0.0014 ± 0.0008	0.0013 ± 0.0007	
	CN		2.1 ± 0.94		2.4 ± 0.6	1.3-2.2
As-Al	R (Å)		3.16 ± 0.022		3.17 ± 0.01	3.11-3.19
	Σ^2 ($Å^2$)		0.0058 ± 0.0017		0.0056 ± 0.0015	0.0009-0.007
	E_0 [d] (eV)	4.88 ± 0.82	4.43 ± 0.93	6.15 ± 1.57	4.70 ± 1.11	
	S_0^2 [e] (Fixed)	0.98	0.98	0.98	0.98	

[a] Coordination number. [b] Interatomic distance. [c] Debye-Waller factor. [d] Energy shift. [e] Amplitude reduction factor. [f] Standard deviation. [g] Selected references of As^V sorbed on aluminum oxides analyzed by EXAFS [16, 27-28].

Table 2.2 Parameters from Langmuir equation for As species sorbed on AAO and ferrihydrite [15].

		AAO				Ferrihydrite		
As Species	pH	B	K_L	r^2	pH	b	K_L	r^2
As^V	5	0.1832	295	0.9834	4	0.1548	10800	0.9999
	7	0.1636	223	0.9917	7	0.1045	372	0.9959
MMA	5	0.1450	109	0.9968	4	0.1738	619	0.9979
	7	0.1163	57	0.9974	7	0.0943	312	0.9968
DMA	5	0.0561	13	0.9881	4	0.0752	144	0.9960
	7	0.0416	2.5	0.9342	7	0.0467	37.5	0.9850

b = sorption maxima (mmol As / mmol Al). K_L = binding constant (L / mmol As).

r^2 = correlation coefficient.

Chapter 3

METHYLARSENIC DISTRIBUTION AND SPECIATION IN SOIL

Abstract

Methylated forms of arsenic (As), monomethylarsenate (MMA) and dimethylarsenate (DMA), have historically been used as herbicides and pesticides. Because of their large application to agriculture fields and the toxicity of MMA and DMA, the distribution, speciation, and sorption of methylated As to soils requires investigation. MMA and DMA were reacted with a soil up to one year under aerobic and anaerobic conditions. Micro synchrotron based X-ray fluorescence (μ-XRF) mapping studies showed that MMA and DMA were heterogeneously distributed in the soil and were mainly associated with iron oxides, goethite and ferrihydrite, in the soil. Micro X-ray absorption near edge structure (μ-XANES) spectra collected from As hotspots showed MMA and DMA were demethylated to arsenate (AsV) over one year incubation under aerobic conditions. MMA was methylated to DMA, and DMA was maintained as DMA over three month incubation under anaerobic conditions. Arsenic-iron precipitation, such as the formation of scorodite ($FeAsO_4 \cdot 2H_2O$), was not observed, indicating that MMA and DMA were associated with iron oxides as sorption complexes.

Introduction

Arsenic (As) occurs in nature both naturally and anthropogenically. The predominate oxidation states for inorganic As species are arsenate (As^{V}, H_3AsO_4) and arsenite (As^{III}, H_3AsO_3). In addition to inorganic forms, organic forms of As also exist in nature; typically occurring in terrestrial environments as MMA ($CH_3H_2AsO_3$) and DMA ($(CH_3)_2HAsO_2$). MMA and DMA have historically been used as herbicides and pesticides in agriculture [1-2]. The primary reason that As has received so much attention is due to its acute toxicity. Arsenic toxicity and the mode of toxin mechanisms depend on its speciation. MMA is known to cause peripheral artery disease related to atherosclerosis, and DMA is known to be a multi cancer promoter [3-4].

The biotransformation of As species is critical in predicting the fate of As in the environment. The methylation/demethylation of As is a biotic process [5-6]. A generally accepted As methylation pathway, the Challenger pathway (Fig. 1.1), involves multi oxidative methylation and reduction steps [7]. In the reactions, the +5 oxidation state species are formed before the 3+ analogue species. For example, As^{III} goes through oxidative methylation to become MMA^{V}. MMA^{V} is reduced to MMA^{III} and goes through another oxidative methylation to become DMA^{V}, which is reduced to DMA^{III}. Also, MMA is an intermediate to form DMA species in this pathway. Recently, an alternative As methylation pathway (Hayakawa mechanism) (Fig. 1.1) has been proposed [8]. The main difference in the newly proposed Hayakawa pathway is 1) the oxidation state of the (3+) species is formed first and oxidized to the analogue (5+) species and 2) MMA and DMA production are not continuous and MMA is also the end product of the methylation pathway. This suggests that the Challenger

pathway is not the only route for methylation/demethylation, and there can be multiple As methylation/demethylation pathways.

There are several studies on MMA and DMA sorption, speciation, or distribution in soils. MMA and DMA sorption maxima on the soils were correlated with the clay fraction and Fe oxide contents [1]. MMA and DMA were detected 1-1.5 year after their application to experimental fields [9]. In a laboratory incubation study, MMA and DMA were mainly demethylated to As^V [10]. However, there are no studies, to our knowledge, on MMA and DMA sorption on soils using X-ray absorption spectroscopy (XAS) and micro-focused synchrotron fluorescence (μ-SXRF) spectroscopy. Such studies would provide direct evidence for binding mechanisms that could not be ascertained using other approaches. The objective of this study is to characterize the *in-situ* behavior of MMA and DMA speciation, localization, and association with soil components using μ-SXRF, μ-X-ray absorption spectroscopy (μ-XAS), and micro X-ray diffraction (μ-XRD).

Materials and Methods

Arsenic compounds

The reagent grades of As^V, MMA, and DMA were used throughout this study. The molecular structures and pKa of As^V MMA and DMA are shown in Fig 1.1 and Table 1.1. MMA^{III} and DMA^{III} were provided by Dr. X. Chris Lee from the University of Alberta, Canada.

Soil Characteristics

A Delaware sandy loam soil (Reybold, Typic Hapludults) was used for this study. The soil was air dried, grounded, and passed through a 2 mm sieve. Soil

pH, organic matter content, and various elemental concentrations (Table 4.1) were measured using standard procedures. Citrate dithionite and ammonium oxalate extractions were conducted to determine total and amorphous Al- and Fe-oxides (Table 4.1) [11].

Arsenic measurement

The total concentration of each arsenic species in solution was determined using high performance liquid chromatography/inductively coupled plasma/mass spectrometry (HPLC–ICP–MS) using a method adapted from Gong et al [12]. The HPLC system consisted of an Agilent 1200 HPLC (Agilent Technologies, Inc., Palo Alto, CA) with a reverse-phase C18 column (Prodigy 3u ODS(3), 150 mm × 4.60 mm, Phenomenex, Torrance, CA). The ICP-MS unit was an Agilent 7500cx model. The mobile phase (pH 5.9) contained 4.7 mM tetrabutylammonium hydroxide, 2 mM malonic acid, and 4% (v/v) methanol at a flow rate of 1.2 mL/min. The injection volume of each sample was 10 μL.

Soil Incubation Studies

Soil incubation studies were conducted via batch experiments. For aerobic samples, a soil suspension (250 g/L), containing 0.01 M $NaNO_3$, was equilibrated with 0.2 mM MMA or DMA in Erlenmeyer flasks, which had vent caps with a 0.22 μm hydrophobic membrane so that the air could enter but not microbes or dust. The flasks were covered with aluminum foil and placed on an orbital rotating shaker, which was placed in a growth chamber at 60 % humidity. The amount of water was maintained by measuring the total weight of the system weekly, assuming that only weight loss was water evaporation through vent caps. The pH of the system was maintained at pH

6 by adding 0.1 M nitric acid or sodium nitrate, and pH measurements were performed at the same time as the measurements of the total weight were made. After incubation times of 1 week, 1 Month, 3 Months, 6 Months, or 1 year, the suspensions were transferred into centrifuge tubes. The suspensions were centrifuged, and supernatants were sampled using syringe filters (Nylon 0.22 μm pore size). The As concentrations were analyzed using HPLC-ICP-MS. The centrifuged soil suspensions were saved as wet pastes for further analysis by μ-SXRF, μ-XAS, and μ-XRD.

Anaerobic samples were prepared with the same concentration of soil and MMA or DMA as for the aerobic samples. The 20 mM MMA and DMA stock solution, 0.01 M $NaNO_3$ solution, and 0.1 M NaOH solution were all prepared in a glove box, and DDW was purged with N_2 for 24 hrs prior to placing it into the glove box. The soils were placed in centrifuge tubes instead of Erlenmeyer flasks and placed in the glove box. They were left in the glove box for one day prior to adding solutions. The addition of solutions was considered the beginning of the incubation time. Test tubes were closed at all the times and shaken periodically to homogenize the system. pH was measured every two weeks and maintained at pH 6 by adding 0.1 M HNO_3 or NaOH. The redox potential of the system was measured before samples were removed for analysis to confirm anaerobic conditions. Test tubes were removed from the glove box for centrifuging. After centrifuging, the samples were placed back in the glove box, and soils and supernatants were separated inside the glove box. The wet soil pastes were placed in a plastic bag filled with N_2 gas, and the plastic bag was placed in a larger plastic bag filled with N_2 gas. Finally, the soil samples were sealed in triple layer plastic bags and transferred to the National Synchrotron Light Source (NSLS) at Brookhaven National Laboratory. The soil samples were kept in a glove box at the

NSLS until each sample was analyzed. The supernatant was filtered through a 0.22 μm syringe filter, and As concentration was analyzed with HPLC-ICP-MS. All sample preparations for HPLC-ICP-MS analysis were performed inside the glove box. Sample vials were removed just before analysis. The maximum time that the vials were left in air was less than 4 hours to minimize the oxidation of reduced As species.

μ-SXRF, μ-XANES, and μ-XRD analysis

The μ-SXRF, μ-XANES, and μ-XRD measurements of the soil samples were performed at beamline X26A at the NSLS. Anaerobic samples were placed in a special sample holder so that the samples were analyzed under anaerobic conditions. Briefly, the sample holder was built with acrylic plastic that had open windows at the front and the back, which were sealed with Kapton film. The front window allowed the X-ray beam to hit the sample and the fluorescence signal from samples was emitted which was measured using a 9 element Ge array detector and silicon drift detector. The back window allowed the X-ray diffraction patterns to be photographed by a detector. μ-SXRF mapping was conducted with a micro-focused beam (≈ 10 μm each side) at 13,000 eV. The size of each map was 0.7 mm by 0.7 mm, and each pixel was 10 μm by 10 μm. Once the high concentration of As hotspots were identified on a map, at least three scans of As μ-XANES spectra were collected from each hotspot. During the course of measurement, the spectra of $CaAsO_4$ were taken between each sample to calibrate the As K-edge as the first derivative of As^V = 11874 eV. The data processing and LCF were performed using the Sixpack/Feff program package [13]. The standard spectra for μ-XANES LCF analysis were As^V, MMA, DMA, or As^{III} that were sorbed on the soil. The standard samples were prepared by reacting 1 g of the soil with 0.1 mM of As^V, MMA, DMA, or As^{III} for 24 hours at pH 6. Arsenic K-edge

(11,867 eV) XAS spectra were collected at Beamline 11-2 at the Stanford Synchrotron Radiation Laboratory. Three spectra per sample were collected, and the Sixpack/Feff program package was used to analyze the data [13]. The LCF was performed using normalized XANES region of spectra. μ-XRD patterns were taken as a transmission pinhole photograph by using a Bruker SMART 1500 (1024 × 1024 pixel) or Rayonix SX-165 (2048 × 2048 pixel) CCD area detector with exposure time ranging from 60 to 120 seconds. The detectors were calibrated with a NIST SRM 674a α-corundum crystal using the Fit2D program. μ-XRD photographs were also integrated using Fit2D to produce 2θ vs. peak intensity graphs. The background spectra of water, mylar, and kapton were subtracted by using XRD-BS before peak analysis. Final peak analysis was performed using the Match! program.

Results and Discussion

Arsenic Distribution Maps

μ-SXRF is an excellent technique to investigate elemental distribution in heterogeneous systems, such as soil, at micron scales but not the distribution of chemical species. Alternatively, indirect chemical species distribution maps, such as scanning at different energy using μ-SXRF, are available. For example, one can collect the same map above the As K-edge energy, at the As^{V} white peak energy, and at the As^{III} white peak energy. By comparing the intensity of fluorescence emitted from the specific energy, one can construct As^{V} or As^{III} distribution maps. However, such map acquisitions require long times and long exposure to X-rays that may lead to beam induced sample damage. Therefore, we focused on regular μ-SXRF analysis. Arsenic was heterogeneously distributed, and several As hotspots were observed on

the μ-SXRF elemental distribution maps (Fig. 3.1). Arsenic distribution in the soil was mainly correlated with Fe distribution, and As hotspots were generally found at Fe hotspots, but Fe hotspots were not necessarily at As hotspots. This could be ascribed to the larger amount of Fe in the soil compared to the amount of added MMA or DMA. The fluorescence counts from Fe were greater than the As counts by an order of magnitude, indicating that the Fe concentration in the soil was much greater than the As concentration (Fig. 3.2). The correlation graphs supported this as there was a linear relation between As counts and Fe counts. Results from maps from different incubation periods and different starting As species (MMA or DMA) showed no other correlations between As distribution and other elements (Fig. 3.1 and 3.2).

Results from Chapter 4 showed that MMA and DMA sorption was also correlated to the Al-oxide content in the soils. It is possible that MMA and DMA distribution is correlated to Al as much as Fe, but the μ-SXRF technique cannot elucidate Al distribution in the soil, since the element is too light to be studied by synchrotron based X-ray techniques. Also, the total amorphous Fe-oxide concentration is at least twice as high as the total amorphous Al-oxide concentration in the Reybold subsoil. The effects of Fe-oxides on MMA and DMA sorption seem to be greater than Al-oxides. Thus, Fe-oxides appear to be a more important sorbent in the Reybold subsoil and greater emphasis is placed on Fe-oxides in this study.

Based solely on μ-SXRF results, it is difficult to assess MMA or DMA distribution. However, the μ-XANES and μ-XRD data (Fig. 3.3 and 3.5) suggest that most of the MMA and DMA was not demethylated in the soil within 1 week of incubation, and the Fe in the soil was mainly goethite and ferrihydrite. It can be concluded that MMA and DMA are mainly sorbed to the Fe oxides. This direct

evidence for MMA and DMA sorption to Fe oxides in soil agrees with the observation that sorption maxima and Fe contents are proportional to each other [14]. This conclusion can also be supported by the strong sorption of As^V, MMA and DMA to goethite and ferrihydrite[15].

μ-XRD Studies

μ-XRD patterns were collected from the As hotspots identified in the μ-SXRF maps. All of the μ-XRD patterns had peaks at 2θ value of 9.5, 12.11, 16.54, 17.8, 18.14, 19.13, 20.58, and 22.44 (Fig. 3.3). These peaks corresponded to quartz. Major Fe oxide minerals identified were goethite and ferrihydrite. Peaks at 2θ value of 8.16, 9.72, 15.17, 15.9, 16.72, and 23.87 corresponded to goethite, and peaks at 2θ value of 8.16, 9.09, 15.9, and 16.6 corresponded to ferrihydrite.

We were unable to identify peaks corresponding to As-Fe bearing minerals, such as scorodite ($FeAsO_4 \cdot 2H_2O$). Scorodite is often observed in the environment where As is introduced as a result of mining [16-18]. One can hypothesize that the one year incubated samples could contain scorodite minerals, since most of the As in the samples was As^V and 1 year would seem to be long enough to form a precipitate, rather than sorption complexes. However, new XRD peaks or increasing intensity of existing peaks with longer incubation times were not observed. Our results are consistent with a study on As^V sorption to goethite for 1 year [19]. This EXAFS study showed that the initial As^V was sorbed to the surface via bidentate binuclear complexes and the surface complexes did not transform to precipitates, such as scorodite. Based on As solution speciation data, there was no detectable As^V in solution except for one sample. It seemed that most of the As^V produced via demethylation was sorbed to the soil and not available in solution to form any Fe-As

bearing minerals. We conclude that scorodite formation is not a major sink for As in the soil.

Solution As and As Sorption in Aerobic Samples

In aerobic samples, only MMA and DMA were detected in the solution of samples that were reacted with MMA (MMA samples) and DMA (DMA samples), respectively (Fig. 3.4 a), b)). In the case of the MMA samples, initial MMA sorption was almost 100 %, and less than 1 % of added MMA was detected in the solution (Fig. 3.4 a)). For the 1 week to 1 year incubated samples, the MMA concentration in solution was consistently low, and changes in concentration were not significant. In contrast, DMA concentrations in the DMA samples decreased over time (Fig. 3.4 b)). The DMA concentration in solution was highest for the 1 week incubated sample and lowest for the 1 year sample. At 1 week incubation, the DMA concentration was 3.34 ppm, which corresponded to approximately 79 % sorption. The DMA concentration dropped to 1.48 ppm (90% sorption) after 1 month of incubation, 0.85 ppm (94.5% incubation) after 3 months of incubation, 0.68 ppm (95.6% sorption) after 6 months of incubation, and 0.60 ppm (96% sorption) after 1 year of incubation.

Under aerobic conditions, MMA samples were demethylated to produce As^V (Fig. 3.5 a), b)). As soon as As^V is produced via demethylation, the As^V is sorbed to the soil due to the strong sorption affinity of As^V to mineral oxides, particularly goethite and ferrihydrite [15]. MMA was also not detected in the solution, indicating the high sorption affinity of MMA to Fe oxides. This observation is consistent with a study of MMA sorption to goethite and ferrihydrite, using a batch system [15]. Possible MMA sorption mechanisms are the formation of inner-sphere and outer-sphere complexes [2, 15]. In this study, we consider that inner-sphere complexes are

due to ligand exchange that are directly bound to the surface and outer-sphere complexes are due to electrostatic attraction or hydrogen bonding to the surface that are not directly bound to the surface. The formation of inner-sphere complexes, particularly a bidentate binuclear complex formation, was observed between MMA and goethite, which is one of main MMA sorbents in the soil [Chapter 4 Desorption study]. Similarly, As^V produced from the demethylation of MMA also forms bidentate binuclear complexes with goethite [20]. The inner-sphere complex formation is often irreversible process, which can explain the very low concentrations of MMA and As^V in the solution phase of the MMA samples [21]. Outer-sphere complex formation, particularly electrostatic attraction, is observed when two opposite charged species exist in solution. At pH 6, the iron oxide surface is positively charged, and MMA is negatively charged ($CH_3AsO_3^-$). Thus, electrostatic attraction could occur. Even though no study has reported the formation of outer-sphere complexes involving MMA or DMA, As^V can form outer-sphere complexes with Fe and Al oxides [22]. Due to the similar molecular structures between As^V, MMA, and DMA, it is reasonable to consider the outer-sphere complex formation of MMA and DMA as a possible sorption mechanism for MMA on iron oxides, contributing to the high sorption.

The lower sorption of DMA to the soil than MMA (Fig. 3.4 a), b)) under aerobic conditions is also analogous to the situation of DMA sorption to pure minerals in batch systems. DMA sorption to goethite, ferrihydrite, and amorphous aluminum oxide is also less than MMA sorption to these oxides [2, 15]. Due to the weaker sorption affinity of DMA, a ppm level of DMA is always detected in the solution of aerobic DMA samples. Possible DMA sorption mechanisms are similar to MMA

sorption mechanisms discussed above. DMA also forms bidentate binuclear complexes with goethite [chapter 4]. The weak sorption affinity of DMA, despite the same inner-sphere bidentate binuclear complex formation, is likely due to the effect of additional methyl group substitution on the As atom, such as size, charge, and geometry effects [2]. The decreasing DMA concentration in the solution over time is largely a result of As speciation changes and is not caused by increasing DMA sorption. As the incubation time increased, more DMA was demethylated to As^{V} by microbes, and this As^{V} was rapidly sorbed to the soil, similar to the observation from MMA samples. The consumption of DMA by microbes leads to decreasing DMA concentration in solution over time. This hypothesis is also supported by the increasing As^{V} peaks in the μ-XANES spectra (Fig. 3.5 c)).

Solution As and As Sorption in Anaerobic Samples

Anaerobic conditions of the samples were verified by measuring the redox potential of each sample. One week incubated samples showed a redox potential of approximately -50 mV, and the remaining samples, 1 month and 3 months incubated samples, had redox potentials between -300 to -350 mV. In the anaerobic samples, As speciation in solution was more varied. The 1 week incubated MMA samples had only MMA^{V} in solution (Fig. 3.4 c)). The MMA^{V} concentration in the solution was 0.065 ppm. After 1 month of incubation, MMA^{V}, DMA^{V}, As^{III}, MMA^{III}, and DMA^{III} were detected at concentrations of 19 ppb, 20 ppb, 1 ppb, 6 ppb, and 2 ppb, respectively. In the 3 month incubated samples, As^{V}, MMA^{V}, DMA^{V}, As^{III}, MMA^{III}, and DMA^{III} were detected at concentrations of 4 ppb, 17 ppb, 27 ppb, 2 ppb, 12 ppb, and 7 ppb, respectively. Unlike the MMA samples, DMA samples showed little variation in As speciation and increasing sorption over time (Fig. 3.4 d)). The 1 week incubated

samples initially contained DMA^{V} and DMA^{III} in solution. The DMA^{V} concentration in the 1 week incubated sample was 2.82 ppm, which corresponded to 82 % sorption, and the DMA^{III} concentration was 3 ppb. After 1 month of incubation, DMA^{V} and DMA^{III} were detected in solution at concentrations of 2.36 ppm and 5 ppb, respectively. After 3 months of incubation, DMA and DMA^{III} were detected in solution at concentrations of 1.76 ppm and 2 ppb, respectively.

In the MMA anaerobic samples, there was a small increase in DMA concentration, and increasing peak intensity was seen in the μ-XANES spectra (Fig. 3.4 c) and 3.5 a), b)), demonstrating that methylation, mainly DMA production, was taking place under anaerobic conditions. Increasing DMA concentration in the solution indicates that DMA production is larger than the capacity of the soil to sorb DMA due to the DMA's relatively lower sorption affinity on goethite and ferrihydrite. The sorption of reduced As species, especially MMA^{III} or DMA^{III} also needs to be mentioned. Due to the instability of these species, which are known to be oxidized to their analogue (5+) species within days, very few sorption studies have been conducted, and the sorption mechanisms are unknown [23]. μXANES spectra do not show peaks corresponding to these species, and MMA^{III} and DMA^{III} are known to have very low sorption affinity to goethite or ferrihydrite [15, 23]. We can assume that MMA^{III} and DMA^{III} sorption is negligible in this study. The total amount of MMA^{III} and DMA^{III} detected in the solution is equivalent to the total MMA^{III} and DMA^{III} produced. There is a possibility that because of their instability, the concentration of MMA^{III} and DMA^{III} can be underestimated. However, our HPLC-ICP-MS analysis is rapid, and the analogue (5+) species concentration is low. The oxidation of MMA^{III} and DMA^{III} should be minimal in this study.

For DMA samples, the decrease in DMA concentration over time can be attributed to continuous DMA sorption on the soil surface (Fig. 3.4 d)). The effect of carbonate on DMA sorption is uncertain, since some studies show decreasing As^{V} sorption to Fe oxides, a very small effect on the As^{V} sorption, or enhanced As^{V} sorption [24-26]. Also, the volatilization of DMA to dimethylarsine or trimethylarsine is uncertain, since the actual measurement of gaseous As species studies showed very little volatilization [10, 27]. High As volatilization rates are reported in studies, using a mass balance equation, and assuming that the missing As in the system is due to volatilization.

We have not conducted any MMA and DMA sorption experiments on Fe-oxide minerals under anaerobic conditions. One possible factor that can affect the MMA and DMA sorption is the reductive dissolution of Fe-oxides. Dissolution will promote the formation of more crystalline Fe-oxide minerals that have lower surface areas, and consequently sorption decreases [28]. Reduced Fe^{2+} species can reduce MMA(V) and DMA(V) to MMA(III) and DMA(III) so that the sorption decreases [15]. Finally, the dissolved Fe can form complexes or precipitate with MMA and DMA. Further research is necessary to address these questions, and such research is discussed in Chapter 5.

μ-XANES Studies in Aerobic Samples

μ-XANES spectra from As hotspots were collected to determine As speciation. The As speciation was determined by analyzing the peak position of the first derivative of the μ-XANES spectra (Fig. 3.5 a), c)). Each As species has a unique peak position that can be used to identify the speciation. For example, As^{III} has a peak position of 11870 eV, DMA 11872 eV, MMA 11873 eV, and As^{V} 11874 eV. The first

derivative of μ-XANES spectra from different incubation periods showed multiple peaks and shifting of the peaks (Fig. 3.5 a), c)). From the LCF of the μ-XANES spectra, we determined the percentage of each As species. For fitting the μ-XANES spectra for the MMA aerobic samples, only MMA and As^V reference spectra were used, since the addition of DMA did not show any improvement in the fitting, and the contribution of DMA to the fitting was less than 1 %. Based on the fitting, MMA samples showed demethylation as the main As biotransformation product. MMA was gradually demethylated to As^V over one year of incubation (Fig. 3.5 a), b)). Initially, MMA was stable until 1 month incubation. The peak due to As^V was hardly recognizable, but the LCF showed that 6 % of the total As was As^V for 1 week incubated samples (Fig 3.5 a), b)). After 1 month of incubation, there was a small peak growing at 11874 eV, which represented As^V, and the LCF showed that 17% of the total As was As^V. The MMA peak gradually became smaller, and the As^V peak was increased in intensity. At 3 months, the peak intensity from MMA and As^V were comparable, and based on the LCF, MMA contributed 70 % and As^V contributed 30 % of the total As (Fig. 3.5 a), b)). The peak from As^V became more intense than the peak from MMA after 3 months of incubation. At 6 months of incubation, 78% of the total As was As^V. After one year of incubation, As^V was the main species, constituting 93 % of the total As.

DMA samples also showed demethylation as the main As biotransformation product. DMA was also demethylated to As^V over one year of incubation (Fig 3.5 c), d)). For the LCF for DMA samples, only DMA and As^V spectra were used in the fitting. MMA spectrum was excluded from the fitting based on a desorption study [Chapter 4], which showed that little MMA was produced and sorbed

to the soil. The peaks from the 1 week incubated samples showed that the most of the As was DMA, but the LCF revealed that 30 % of the total As was As^V (Fig 3.5 c), d)). After 1 month of incubation, the peak intensity from As^V was already higher than the peak from DMA. The LCF showed that 58 % of the total As was DMA and 42 % was As^V. The intensity of the DMA peak gradually decreased from 3 months to 6 months of incubation. 35 % of the total As was DMA in the 3 month incubated samples, and 26 % was DMA in the 6 month incubated samples. After one year of incubation, the As^V peak was dominant (Fig. 3.5 c), d)). The LCF showed that 94 % of the total As was As^V, and the peak due to DMA was insignificant. As a biological control, the same MMA and DMA samples were incubated for 1 month with an addition of 10 mM sodium azide. μ-XANES analysis of these samples (data not shown) showed only MMA or DMA peaks indicating that the methylation/demethylation was a biotic process.

Our results show that from the analysis of μ-XANES spectra, the first derivative peak positions and the LCF can elucidate qualitative information on *in-situ* As speciation. The quantification between the two analyses was not always consistent. For example, the As^V peak intensity is higher than the DMA peak intensity in the aerobic DMA incubated samples, but the LCF analyses showed a higher percentage of DMA than As^V (Fig. 3.5 c), d)). This inconsistency demonstrates the limitation in μ-XANES analyses as a technique for speciation quantification. However, μ-XANES data can show the general trends in As speciation over time under different environmental conditions.

MMA and DMA demethylation to As^V under aerobic conditions agrees with other studies that were conducted under similar conditions [10, 29]. These

observations indicate that a positive redox potential, indicating an oxidized condition, is the one of the factors that triggers the demethylation. μ-XANES studies show that DMA seems to be directly demethylated to As^V, which contradicts the Challenger methylation scheme. Based on the Challenger methylation scheme (Fig 1.1 a)), DMA is demethylated to MMA first, and then MMA is transformed to As^V. μ-XANES spectra themselves could not prove that no MMA is produced. It is possible that a small amount of MMA is produced, but this was not evident from the μ-XANES spectra (Fig. 3. 5 c)). However, assuming MMA is the intermediate of demethylation before the production of As^V, the amount of MMA produced should be higher than or equal to the amount of As^V produced. This suggests that the MMA peaks should be observed from μ-XANES spectra because MMA has strong sorption affinity to Fe oxides. Inconsistency between our observation and the Challenger mechanism can be an indication that there is more than one demethylation pathway that was not identified. For example, the Hayakawa methylation scheme (Fig. 1. 1 b)) proposes that MMA is not an intermediate of As^V methylation before the production of DMA. DMA can be produced without MMA. It is possible that there are other demethylation pathways, in which As^V can be produced without MMA, and MMA is produced from the methylation of As^V but not the demethylation of DMA.

The rate of demethylation is different for MMA and DMA. The faster rate of DMA demethylation is partially caused by its lower sorption affinity to the soil. The amount of DMA desorption from Fe and Al oxides, using phosphate as a desorbing agent, is higher than desorption studies on As^V or MMA [2, 15]. In our study, a part of applied DMA always stays in the solution phase, which is available for microbes to demethylate. Once As^V is produced, As^V can replace the sorbed DMA on

the surface that leads to more DMA being available for further demethylation. The rate of demethylation can become faster. MMA demethylation, on the other hand, is slower. Most of the applied MMA is sorbed to the soil, and very little MMA is in solution first so that the initial As^V production is small. The small amount of As^V can replace only a small amount of MMA from the surface. More time is needed to produce large amounts of As^V. In addition, it is more difficult for As^V to replace sorbed MMA than to replace DMA due to MMA's stronger sorption affinity. The actual rate of single MMA or DMA molecule demethylation can be the similar, but the constant presence of DMA in the solution enhanced a rapid rate of DMA demethylation compared to MMA demethylation.

μ-XANES Studies in Anaerobic Samples

Under anaerobic incubation, the MMA samples showed methylation as the main As biotransformation product. MMA was methylated to DMA over 3 months of incubation (Fig 3.6 a)). The As^V reference spectrum was not included in the LCF because the addition of the As^V spectrum did not improve the fitting, and the contribution of the spectrum to the fitting was less than 1 %. MMA^{III} and DMA^{III} spectra were also not included in the fitting since the sorption affinity was low based on the solution analysis, and their sorption was negligible [15]. According to the peak intensities from μ-XANES spectra, MMA methylation was observed at one week (Fig. 3.6 a), b)). At 1 week, there was an enhanced peak due to DMA. The LCF showed 16 % of the total As was DMA. At 1 month, the peak due to DMA was not obvious, but the LCF showed 15 % of the total As was DMA. After 3 months of incubation, the peak due to MMA was still dominant, but the peak due to DMA was more obvious than before. The LCF showed 27 % of the total As was DMA (Fig. 3.6 a), b)). The

peak due to As^{III} was consistently observed for all incubation periods, contributing 2-6 % of the total As species based on the LCF. The DMA samples did not show significant changes in As speciation. The only peaks recognized from the μ-XANES spectra were DMA and As^{III} (Fig. 3.6 c), d)). The LCF analysis showed that DMA was 98-99 % of the total As at all times and As^{III} was about 1-2 %. The MMA standard spectrum was not included in the fitting, since it did not show significant contribution to the fitting (< 1 %). The fitting was performed using DMA and As^{III} standard spectra. As a biological control, the same samples were incubated for 1 month with an addition of 10 mM sodium azide. The solution phase analysis of these samples (data not shown) showed no signs of speciation changes indicating that methylation/demethylation is a biotic process. Due to the limited beam time, μ-XANES analysis was not performed on these samples.

Our study showed that at a lower redox potential, methylation is favored over demethylation. This observation is similar to other studies that have reported As^{V} or MMA methylation to MMA or DMA under anaerobic conditions [30-31]. Although the exact mechanism of methylation is still unclear, two recognized mechanisms favor reduced conditions for the methylation. Under the Challenger mechanism, oxidation state 5+ species have to be reduced at first to undergo further oxidative methylation. Reduced species, such as As^{III} or MMA^{III}, are more unstable than oxidized species, such as As^{V} or MMA^{V}, under normal conditions and can be easily oxidized [23]. Lower redox potential conditions can stabilize reduced species. In the Hayakawa mechanism, the methylation process requires reduced glutathione. This reduced species is more stable under reduced conditions [8]. Methylation is again favored under reduced conditions. A thermodynamic analysis of the Challenger mechanism

also supports methylation being favored under reduced conditions (pe < 0) [32]. However, there are studies, showing that demethylation is still observed under anaerobic condition, especially DMA demethylation to MMA [30]. This variation in the methylation/demethylation of As under anaerobic conditions indicates that this process highly depends on not only environmental conditions but also on the composition of microbial communities in soils.

Environmental Significance

MMA and DMA are generally minor components of the total As in the environment but can sometimes be 10-50 % of total As in sea water, ground water, river water, lake water, and soil [33-35]. Arsenic speciation changes are very dynamic processes, and the methylation/demethylation of As is commonly observed in the environment, yet the exact mechanisms and factors affecting the process are largely unknown. A better understanding of As speciation is essential to predict the fate of As in the environment. μ-SXRF studies provided the direct evidence for MMA and DMA being associated with iron oxides in soil, similar to As^V association with iron oxide. Due to the strong sorption affinity of sorbed As species, extraction methods may alter As species on the mineral surface. μ-SXRF and μ-XANES analyses clearly demonstrated the capability to determine *in-situ* qualitative As speciation of sorbed As species under aerobic or anaerobic conditions. Our findings also suggest that under anaerobic conditions, the presence of organoarsenicals, MMA and DMA, can be greater than what was previously thought.

REFERENCES

(1)Dickens, R.; Hiltbold, A. E., Movement and persistence of methanearsonates in soil. *Weeds* **1967,** *15*, (4), 299-304.

(2)Shimizu, M.; Ginder-Vogel, M.; Parikh, S. J.; Sparks, D. L., Molecular scale assessment of methylarsenic sorption on aluminum oxide. *Environ. Sci. Technol.* **2010,** *44*, (2), 612-617.

(3)Tseng, C. H.; Huang, Y. K.; Huang, Y. L.; Chung, C. J.; Yang, M. H.; Chen, C. J.; Hsueh, Y. M., Arsenic exposure, urinary arsenic speciation, and peripheral vascular disease in blackfoot disease-hyperendemic villages in Taiwan *Toxicol. Appl. Pharmacol.* **2006,** *211*, (2), 175-175.

(4)Yamanaka, K.; Ohtsubo, K.; Hasegawa, A.; Hayashi, H.; Ohji, H.; Kanisawa, M.; Okada, S., Exposure to dimethylarsinic acid, a main metabolite of inorganic arsenics, strongly promotes tumorigenesis initiated by 4-nitroquinoline 1-oxide in the lungs of mice. *Carcinogenesis* **1996,** *17*, (4), 767-770.

(5)Cullen, W. R.; Reimer, K. J., Arsenic speciation in the environment. *Chem. Rev.* **1989,** *89*, (4), 713-764.

(6)Turpeinen, R.; Pantsar-Kallio, M.; Haggblom, M.; Kairesalo, T., Influence of microbes on the mobilization, toxicity and biomethylation of arsenic in soil. *Sci. Total Environ.* **1999,** *236*, (1-3), 173-180.

(7)Challenger, F., Biological methylation. *Chem. Rev.* **1945,** *36*, (3), 315-361.

(8)Hayakawa, T.; Kobayashi, Y.; Cui, X.; Hirano, S., A new metabolic pathway of arsenite: Arsenic-glutathione complexes are substrates for human arsenic methyltransferase Cyt19. *Arch. Toxicol.* **2005,** *79*, (4), 183-191.

(9)Akkari, K. H.; Frans, R. E.; Lavy, T. L., Factors affecting degradation of MSMA in soil. *Weed Sci.* **1986,** *34*, (5), 781-787.

(10)Gao, S.; Burau, R. G., Environmental factors affecting rates of arsine evolution from and mineralization of arsenicals in soil. *J. Environ. Qual.* **1997,** *26*, (3), 753-763.

(11)Burt, R. (Ed.), Soil Survey Laboratory Methods Manual. Soil Survey Investigations Report No. 42 Version 4.0. 2004. Lincoln, NE. Natural Resources Conservation Service, U. S. Department of Agriculture.

(12)Gong, Z.; Jiang, G. F.; Cullen, W. R.; Aposhian, H. V.; Le, X. C., Determination of arsenic metabolic complex excreted in human urine after administration of sodium 2,3-dimercapto-1-propane sulfonate. *Chem. Res. Toxicol.* **2002,** *15*, (10), 1318-1323.

(13)Webb, S. M., SIXpack: a graphical user interface for XAS analysis using IFEFFIT. *Phy. Scr.* **2005,** *T115*, 1011-1014.

(14)Woolson, E. A., Persistence and chemical distribution of arsanilic acid in three soils. *J. Agric. Food Chem.* **1975,** *23*, (4), 677-681.

(15)Lafferty, B. J.; Loeppert, R. H., Methyl arsenic adsorption and desorption behavior on iron oxides. *Environ. Sci. Technol.* **2005,** *39*, (7), 2120-2127.

(16)Chen, N.; Jiang, D. T.; Cutler, J.; Kotzer, T.; Jia, Y. F.; Demopoulos, G. P.; Rowson, J. W., Structural characterization of poorly-crystalline scorodite, iron(III)-arsenate co-precipitates and uranium mill neutralized raffinate solids using X-ray absorption fine structure spectroscopy. *Geochim. Cosmochim. Acta* **2009,** *73*, (11), 3260-3276.

(17)Walker, S. R.; Parsons, M. B.; Jamieson, H. E.; Lanzirotti, A., Arsenic mineralogy of near-surface tailings and soils: Influences on arsenic mobility and bioaccessibility in the nova scotia gold mining districts. *Can. Mineral.* **2009,** *47*, (3), 533-556.

(18)Dove, P. M.; Rimstidt, J. D., The solubility and stability of scorodite, $FeAsO_4 \cdot 2H_2O$. *Am. Miner.* **1985,** *70*, (7-8), 838-844.

(19)O'Reilly, S. E.; Strawn, D. G.; Sparks, D. L., Residence time effects on arsenate adsorption/desorption mechanisms on goethite. *Soil Sci. Soc. Am. J.* **2001,** *65*, (1), 67-77.

(20)Fendorf, S.; Eick, M. J.; Grossl, P.; Sparks, D. L., Arsenate and chromate retention mechanisms on goethite .1. Surface structure. *Environ. Sci. Technol.* **1997,** *31*, (2), 315-320.

(21)Sparks, D. L., *Environmental Soil Chemistry*. 2nd ed.; Academic Press: Boston, 2002.

(22)Catalano, J. G.; Park, C.; Fenter, P.; Zhang, Z., Simultaneous inner- and outer-sphere arsenate adsorption on corundum and hematite. *Geochim. Cosmochim. Acta* **2008,** *72*, (8), 1986-2004.

(23)Gong, Z. L.; Lu, X. F.; Cullen, W. R.; Le, X. C., Unstable trivalent arsenic metabolites, monomethylarsonous acid and dimethylarsinous acid. *J. Ana. At. Spectrom.* **2001,** *16*, (12), 1409-1413.

(24)Arai, Y.; Sparks, D. L.; Davis, J. A., Effects of dissolved carbonate on arsenate adsorption and surface speciation at the hematite-water interface. *Environ. Sci. Technol.* **2004,** *38*, (3), 817-824.

(25)Stachowicz, M.; Hiemstra, T.; van Riemsdijk, W. H., Arsenic-bicarbonate interaction on goethite particles. *Environ. Sci. Technol.* **2007,** *41*, (16), 5620-5625.

(26)Radu, T.; Subacz, J. L.; Phillippi, J. M.; Barnett, M. O., Effects of dissolved carbonate on arsenic adsorption and mobility. *Environ. Sci. Technol.* **2005,** *39*, (20), 7875-7882.

(27)Huysmans, K. D.; Frankenberger, W. T., Evolution of trimethylarsine by a *Penicillium* Sp isolated from agricultural evaporation pond water. *Sci. Total Environ.* **1991,** *105*, 13-28.

(28)Kocar, B. D.; Herbel, M. J.; Tufano, K. J.; Fendorf, S., Contrasting effects of dissimilatory iron(III) and arsenic(V) reduction on arsenic retention and transport. *Environ. Sci. Technol.* **2006,** *40*, (21), 6715-6721.

(29)Woolson, E. A.; Aharonson, N.; Iadevaia, R., Application of the high-performance liquid-chromatography flameless atomic-absorption method to the study of alkyl arsenical herbicide metabolism in soil. *J. Agric. Food Chem.* **1982,** *30*, (3), 580-584.

(30)Sierra-Alvarez, R.; Yenal, U.; Field, J. A.; Kopplin, M.; Gandolfi, A. J.; Garbarino, J. R., Anaerobic biotransformation of organoarsenical pesticides monomethylarsonic acid and dimethylarsinic acid. *J. Agric. Food Chem.* **2006,** *54*, (11), 3959-3966.

(31)Feng, M.; Schrlau, J. E.; Snyder, R.; Snyder, G. H.; Chen, M.; Cisar, J. L.; Cai, Y., Arsenic transport and transformation associated with MSMA application on a golf course green. *J. Agric. Food Chem.* **2005,** *53*, (9), 3556-3562.

(32)Dombrowski, P. M.; Long, W.; Farley, K. J.; Mahony, J. D.; Capitani, J. F.; Di Toro, D. M., Thermodynamic analysis of arsenic methylation. *Environ. Sci. Technol.* **2005,** *39*, (7), 2169-2176.

(33)Braman, R. S.; Foreback, C. C., Methylated forms of arsenic in environment. *Science* **1973,** *182*, (4118), 1247-1249.

(34)Bednar, A. J.; Garbarino, J. R.; Ranville, J. F.; Wildeman, T. R., Presence of organoarsenicals used in cotton production in agricultural water and soil of the southern United States. *J. Agric. Food Chem.* **2002,** *50*, (25), 7340-7344.

(35)Marin, A. R.; Pezeshki, S. R.; Masschelen, P. H.; Choi, H. S., Effect of dimethylarsenic acid (DMAA) on growth, tissue arsenic, and photosynthesis of rice plants. *J. Plant Nutr.* **1993,** *16*, (5), 865-880.

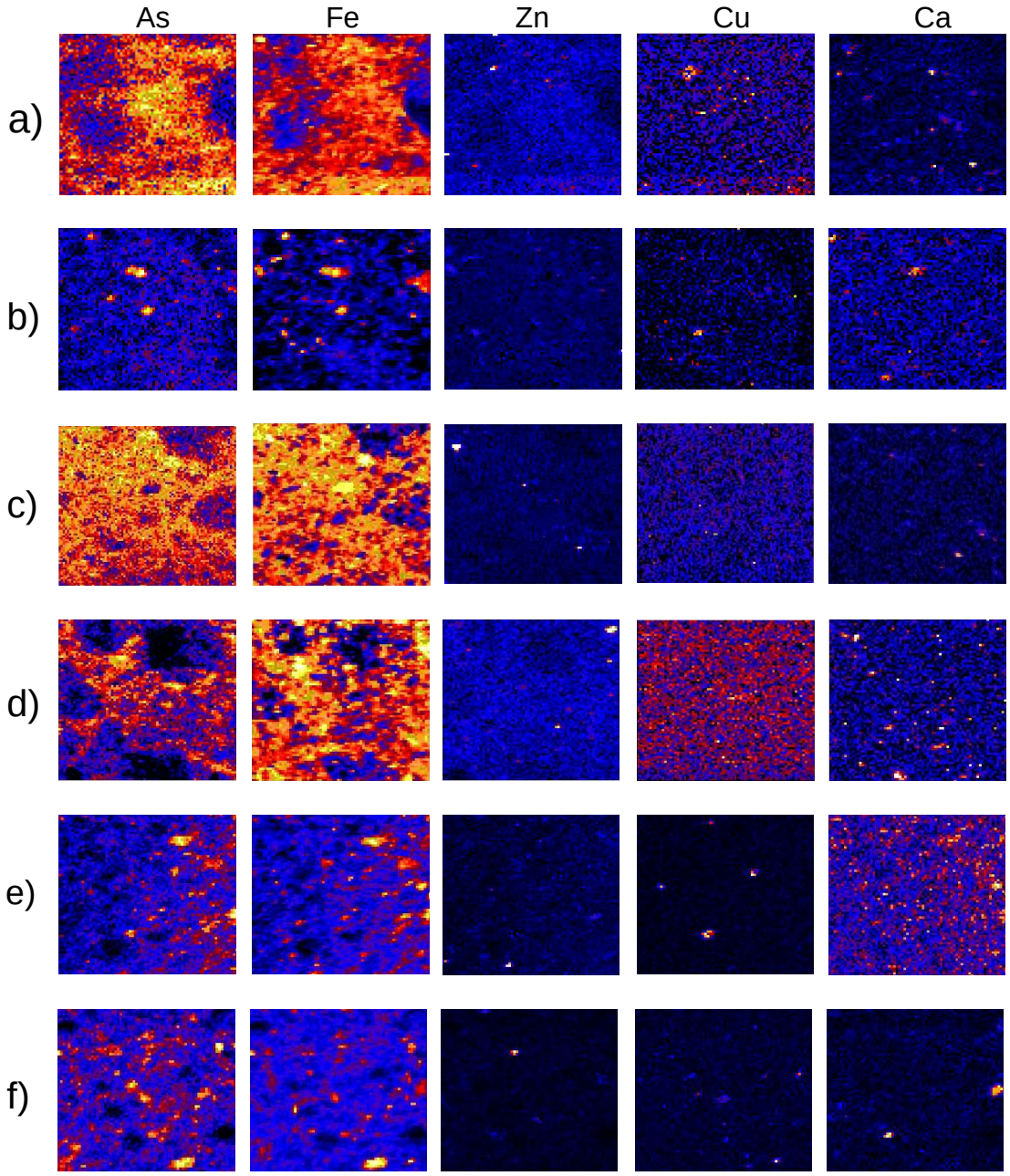

Figure 3.1 Selected μ-SXRF maps for As, Fe, Zn, Cu, and Ca. a) MMA incubated for 1 week under aerobic conditions (MMA 1 week aerobic), b) DMA 3 month aerobic, c) DMA 1 year aerobic, d) DMA 1 week anaerobic, e) MMA 1 month anaerobic, and f) MMA 3 month anaerobic.

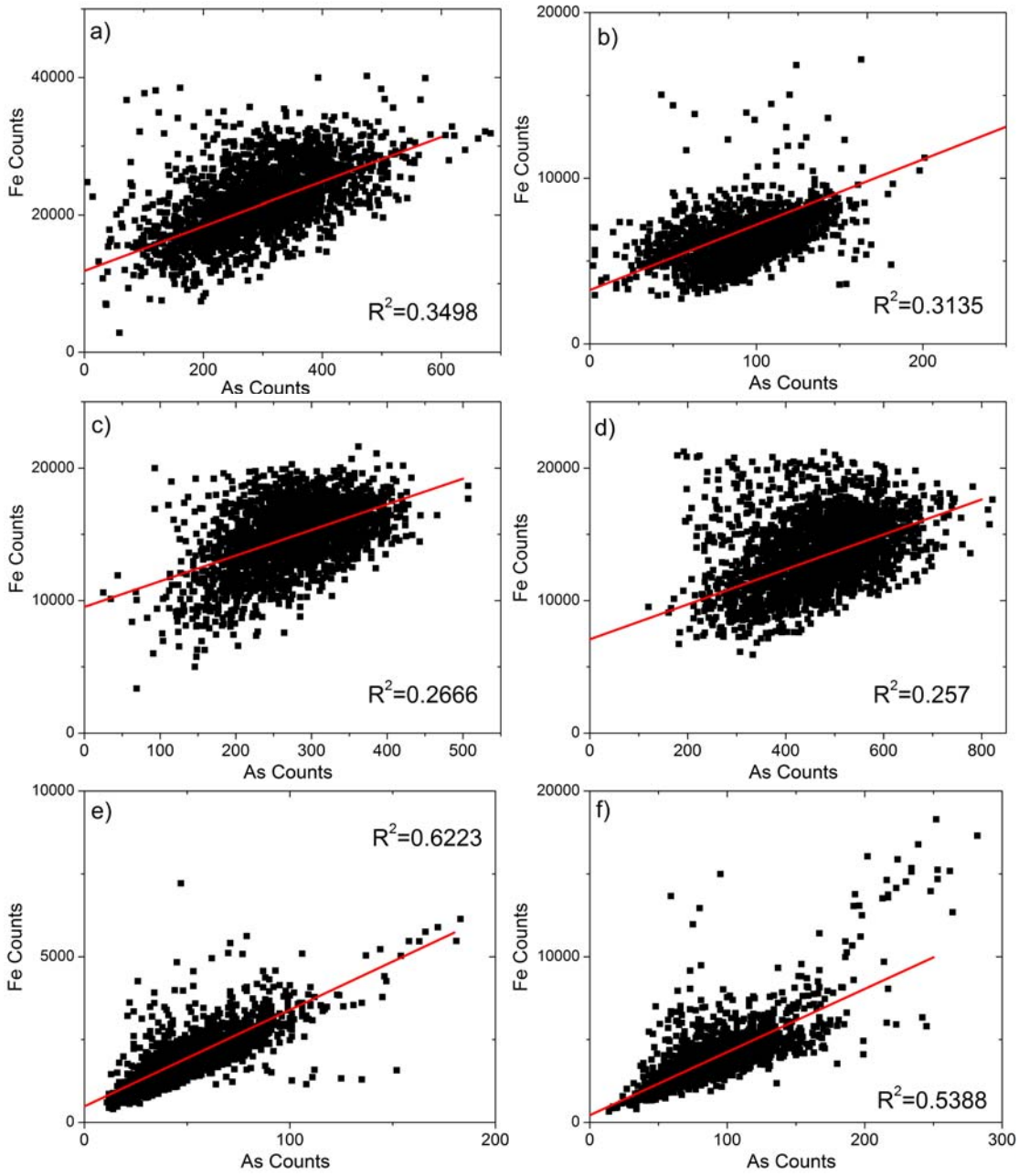

Figure 3.2 Arsenic and Fe fluorescence count correlation plots from μ-SXRF maps. a) MMA incubated for 1 week under aerobic conditions (MMA 1 week aerobic), b) DMA 3 month aerobic, c) DMA 1 year aerobic, d) DMA 1 week anaerobic, e) MMA 1 month anaerobic, and f) MMA 3 month anaerobic.

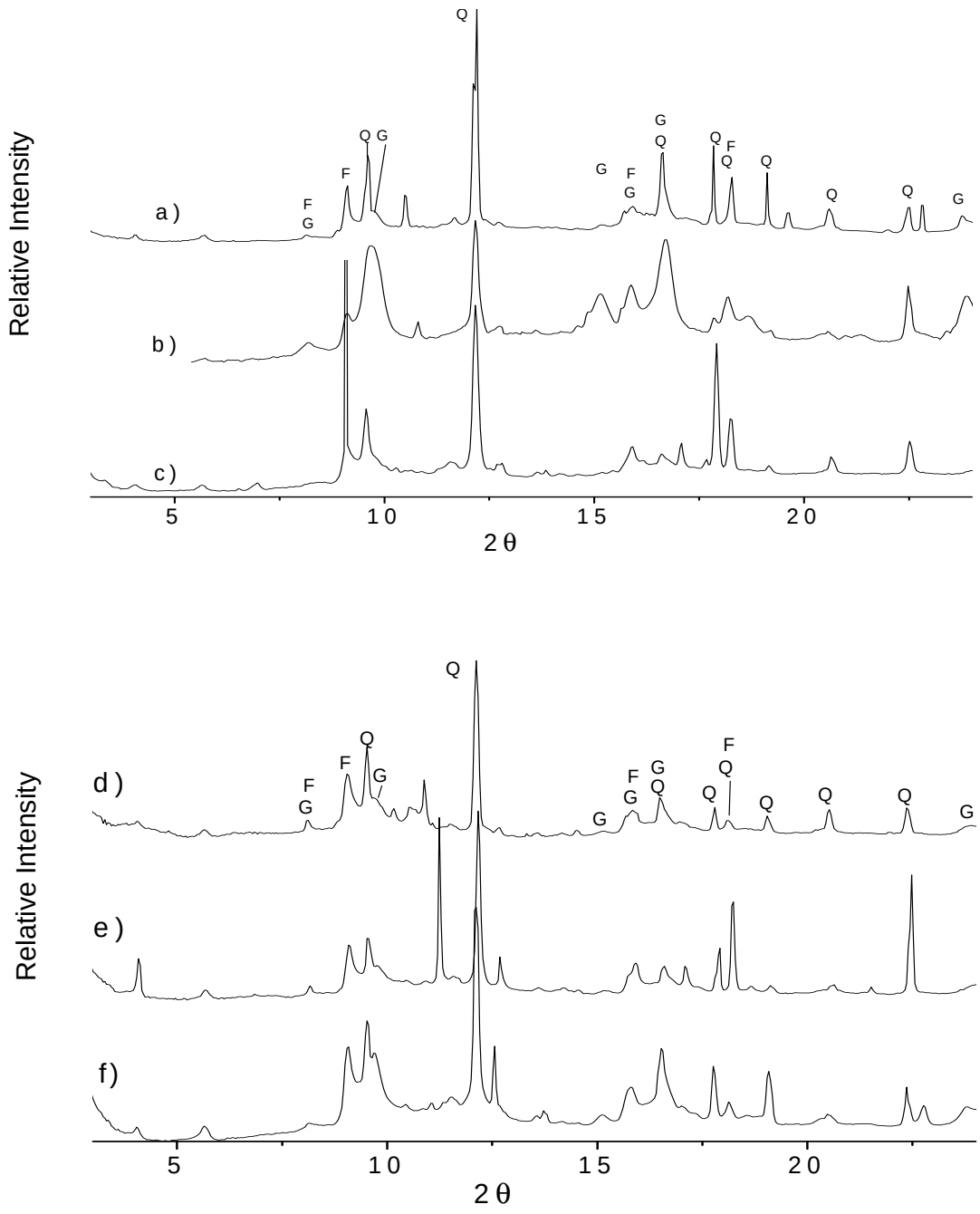

Figure 3.3 μ-XRD patterns in 2θ spacing. a) MMA incubated for 1 week under aerobic conditions (MMA 1 week aerobic), b) DMA 3 month aerobic, c) DMA 1 year aerobic, d) DMA 1 week anaerobic, e) MMA 1 month anaerobic, and f) MMA 3 month anaerobic.

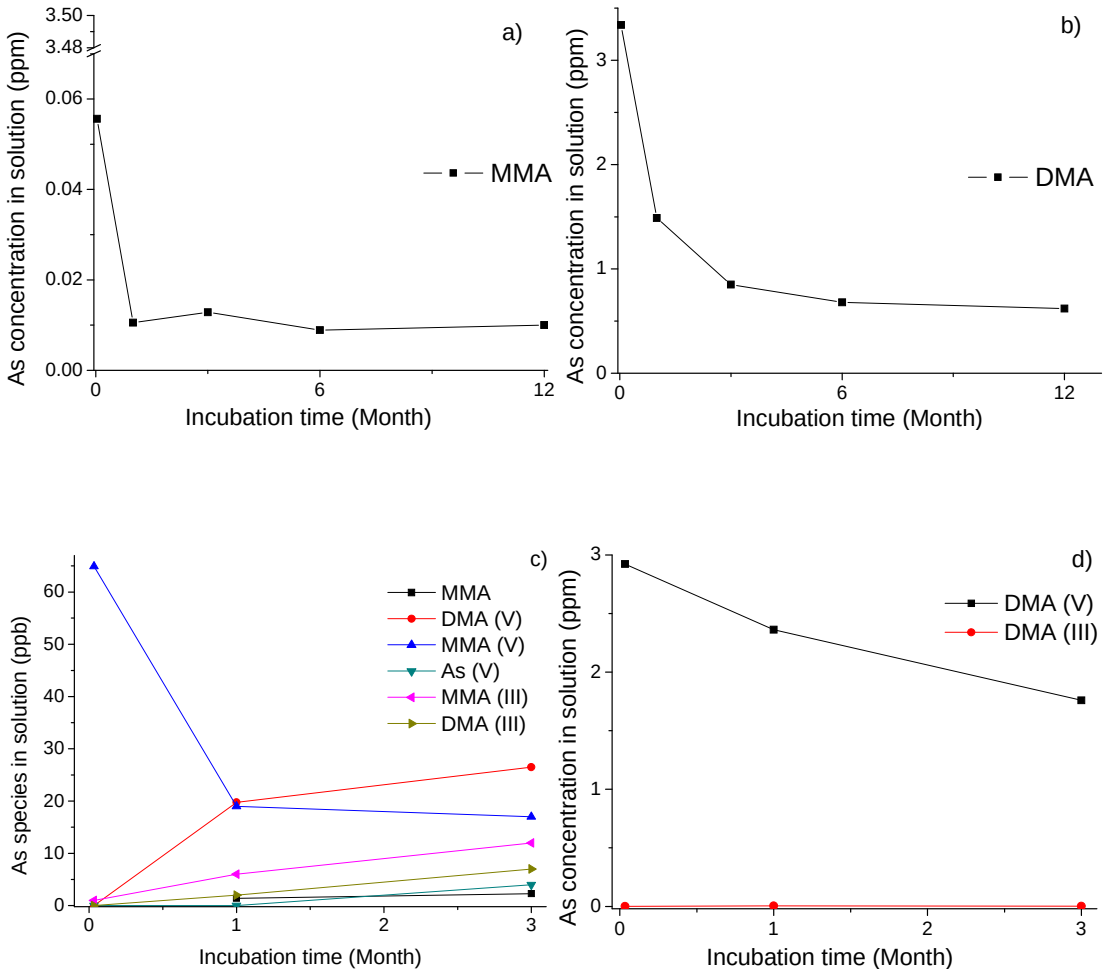

Figure 3.4 As species concentration in solution. a) MMA samples incubated under aerobic conditions, b) DMA samples incubated under aerobic conditions, c) MMA samples incubated under anaerobic conditions, and d) DMA samples incubated under anaerobic conditions.

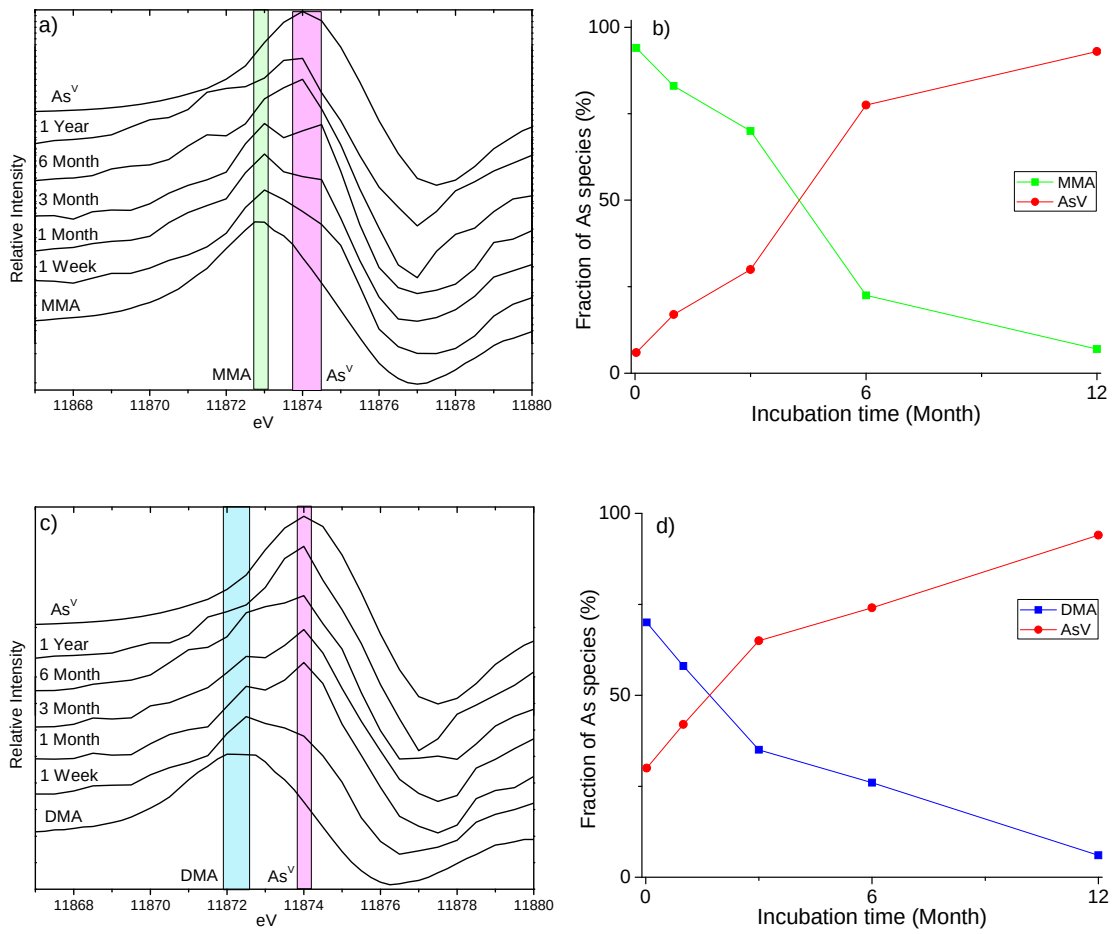

Figure 3.5 μ-XANES spectra. a) the first derivative for MMA aerobic incubated samples, b) As species in percentage from the LCF for MMA aerobic samples, c) the first derivative for DMA aerobic incubated samples, and d) As species in percentage from the LCF for DMA aerobic samples.

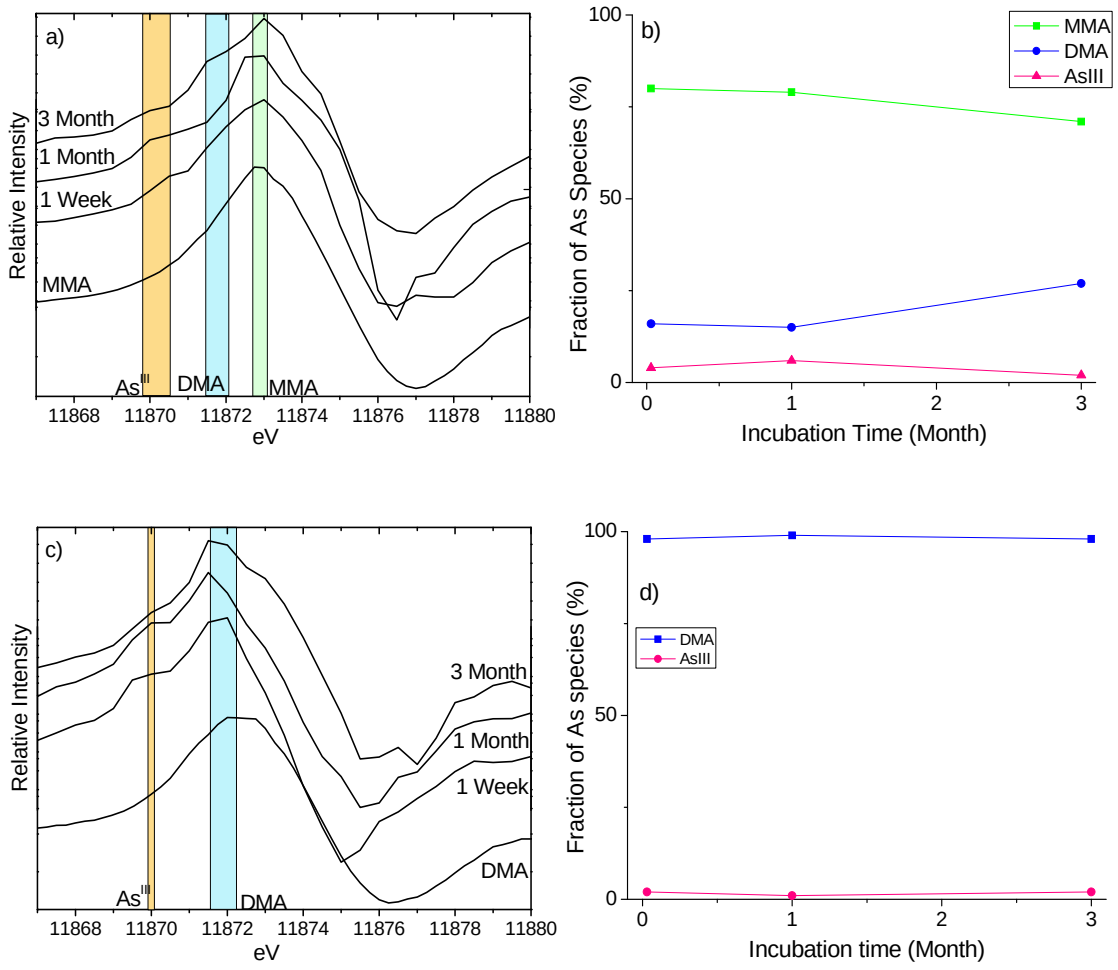

Figure 3.6 μ-XANES spectra. a) the first derivative of MMA anaerobic incubated samples, b) As species in percentage from the LCF for MMA anaerobic samples, c) the first derivative for DMA anaerobic incubated samples, and d) As species in percentage from the LCF for DMA anaerobic samples.

Chapter 4

METHYLARSENIC SORPTION AND DESORPTION ON SOILS

Abstract

Methylated forms of arsenic (As), monomethylarsenate (MMA) and dimethylarsenate (DMA), have historically been used as herbicides and pesticides. Because of their large application to agriculture fields and the toxicity of MMA and DMA, the persistency of these compounds in the environment is of great concern. MMA and DMA sorption and desorption were investigated in soils, varying in mineralogical and organic matter contents. Sorption studies showed that Al/Fe-oxides were the main sorbents in the soils, and the sorption capacity increased as Al/Fe concentration in the soils increased. MMA sorption was greater than DMA sorption, and the rate of MMA sorption was also faster than the DMA sorption rate. Other potential sorbents, such as clay minerals, quartz, and organic matter did not affect MMA and DMA sorption as much as Al/Fe content did. EXAFS studies showed that both MMA/DMA-Fe interatomic distances were around 3.3 Å, which were indicative of inner-sphere complex formation, particularly bidentate binuclear complex formation. Desorption studies showed that not all of the sorbed MMA or DMA was desorbed due to the strong binding between MMA and DMA and iron oxides in the surface via inner-sphere complex formation. The amount of the desorbed MMA and DMA decreased as the sorption residence time increased. For example, 77 % of sorbed MMA was desorbed from the Reybold subsoil after one day residence time,

and 66 % of sorbed MMA were desorbed from the same soil after six months of residence time. The decreases in the desorption were likely due to As speciation changes over time. As residence time increased more MMA was demethylated to As^{V} which was more strongly bound to the surface. This study highlights that MMA and DMA behavior is not only determined by sorption/desorption but also by methylation/demethylation processes.

Introduction

The widespread presence of As throughout the world naturally or anthropogenically is of great concern. Natural phenomena, such as weathering and biological activities, along with agricultural uses and industrial activities, are responsible for As introduction to the environment [1-3]. The most predominate oxidation states for the inorganic As species are As^{V} (H_3AsO_4) and arsenite (As^{III}, H_3AsO_3). In addition to inorganic forms, organic forms of As also exist in nature; typically occurring in terrestrial environments as MMA ($CH_3H_2AsO_3$) and DMA ($(CH_3)_2HAsO_2$). MMA and DMA have historically been used as herbicides and pesticides in agriculture [3-4].

The agricultural application of MMA and DMA often leads to MMA and DMA sorption to soil constituents. MMA and DMA were detected in soils 1.5 years after application, and the half life of MMA and DMA were estimated to be 20 and 22 days, respectively [5]. Studies have shown that MMA and DMA are mainly sorbed to Fe-oxides in the soil [4, 6]. However, MMA and DMA do not always sorb to the soil and can percolate into the groundwater. MMA has been used as a common pesticide at golf courses in Florida and has been linked to the elevated concentration of As in the groundwater beneath the golf courses [7]. Another study has shown that inorganic As

species, As^{III} and As^{V}, are detected in the surface water and groundwater nearby or beneath agricultural fields that have received MMA and DMA as herbicides and pesticides [8]. These studies highlight that upon the application of MMA and DMA, they are subject to various biogeochemical processes with natural components in the environment, such as sorption, desorption, reduction, oxidation, methylation, and demethylation.

Despite the large application and the toxicity of MMA and DMA, little information is available about MMA and DMA behavior in the environment. MMA and DMA application is generally continuous for years, yet the effect of long term application/contact time is not understood well. Studies on As^{V} have shown that As^{V} desorption from γ-Al_2O_3 is affected by residence time [9]. The desorption of As^{V} is decreased as the residence time increases. XANES studies show that aged samples have features similar to an Al-As bearing mineral mansfieldite. On the other hand, the desorption of As^{V} from goethite is not significantly affected by residence time [10]. EXAFS studies have revealed that aged samples do not have any features similar to As-Fe bearing minerals, such as scorodite. Residence time effects can vary, and the effect of residence time on MMA and DMA sorption to soils is not known. In addition, as is discussed in Chapter 3, the biotransformation of As species is critical to predict the fate of As in the environment. The long term incubation of MMA and DMA can cause the biotransformation of As species, and the effect of biotransformation on desorption is not understood well. It is known that As^{V} forms inner-sphere complexes, especially bidentate binuclear complexes with ferrihydrite, goethite, gibbsite, and γ-Al_2O_3, and MMA and DMA form bidentate binuclear complexes [3, 11-13]. MMA and DMA sorption mechanisms to iron oxides, such as

goethite, are not understood well. Investigations on the sorption mechanisms would help to predict the sorption/desorption behaviors of MMA and DMA in soils. Therefore, the objective of this study is to elucidate the soil characteristics that affect MMA and DMA sorption, investigate residence time effects on MMA and DMA desorption, and identify sorption mechanisms between MMA and DMA and goethite. Goethite was chosen as a model Fe-oxide due to its presence in soils.

Materials and Methods

Materials

Reagent grades As^{V}, MMA, and DMA were used throughout this study. The molecular structures and pKa of As^{V}, MMA, and DMA are shown in Fig. 1.1 and Table 1.1. Goethite was synthesized according to the method described by Schwertmann and Cornell [14]. XRD analysis shown that the product was goethite.

Soil Characteristics

The soils that were studied include topsoils and subsoils of a sandy soil (Fort Mott, Areic Hapludult), a high organic matter (OM) soil (Mullica, Typic Umbraquept), a sandy loam soil (Reybold, Typic Hapludults), and a high iron (Fe) soil (Cecil, Typic Kanhapludults). The soils were air dried, ground, passed through a 2 mm sieve, and stored in a refrigerator until experiments were conducted. Soil pH, organic matter concentration, and various elemental concentrations were measured by the Soil Testing Laboratory at the University of Delaware, using standard methods (Table 4.1). Citrate dithionite (CD) and ammonium oxalate (Ox) extractions were performed to determine total and amorphous Al/Fe-oxides, respectively (Table 4.1) [15].

Arsenic measurements

The total concentration of each arsenic species in solution was determined by high performance liquid chromatography/inductively coupled plasma/mass spectrometry (HPLC–ICP–MS), using a method adapted from Gong et al [16]. The HPLC system consisted of an Agilent 1200 HPLC (Agilent Technologies, Inc., Palo Alto, CA) with a reverse-phase C18 column (Prodigy 3u ODS(3), 150 mm × 4.60 mm, Phenomenex, Torrance, CA). The ICP-MS unit was an Agilent 7500cx model. The mobile phase (pH 5.9) contained 4.7 mM tetrabutylammonium hydroxide, 2 mM malonic acid, and 4% (v/v) methanol at a flow rate of 1.2 mL/min. The injection volume of each sample was 10 μL.

Sorption Isotherm Studies

Sorption isotherms were determined via batch experiments at pH 6 with various arsenic concentrations, ranging from 50 μM to 2 mM. Soil suspensions (50 g/L) containing 0.01 M $NaNO_3$ were placed in 50 mL centrifuge tubes and equilibrated at pH 6 for 24 h using rotating shakers (30 RPM) prior to arsenic addition. 20 mM and 1 mM MMA and DMA stock solutions were also prepared at pH 6. Throughout the experiments, the pH of solutions and samples were adjusted with 0.1 M HNO_3 or 0.1 M NaOH. After the arsenic solution was added, the suspension was equilibrated for 24 hrs using rotating shakers. The pH was measured and adjusted three times daily to maintain pH 6. The suspensions were centrifuged, and supernatants were collected using 0.22 μm pore size Nylon syringe filters. The arsenic concentrations were analyzed using HPLC-ICP-MS.

Sorption Kinetics Studies

Sorption kinetics experiments were conducted using a 50 g/L soil suspension and 0.1 mM MMA or DMA in 0.01 M $NaNO_3$ at pH 6 with 1 mM MES buffer. The samples were reacted for various time periods (10 min, 30 min, 1 h, 2 h, 6 h, 12 h, 24 h, 48 h, and 96 h) by placing them on rotating shakers at 30 RPM. Suspensions were filtered through 0.22 μm pore size filters. The arsenic concentrations were analyzed using HPLC-ICP-MS.

Desorption Studies

Desorption studies were conducted using phosphate as a desorbing agent. Prior to desorption, 50 g/L soil suspensions were reacted with 0.1 mM MMA or DMA in a 0.01 M $NaNO_3$ solution at pH 6 for 24 hrs. After centrifuging, the supernatants were decanted, and the wet soils were saved for the desorption study. The weights of all bottles and soils were recorded to calculate water content in the wet soils. The soils were kept in open top bottles covered with kimwipes and aluminum foil to block light and kept in a growth chamber with humidity of 60 % for up to 6 months. The water content of the soils was maintained at 75 % field capacity by measuring the total weight of the system (container, soil, and water). The systems were weighed every week, and if needed, water was added. The soils were mixed and homogenized weekly. After 1 day, 1 month, 3 months, and 6 months, small amounts of soils were collected for the desorption experiments. Approximately 1 g of each soil was placed in 50 mL centrifuge tubes and equilibrated with 1 mM phosphate solution, which had a concentration 10 × higher than the initial concentrations of MMA or DMA, at pH 6 for 24 hrs. The tubes were centrifuged, and the supernatants were removed for As

speciation analysis. Fresh 1 mM phosphate solution was added, and desorption experiments were repeated for 1 week.

X-Ray Absorption Spectroscopy (XAS) Investigations

All XAS samples were prepared by reacting 0.1 mM MMA or DMA with 25 g/L goethite suspensions at pH 5 for MMA and pH 6 for DMA samples. After 48 hr of reaction, samples were centrifuged and washed with 0.01 M $NaNO_3$ three times to remove excess As compounds. After the third centrifugation, the wet paste was kept moist by sealing the tubes and saving them for analysis. Arsenic K-edge (11,867 eV) XAS spectra were collected at beamline X11A at the National Synchrotron Light Source (NSLS) at Brookhaven National Laboratory. Five spectra per sample were collected, and the SIXPack/IFEFFIT program package was used to analyze the data [17]. The inflection point of all studied samples did not change between the first and last scan. First, five spectra of MMA or DMA samples were averaged. The averaged spectra were normalized with respect to E_0, and then the Autobk value was set at the half distance to neighboring atoms. Next, the data were converted from E space to κ space and weighted by κ^3 to compensate for dampening of the XAFS amplitude with increasing κ space. Fourier transformation was then performed over the k-space range from 2.8 to 10.5 $Å^{-1}$ for MMA and from 2.8 to 12.5 $Å^{-1}$ for DMA to obtain the radial distribution functions (RDF). Final fitting of the spectra was conducted on Fourier transformed κ^3 weighted spectra in R space. The WebAtoms and FEFF7 code were utilized to calculate single scattering theoretical spectra for As–O and As–Al backscatters using an input file based on the structural refinement of mansfieldite ($AlAsO_4 \cdot 2H_2O$) minerals. During the fitting process, the coordination numbers for MMA and DMA, As-O and As-C, and As-O-O were fixed to reduce adjustable

parameters. Only the As-O-O multiple scattering path was included in the fitting since FEFF simulations showed only this path had an amplitude contribution over 10 %. Other paths, such as As-C-O and As-C-C, had less than 10 % of contributions.

Results and Discussion

Al- and Fe-oxides as sorbents

Soil extraction results showed that MMA and DMA sorption was linearly correlated with CB extracted Al/Fe-oxide concentration in soils (Fig. 4.3). Soils with higher CB extracted Al/Fe-oxides had higher MMA and DMA sorption. The linear correlation coefficient R^2 values for MMA and DMA sorption vs. both CB and Ox extracted Al/Fe-oxides were higher for Fe-oxides than Al-oxides, suggesting that Fe-oxides might be playing more significant roles in MMA and DMA sorption than Al-oxides. In addition, poor linear correlation between Ox extracted Al-oxides and MMA and DMA sorption was observed (Fig 4.3). One possible explanation for the observation is that Fe-oxide concentrations in soils are generally at least twice higher than Al-oxides in the soils, except the Mullica soils, which had a higher Al-oxide than Fe-oxide concentration (Fig 4.3 and Table 4.1). The total Al-oxides ranged from 1000 to 5500 ppm, while the total Fe-oxides ranged from 0 to 16000 ppm. Soils with higher Al-oxide contents also contained larger amount of Fe-oxides, such as the Reybold and Cecil soils that had high MMA and DMA sorption. It is possible that the higher Fe-oxide concentration overshadowed the effects of Al-oxides on MMA and DMA sorption on the soils. However, studies from Chapter 2 showed that MMA and DMA sorption maxima for amorphous aluminum oxide were similar to ferrihydrite. If other sorption studies were conducted with soils that had higher Al-oxide concentration than

Fe-oxides, we could have observed a greater contribution of Al-oxides to MMA and DMA sorption.

The effect of Organic Matter on sorption

OM is generally a negatively charged component and can interact with positively charged species. In general, Al/Fe-oxides have high PZC values and are positively charged at pH 6. OM can sorb to Al/Fe-oxides and compete with As for the same binding sites on Al/Fe-oxides, resulting in less As sorption to the oxides [18]. In addition, the sorption of OM on Al/Fe oxides lowers the PZC of the oxides [19], causing the Al/Fe oxide surfaces to be less positively charged, which results in less electrostatic attraction and therefore, less sorption.

The Mullica topsoil, which had the highest OM % in the soils, sorbed the least amount of MMA and DMA at lower initial MMA and DMA concentrations (Fig. 4.1). The Mullica topsoil had the second lowest Fe-oxide concentration but had over 1000 ppm Al-oxide (Table 4.1), which was higher than the other soils that had higher MMA and DMA sorption than the Mullica topsoil. It is possible that MMA and DMA competed for the same binding sites with OM in the Mullica soil, and many available binding sites were preoccupied by OM, resulting in lower MMA and DMA sorption to the Mullica soil. However, as the initial MMA and DMA concentrations increased, the sorption amount increased. At initial concentrations of 2 mM, the Mullica topsoil had the fourth highest sorption. This is likely due to either As-O or methyl groups forming a complex with OM. Arsenate binding to OM, through As-O, has been documented [20], and OM is the principal sorbent of hydrophobic compounds, which include methyl group [21]. However, methylated tin sorption on fulvic acid was higher for monomethyltintrichloride, $MeSnCl_3$, than dimethyltindichloride, Me_2SnCl_2. The

demethylated tin had higher hydrophobicity due to two methyl groups. Further research on MMA and DMA interaction with OM are necessary to elucidate binding mechanisms.

In this study, a clear correlation between OM % and MMA and DMA sorption was not observed (Fig 4.3). In addition, the sorption data were plotted against OM % divided by CB extracted Fe-oxide (OM % / CB extracted Fe-oxide), but a clear linear correlation was not observed (data not shown). It is possible that the effect of Fe-oxides on MMA and DMA sorption is much greater than OM, which masks a correlation between OM and MMA and DMA sorption. Further sorption studies on more soils with various OM % would be required to determine the effect of OM on MMA and DMA sorption.

Sorption Isotherms

Sorption isotherms for MMA and DMA show that MMA exhibits higher sorption capacity than DMA (Fig. 4.1). For both MMA and DMA sorption samples, the highest sorption occurred in the Cecil subsoil, which contained the highest amount of Fe (Table 4.1). At the initial MMA or DMA concentrations of 2 mM, the overall order of the four highest MMA and DMA sorption on the soils was: Cecil subsoil > Reybold subsoil > Cecil topsoil > Mullica topsoil. The sorption capacity order was approximately proportional to the Al/Fe-oxide concentration in the soils (Fig. 4.3). Based on the Fe mineralogy, MMA and DMA were mainly sorbed to goethite in the Reybold soils and hematite in the Cecil soils. MMA and DMA sorption to other soil components, such as clay minerals and quartz, are likely little, since As^V sorption to these minerals are also minimal [22-23]. The Fort Mott soils, which were the sandiest, sorbed the least amounts of both MMA and DMA. These studies clearly show that

Al/Fe-oxides are likely the major sorbents for MMA and DMA in the soils. This observation is consistent with high As sorption on Al/Fe-oxides and on soils with high Al/Fe concentrations [3, 11, 24-26]. MMA and DMA also have a high sorption affinity to ferrihydrite and goethite [27]. As previous studies have pointed out, As sorption on Al/Fe-oxides involves specific sorption mechanisms.

Possible sorption mechanisms between MMA or DMA and Al/Fe-oxides are inner-sphere complexes and outer-sphere complexes. In this study, we consider that inner-sphere complexes are due to ligand exchange that are directly bound to the surface and outer-sphere complexes are due to electrostatic attraction or hydrogen bonding to the surface that are not directly bound to the surface. Electrostatic attraction can occur when MMA and DMA, which are negatively charged, are sorbed on the Al/Fe-oxide surface, which is positively charged. In this study, most experiments were conducted at pH 6. MMA and DMA are negatively charged at pH 6 based on their pKa values (Table 1.1). The Al/Fe-oxide surface is positively charged at pH 6, since the PZCs of those oxides are often above pH 8 [3, 11, 27-28]. Thus, the experimental conditions in this study would promote the electrostatic attraction of MMA or DMA to the Al/Fe-oxide surface. The electrostatic attraction of MMA or DMA to the Al/Fe-oxide surface can decrease when pH increases and the Al/Fe-oxide surface becomes less positive or even negative. MMA and DMA sorption to amorphous aluminum oxide and goethite is higher at low pH and lower at high pH [3, 27]. The high MMA and DMA sorption at low pH is most probably due to electrostatic attraction. Another possible sorption mechanism is inner-sphere complex formation. EXAFS studies (Fig. 4.5) have shown that MMA and DMA form inner-sphere bidentate binuclear complexes with goethite. Further discussion is in the

EXAFS section. No studies have been reported on outer-sphere complex formation between MMA and DMA and Fe-, Al-, or Mn-oxides, but simultaneous inner and outer-sphere formation has been reported for As^V sorption to hematite [29]. Due to the similar molecular geometry of As^V, MMA, and DMA, it is reasonable to consider that MMA and DMA could form both inner and outer-sphere complexes simultaneously.

Sorption Kinetics Studies

The sorption kinetics experiments revealed biphasic sorption characteristics: fast initial sorption followed by slow continuous sorption (Fig. 4.2), similar to other sorption kinetics studies [3, 30-31]. The possible slow continuous sorption could be attributed to diffusion into the interiors of aggregates and different sites of reactivity [10, 30].

Similar to the sorption isotherm studies, the MMA and DMA sorption rates are also approximately proportional to the Al/Fe concentration in the soils (Fig. 4.3a). Among MMA sorption samples, the Cecil subsoil had the fastest sorption rate. Almost 100 % of the initial MMA was sorbed within 1 hour of reaction. Initial MMA sorption on the Reybold subsoil was only 70 %, but the fast initial sorption continued for the first 6 hours. By the end of the 96 hr reaction period, total sorption was close to what was observed for the Cecil subsoil. The third highest amount of MMA sorption was observed for the Cecil topsoil with 63 % sorption. The other soils had similar amounts of MMA sorption ranging from 20 to 34 % (Fig. 4.2). Most rapid sorption on all soils took place within the first 24 hrs. DMA sorption on these soils showed a similar trend but the sorption capacity was lower than MMA sorption, the Cecil subsoil sorbing 95 %, the Reybold subsoil sorbing 67%, and the Cecil topsoil sorbing 45 %. The remaining five soils had around 25 % sorption at 96 hr. For the Cecil

subsoil, the Reybold subsoil, and the Cecil topsoil, the rapid sorption continued for the first 24 hr. For the other five soils, the rapid sorption continued for only first 6 hr.

The MMA and DMA sorption kinetics were independent of OM % (Fig. 4.3b). MMA sorption was consistently higher than DMA sorption in both the isotherm and kinetics studies. Similar trends have been reported for MMA and DMA sorption to ferrihydrite, goethite, and amorphous aluminum oxides [3, 27]. The main cause of lower sorption for DMA is possibly due to the additional methyl group substitution. The additional methyl group eliminates a deprotonation site from DMA so that DMA is less negatively charged at any given pH, which leads to less electrostatic attraction to the positively charged Fe and Al oxide mineral surfaces at acidic pH. Less electrostatic attraction can affect the rate and amount of outer-sphere complex formation [29, 32]. Additional methyl groups also make the DMA molecule larger, occupying more space per molecule. Less hydrogen bonding is formed with the oxide surface oxy/hydroxyl groups. Thus, fewer binding sites are available for inner- and outer-sphere complex formation.

Desorption

Phosphate was used as a desorbing agent for this study since several studies showed that phosphate could effectively remove sorbed MMA and DMA [3, 27]. The desorption ratio was calculated as desorbed As to sorbed As (desorbed As^V or MMA or DMA / sorbed MMA or DMA) %. As^V and DMA were produced as a result of methylation and demethylation of MMA or DMA. Results from the desorption of MMA and DMA reacted samples (MMA samples and DMA samples) varied from soil to soil (Fig. 4.4), and no significant correlations between the amount of desorption and

specific soil characteristics, such as Fe concentrations or OM % in the soils, were observed.

In MMA samples, after 1 day of sorption, 64 – 84 % of sorbed MMA was desorbed, and all of the desorbed As was MMA (Fig. 4.4 a - d)). The total desorbed As, a sum of desorbed MMA, DMA, and As^V, decreased over time (Fig. 4.4). After 6 months of residence time, 42 – 77 % of sorbed As was desorbed. The Cecil subsoil had the highest total As retention. After 1 day of sorption, 65 % of sorbed MMA was desorbed. The desorption % decreased to 58 % for 1 month and 49 % for 3 months samples. The percentage finally dropped to 42 % after 6 months of incubation. In DMA samples, the average As desorption was higher than for the MMA samples. After 1 day of sorption, 73 – 88 % of sorbed DMA was desorbed (Fig. 4 e – g)). The total desorbed As, a sum of desorbed MMA, DMA, and As^V, also decreased over time. Among the soil samples, the Fort Mott topsoil retained the highest amount of As (Fig. 4.4 e)). After 1 day of sorption, 77 % of the sorbed DMA was desorbed. The desorption % decreased to 74 % for the 1 month and 64 % for the 3 month samples. The desorption percentage finally dropped to 56 % after 6 months incubation.

There are several possible explanations for decreasing total As desorption with longer residence times. The MMA and DMA desorption is often limited by diffusion processes [30]. At the fast initial MMA and DMA sorption phase, MMA or DMA can be sorbed on the exterior of mineral particles, where can be accessible over short times. At longer reaction times, MMA and DMA diffuse into the interior of particles and micro-pores. The MMA and DMA from the interiors of particles have to diffuse out to be desorbed. In theory, if the diffusion into the interior of particles takes a month, the diffusion from the interior of particles requires the same amount of time.

Soils are heterogeneous systems that consist of networks of macro- and micro- pores/ particles that promote diffusion processes. Thus, one week might not be long enough to desorb MMA and DMA, and they would remain in the soils. Another possible explanation for the less desorption at longer residence times could be due to a transformation in sorption complexation. As discussed earlier, some sorption could occur via electrostatic attraction or outer-sphere complex formation. Over time, MMA or DMA sorbed via electrostatic attraction or outer-sphere complexes may transform to inner-sphere complexes, causing the MMA and DMA to be more difficult to desorb. Also, the formation of stable surface precipitate/sorption complexes is possible as observed in other studies [9]. The surface precipitate develops at longer times. Even though our systems had a water content of 75 % field capacity, it could be a possible that a part of Al/Fe-oxide surface can be dissolved at mineral/water interface. The dissolved Al/Fe ions are positively charged and can be electrostatically attracted to the sorbed MMA or DMA, which are negatively charged. During 6 month residence time, surface precipitate can be formed. Another possible explanation for less desorption at longer residence times is due to the increasing sorption of As^{V}. This study has shown that a portion of sorbed MMA and DMA is demethylated to As^{V}. The sorbed As^{V} is not desorbed as easily as sorbed MMA or DMA, since it is documented that As^{V} has a higher sorption affinity than MMA and DMA [3, 27]. In the soil samples, demethylation increases over time, and there is concurring desorption.

Surface precipitate formation could be the cause for the lower As desorption from MMA samples reacted with the Cecil subsoils. When both MMA and DMA form bidentate binuclear complexes with Fe-oxides (Table 4.2), MMA still has an oxy/hydroxyl group that is not involved in the complex formation. The

oxy/hydroxyl group is negatively charged and can electrostatically attract positively charged Fe ions, while DMA has only two methyl groups not involved in the complex formation. Methyl groups are neutral functional groups and cannot electrostatically attract Fe ions. The formation of surface precipitates in DMA samples are less likely compared to MMA samples, and there is known MMA-Fe bearing ferric methanearsnonate precipitate that has been used to control sheath blight of rice plants [33]. Since in many cases, DMA samples had a higher demethylation rate (Fig. 4.4), the demethylation of DMA to As^V in the Cecil subsoil is likely higher than the rate of MMA demethylation to As^V. If more As^V is produced in the Cecil subsoil that is reacted with DMA, the As desorption from the Cecil subsoil should be lower than from the MMA samples due to the As^V strong sorption affinity to Al/Fe-oxides. However, the As desorption from the Cecil subsoil reacted with MMA is lower than the DMA samples, which indicates that the demethylation does not cause a residence time effect. The larger amount of As retention in the Cecil subsoil reacted with MMA is possibly due to surface precipitates, while the As retention in the Cecil subsoil reacted with DMA is possibly due to the increasing sorption as As^V.

A part of MMA and DMA sorption was irreversible, and phosphate could not remove all of the sorbed MMA or DMA, even when the residence time was only one day (Fig. 4.4). As the EXAFS studies (Table 4.2) suggest, the irreversible sorption is likely due to inner-sphere complex formation, since the inner-sphere complexes are often irreversibly sorbed [34]. The irreversible sorption behavior is consistent with MMA and DMA desorption studies on goethite, ferrihydrite, and amorphous aluminum oxide [3, 27]. The type of inner-sphere complex is the same for MMA and DMA, but the amount of desorption is higher for DMA. The same trend was reported

for MMA and DMA sorption on Al oxide [3]. The possible explanation for this is that the DMA bidentate binuclear complex is not as strong as the MMA bidentate binuclear complex, and the complex formation can be reversible to some extent [3]. Another possibility is that MMA and DMA simultaneously form both inner and outer-sphere complexes, and the ratio of inner-sphere complexes to outer-sphere complexes is different. DMA could form a larger proportion of outer-sphere complexes than As^V or MMA does, which can be easily desorbed. Further sorption mechanism studies, such as resonance anomalous X-ray reflectivity measurement, can help to verify such speculation.

Demethylation was consistently observed in both MMA and DMA samples. In MMA samples, as residence time increased, more As^V and DMA were desorbed from the soils (Fig. 4.4 c, d)). Desorbed As^V ranged from less than 1 % to 14 % of sorbed MMA after six months of incubation. The Fort Mott topsoil had the largest amount of demethylation. After 1 month of incubation, 6.5 % of sorbed MMA was demethylated to As^V. The demethylation % increased from 11 % for the three month samples to 14 % for the 6 month samples. Desorbed As^V ranged from 1.5 % to 39 % of sorbed DMA for the six month samples. With DMA samples, the Fort Mott topsoil also had the highest demethylation. After 1 month of incubation, 15 % of the sorbed DMA was demethylated to As^V. The demethylation % increased from 24 % for the three month samples to 39 % for the six month samples. The As^V desorption (39 %) was larger than DMA desorption (17 %). The Fort Mott topsoil does not possess specific soil physicochemical characteristics that are different from the other soils. It may be that the Fort Mott topsoil has some unique microbial community that is

capable of demethylating MMA and DMA at a rapid rate. The difference in the rate of demethylation depends on the variation in microbial communities in each soil.

The effect of soil constituents, such as the effect of OM, on demethylation is not clear. Topsoils have higher rates of demethylation and higher OM % compared to corresponding subsoils (Fig. 4.4 and Table 4.1). It is possible that the OM is enhancing microbial activity, but other studies have shown that the addition of cellulose or carbohydrates actually retard methylation/demethylation [35-36]. A clear conclusion on the effect of OM cannot be made, but it is possible that microbial community diversity could affect the degree of demethylation.

The higher degree of DMA demethylation over MMA demethylation is consistent with the soil incubation study from Chapter 3. As is discussed in Chapter 3, there is weaker sorption affinity for DMA that can promote more demethylation by microbes. Another study also has shown higher DMA demethylation than MMA demethylation [35]. DMA demethylation to As^V is 73 %, while MMA demethylation to As^V was 43 % over 70 days incubation. As discussed earlier, the higher sorption affinity of As^V can enhance the retention of As in the soils. A part of As^V produced via demethylation is retained in the soils so that the actual As^V production is larger than the As^V desorbed.

EXAFS Studies

Based on the fit for MMA sorption on goethite, the As-O bond distance was calculated to be 1.70 Å, while the As-C bond distance was 1.89 Å (Table 4.2). The As-O and As-C bond distances from this study agreed with other experimental studies and XAS investigations, which indicated that MMA still maintained tetrahedral geometry upon sorption [3, 37-38]. MMA sorption resulted in a new peak

due to a second neighboring atom in the Fourier transformed κ^3 weighted spectra in R space (Fig 4.5b). This indicated the formation of inner-sphere complexes. Approximately, 1.8 Fe atoms were located at an As-Fe interatomic distance of 3.31 Å (Table 4.2). The coordination number and As-Fe distances were indicative of MMA-goethite bidentate binuclear complexes. This observation agrees with MMA-nanocrystalline titanium oxide bidentate binuclear complex formation and MMA-amorphous aluminum oxide bidentate binuclear complex formation observed in earlier studies [3, 10, 12, 38-40].

Based on the fit for DMA sorption on goethite, the As-O bond distance was calculated to be 1.71 Å, while the As-C bond distance was 1.91 Å (Table 4.2). The As-O and As-C bond distances from this study agree with other experimental studies and XAS investigations [3, 37-38]. DMA sorption also resulted in new second neighboring atom peak formation in the Fourier transformed κ^3 weighted spectra in R space (Fig 4.5b) with 1.9 Fe atoms located at an As-Fe interatomic distance of 3.30 Å (Table 4.2). The coordination number and As-Fe distances were indicative of DMA-goethite bidentate binuclear complexes, which is consistent with published EXAFS studies and density functional theory (DFT) studies, reporting As-Fe bidentate binuclear complex formation [12, 40].

It has been reported that DMA forms monodentate mononuclear complexes with nanocrystalline titanium oxide and bidentate binuclear and bidentate binuclear complexes with amorphous aluminum oxide [3, 38]. The difference in the type of DMA surface complexes could be due to differences in experimental conditions and the surface charge of titanium oxide and iron oxide [3]. The As-Fe interatomic distance of 3.30 Å is too close for As-Fe monodentate mononuclear

complex formation. The As-Fe interatomic distance for monodentate mononuclear complexes is 3.6 Å based on EXAFS studies and 3.67 Å based on DFT calculations [12, 40]. The coordination number itself cannot be conclusive due to the large standard deviation. Considering both interatomic distance and coordination number, we conclude that DMA forms bidentate binuclear complexes with goethite. In addition to inner-sphere complex formation, it is likely that both MMA and DMA also simultaneously form outer-sphere complexes with goethite, like As^V does [29]. The As-Fe interatomic distance in outer-sphere complexes is greater than 5 Å. With the long interatomic distances, the As-Fe scattering becomes extremely weak, and the variation in the interatomic distance increases the Debye-Waller factor to an extremely large value such that the As-Fe peak observed in Fourier transformed spectra is not intense enough to be fit. The EXAFS spectroscopy technique is not suitable for studying the longer interatomic distances of outer-sphere complexes. The exact mechanisms of MMA and DMA sorption to iron oxides are not clear and further studies are needed.

Environmental Significance

MMA and DMA are generally minor components of the total As in the environment but can sometimes reach 10-50 % of total As [8, 41-42]. A better understanding of MMA and DMA sorption/desorption is critical to predict the fate of these chemicals in the environment. Our study revealed that MMA and DMA are mainly sorbed to Al/Fe-oxides in soils, and the sorption rate and capacity depends on the quantity of Fe and Al. A part of the irreversible MMA and DMA sorption is due to the strong inner-sphere bidentate binuclear complex formation between MMA and DMA and the goethite surface, similar to As^V sorption on goethite. The decreasing

desorption of MMA and DMA over time suggests a possible accumulation of As as either organic or inorganic species during long term agricultural applications. When these fields are used for agricultural production, the uptake of As by plants is possible. Accordingly, MMA and DMA sorption/desorption and biotransformation can play an important role in total arsenic cycling in the environment. Understanding MMA and DMA sorption mechanisms are also useful for establishing important parameters for surface complexation model development.

REFERENCES

(1)Fish, R. H.; Walker, W.; Tannous, R. S., Organometallic geochemistry 2.The molecular characterization of trace organometallic and inorganic-compounds of arsenic found in green river formation oil-shale and its pyrolysis product. Energy Fuels 1987, 1, (3), 243-247.

(2)Cullen, W. R.; Reimer, K. J., Arsenic speciation in the environment. Chem. Rev. 1989, 89, (4), 713-764.

(3)Shimizu, M.; Ginder-Vogel, M.; Parikh, S. J.; Sparks, D. L., Molecular scale assessment of methylarsenic sorption on aluminum oxide. Environ. Sci. Technol. 2010, 44, (2), 612-617.

(4)Dickens, R.; Hiltbold, A. E., Movement and persistence of methanearsonates in soil. Weeds 1967, 15, (4), 299-304.

(5)Woolson, E. A.; Aharonson, N.; Iadevaia, R., Application of the high-performance liquid-chromatography flameless atomic-absorption method to the study of alkyl arsenical herbicide metabolism in soil. J. Agric. Food Chem. 1982, 30, (3), 580-584.

(6)Wauchope, R. D., Fixation of arsenical herbicides, phosphate, and arsenate in alluvial soils. J. Environ. Qual. 1975, 4, (3), 355-358.

(7)Feng, M.; Schrlau, J. E.; Snyder, R.; Snyder, G. H.; Chen, M.; Cisar, J. L.; Cai, Y., Arsenic transport and transformation associated with MSMA application on a golf course green. J. Agric. Food Chem. 2005, 53, (9), 3556-3562.

(8)Bednar, A. J.; Garbarino, J. R.; Ranville, J. F.; Wildeman, T. R., Presence of organoarsenicals used in cotton production in agricultural water and soil of the southern United States. J. Agric. Food Chem. 2002, 50, (25), 7340-7344.

(9)Arai, Y.; Sparks, D. L., Residence time effects on arsenate surface speciation at the aluminum oxide-water interface. Soil Sci. 2002, 167, (5), 303-314.

(10)O'Reilly, S. E.; Strawn, D. G.; Sparks, D. L., Residence time effects on arsenate adsorption/desorption mechanisms on goethite. Soil Sci. Soc. Am. J. 2001, 65, (1), 67-77.

(11)Arai, Y.; Elzinga, E. J.; Sparks, D. L., X-ray absorption spectroscopic investigation of arsenite and arsenate adsorption at the aluminum oxide-water interface. J. Colloid Interface Sci. 2001, 235, (1), 80-88.

(12)Fendorf, S.; Eick, M. J.; Grossl, P.; Sparks, D. L., Arsenate and chromate retention mechanisms on goethite .1. Surface structure. Environ. Sci. Technol. 1997, 31, (2), 315-320.

(13)Ladeira, A. C. Q.; Ciminelli, V. S. T.; Duarte, H. A.; Alves, M. C. M.; Ramos, A. Y., Mechanism of anion retention from EXAFS and density functional calculations: Arsenic (V) adsorbed on gibbsite. Geochim. Cosmochim. Acta 2001, 65, (8), 1211-1217.

(14)Schwertmann, U.; Cornell, R. M., Iron oxides in the laboratory. VCH: Weinheim, 1991.

(15)Burt, R. (Ed.), Soil Survey Laboratory Methods Manual. Soil Survey Investigations Report No. 42 Version 4.0. 2004. Lincoln, NE. Natural Resources Conservation Service, U. S. Department of Agriculture.

(16)Gong, Z.; Jiang, G. F.; Cullen, W. R.; Aposhian, H. V.; Le, X. C., Determination of arsenic metabolic complex excreted in human urine after administration of sodium 2,3-dimercapto-1-propane sulfonate. Chem. Res. Toxicol. 2002, 15, (10), 1318-1323.

(17)Webb, S. M., SIXpack: a graphical user interface for XAS analysis using IFEFFIT. Phy. Scr. 2005, T115, 1011-1014.

(18)Redman, A. D.; Macalady, D. L.; Ahmann, D., Natural organic matter affects arsenic speciation and sorption onto hematite. Environ. Sci. Technol. 2002, 36, (13), 2889-96.

(19)Harter, R. D.; Naidu, R., Role of metal-organic complexation in metal sorption by soils. In Advances in Agronomy, Vol 55, Academic Press Inc: San Diego, 1995; Vol. 55, pp 219-263.

(20)Buschmann, J.; Kappeler, A.; Lindauer, U.; Kistler, D.; Berg, M.; Sigg, L., Arsenite and arsenate binding to dissolved humic acids: Influence of pH, type of humic acid, and aluminum. Environ. Sci. Technol. 2006, 40, (19), 6015-6020.

(21)Xing, B. S.; Pignatello, J. J., Competitive sorption between 1,3-dichlorobenzene or 2,4-dichlorophenol and natural aromatic acids in soil organic matter. Environ. Sci. Technol. 1998, 32, (5), 614-619.

(22)Goldberg, S., Competitive adsorption of arsenate and arsenite on oxides and clay minerals. Soil Sci. Soc. Am. J. 2002, 66, (2), 413.

(23)Ladeira, A. C. Q.; Ciminelli, V. S. T., Adsorption and desorption of arsenic on an oxisol and its constituents. Water Res. 2004, 38, (8), 2087-2094.

(24)Jain, A.; Raven, K. P.; Loeppert, R. H., Arsenite and arsenate adsorption on ferrihydrite: Surface charge reduction and net OH- release stoichiometry. Environ. Sci. Technol. 1999, 33, (8), 1179-1184.

(25)Woolson, E. A., Persistence and chemical distribution of arsanilic acid in three soils. J. Agric. Food Chem. 1975, 23, (4), 677-681.

(26)Dixit, S.; Hering, J. G., Comparison of arsenic(V) and arsenic(III) sorption onto iron oxide minerals: Implications for arsenic mobility. Environ. Sci. Technol. 2003, 37, (18), 4182-4189.

(27)Lafferty, B. J.; Loeppert, R. H., Methyl arsenic adsorption and desorption behavior on iron oxides. Environ. Sci. Technol. 2005, 39, (7), 2120-2127.

(28)Shibata, J.; Fuerstenau, D. W., Flocculation and flotation characteristics of fine hematite with sodium oleate. Int. J. Miner. Process. 2003, 72, (1-4), 25-32.

(29)Catalano, J. G.; Park, C.; Fenter, P.; Zhang, Z., Simultaneous inner- and outer-sphere arsenate adsorption on corundum and hematite. Geochim. Cosmochim. Acta 2008, 72, (8), 1986-2004.

(30)Fuller, C. C.; Davis, J. A.; Waychunas, G. A., Surface-Chemistry of Ferrihydrite .2. Kinetics of Arsenate Adsorption and Coprecipitation. Geochim. Cosmochim. Acta 1993, 57, (10), 2271-2282.

(31)Raven, K. P.; Jain, A.; Loeppert, R. H., Arsenite and arsenate adsorption on ferrihydrite: Kinetics, equilibrium, and adsorption envelopes. Environ. Sci. Technol. 1998, 32, (3), 344-349.

(32)Sposito, G., The operational definition of the zero-point of charge in soils. Soil Sci. Soc. Am. J. 1981, 45, (2), 292-297.

(33)Odanaka, Y.; Tsuchiya, N.; Matano, O.; Goto, S., Metabolic fate of the arsenical fungicide, ferric methanearsonate, in soil. J. Pestic. Sci. 1985, 10, (1), 31-39.

(34)Sparks, D. L., Environmental Soil Chemistry. 2nd ed.; Academic Press: Boston, 2002.

(35) Gao, S.; Burau, R. G., Environmental factors affecting rates of arsine evolution from and mineralization of arsenicals in soil. J. Environ. Qual. 1997, 26, (3), 753-763.

(36)Huysmans, K. D.; Frankenberger, W. T., Evolution of trimethylarsine by a Penicillium Sp isolated from agricultural evaporation pond water. Sci. Total Environ. 1991, 105, 13-28.

(37)Grundler, H. V.; Schumann, H. D.; Steger, E., Raman and infrared spectroscopic investigation of alkyl derivatives of arsenic acid .6. AsO bond - calculation of force constants and vibrational energy-distribution in compounds of type RAsO3X2 and R2AsO2X. J. Mol. Struct. 1974, 21, (1), 149-157.

(38)Jing, C. Y.; Meng, X. G.; Liu, S. Q.; Baidas, S.; Patraju, R.; Christodoulatos, C.; Korfiatis, G. P., Surface complexation of organic arsenic on nanocrystalline titanium oxide. J. Colloid Interface Sci. 2005, 290, (1), 14-21.

(39)Foster, A. L.; Brown, G. E.; Tingle, T. N.; Parks, G. A., Quantitative arsenic speciation in mine tailings using X-ray absorption spectroscopy. Am. Miner. 1998, 83, (5-6), 553-568.

(40)Sherman, D. M.; Randall, S. R., Surface complexation of arsenie(V) to iron(III) (hydr)oxides: Structural mechanism from ab initio molecular geometries and EXAFS spectroscopy. Geochim. Cosmochim. Acta 2003, 67, (22), 4223-4230.

(41)Braman, R. S.; Foreback, C. C., Methylated forms of arsenic in environment. Science 1973, 182, (4118), 1247-1249.

(42)Marin, A. R.; Pezeshki, S. R.; Masschelen, P. H.; Choi, H. S., Effect of dimethylarsenic acid (DMAA) on growth, tissue arsenic, and photosynthesis of rice plants. J. Plant Nutr. 1993, 16, (5), 865-880.

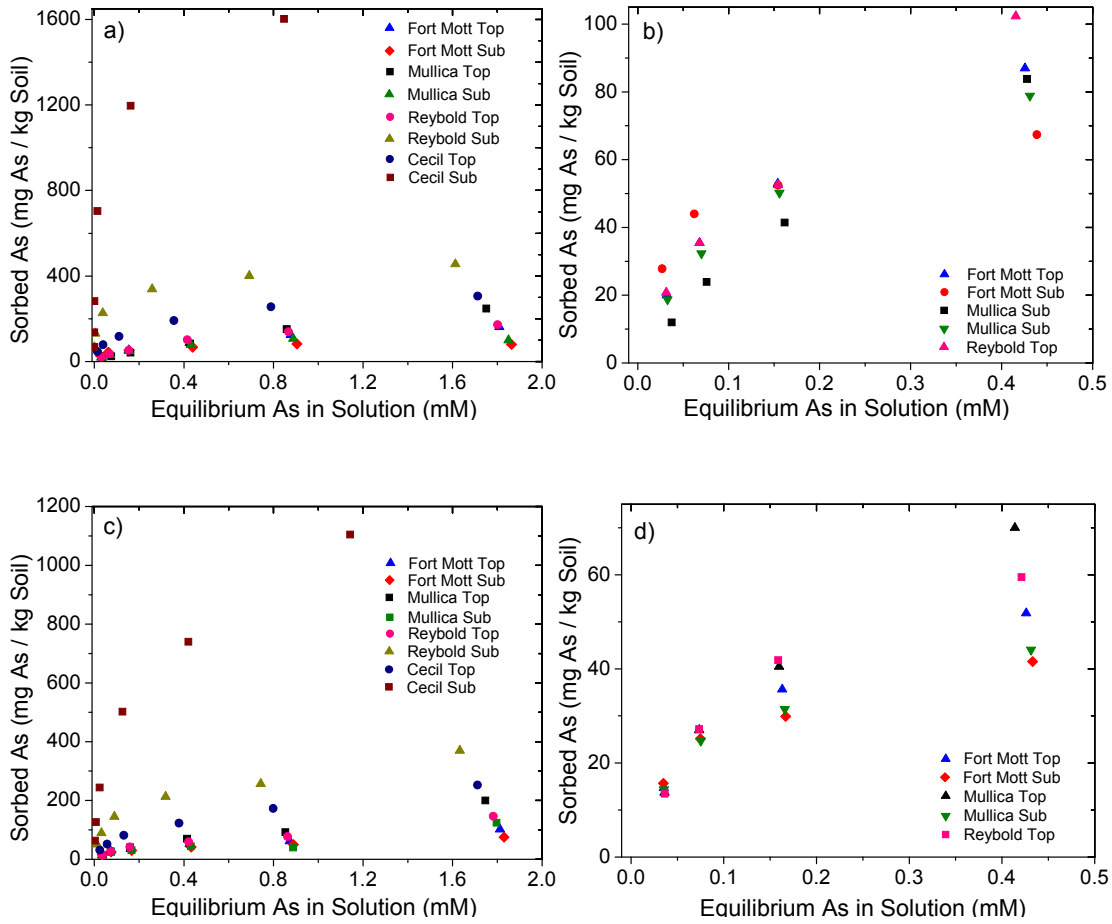

Figure 4.1 Sorption isotherm studies. a) MMA sorption to soils, b) MMA sorption at lower equilibrium MMA solution concentrations, c) DMA sorption to soils, and d) DMA sorption at lower equilibrium DMA solution concentrations.

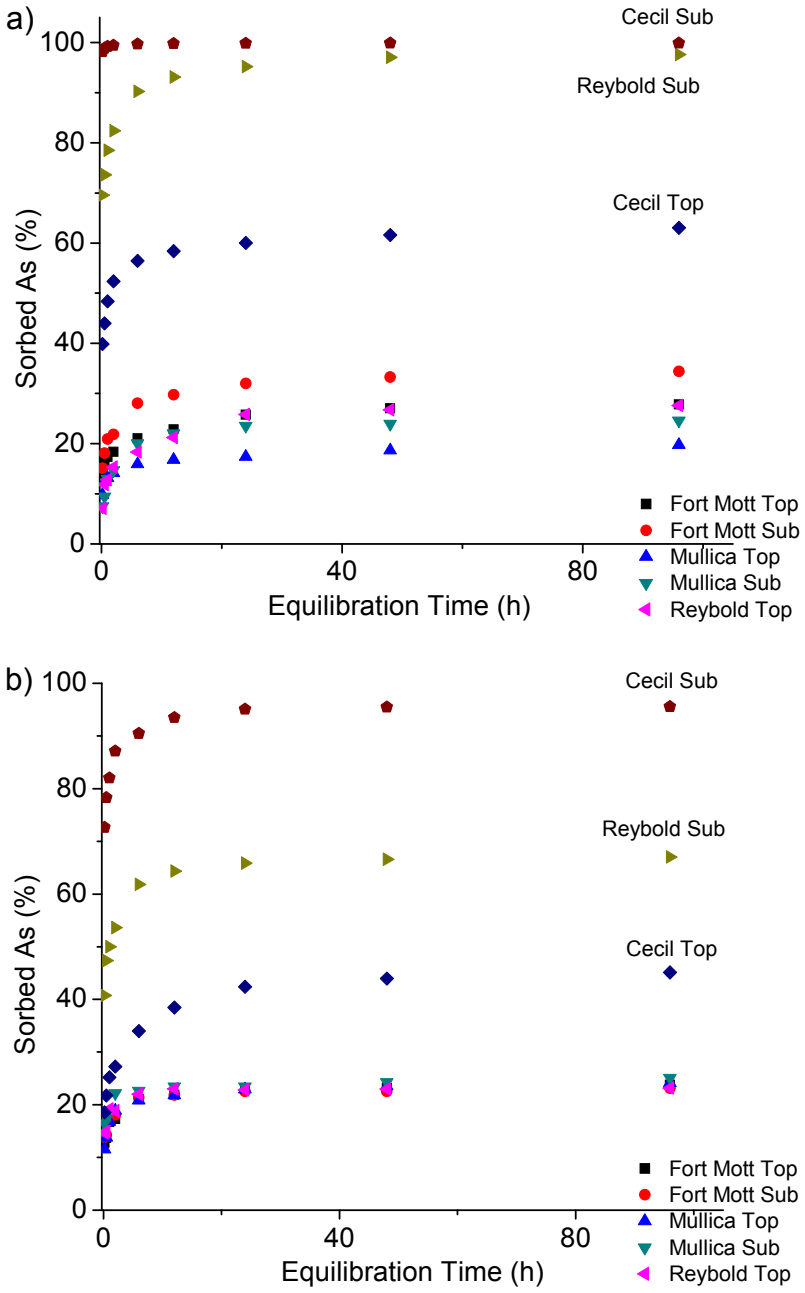

Figure 4.2 MMA (a) and DMA (b) sorption kinetics.

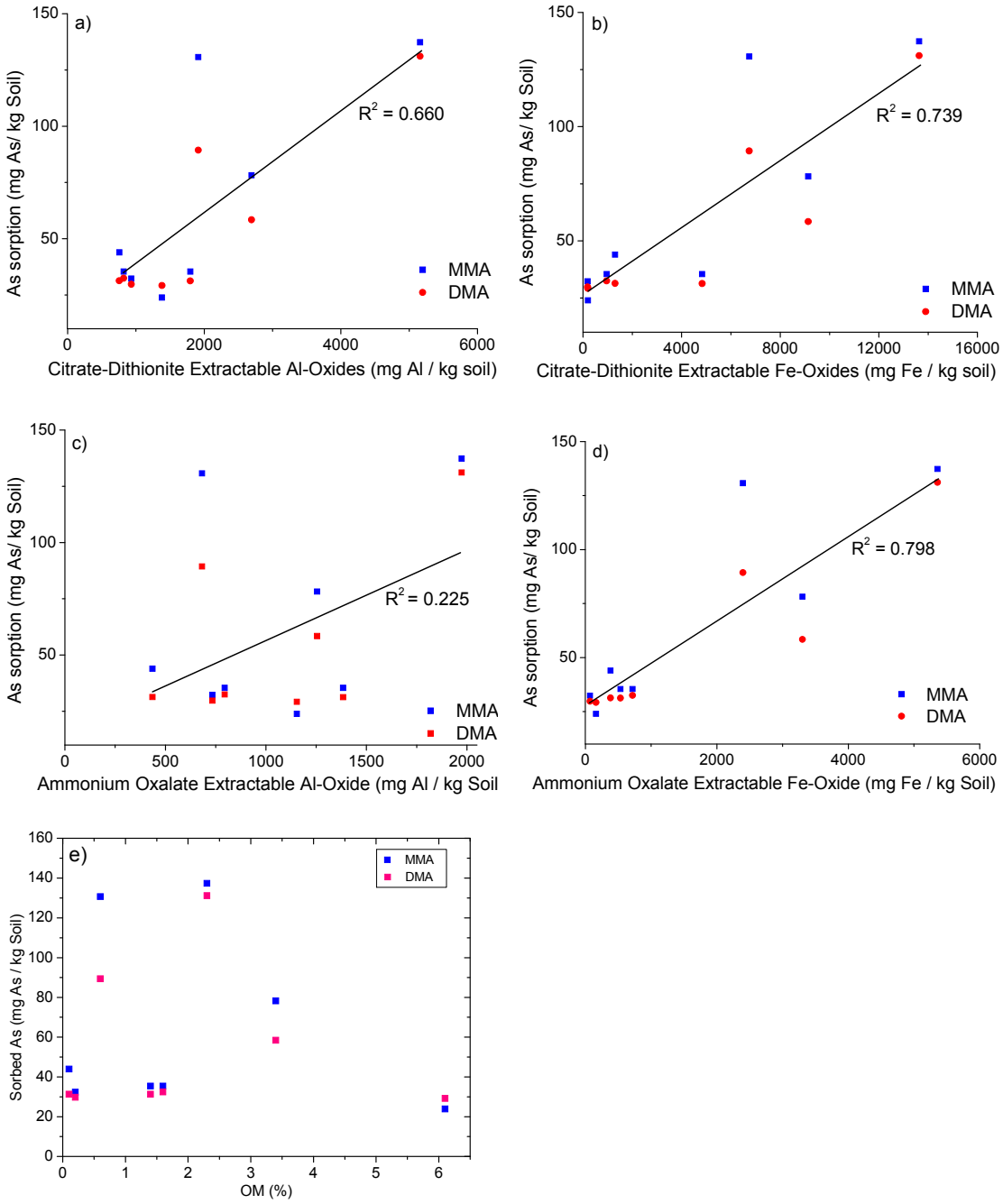

Figure 4.3 The relation between MMA and DMA sorption and Fe and OM contents. MMA and DMA sorption versus total Al-oxide a), total Fe-oxide b), amorphous Al-oxide c), and amorphous Fe-oxide d) in the soils, and (e) MMA and DMA sorption versus OM concentration in the soils.

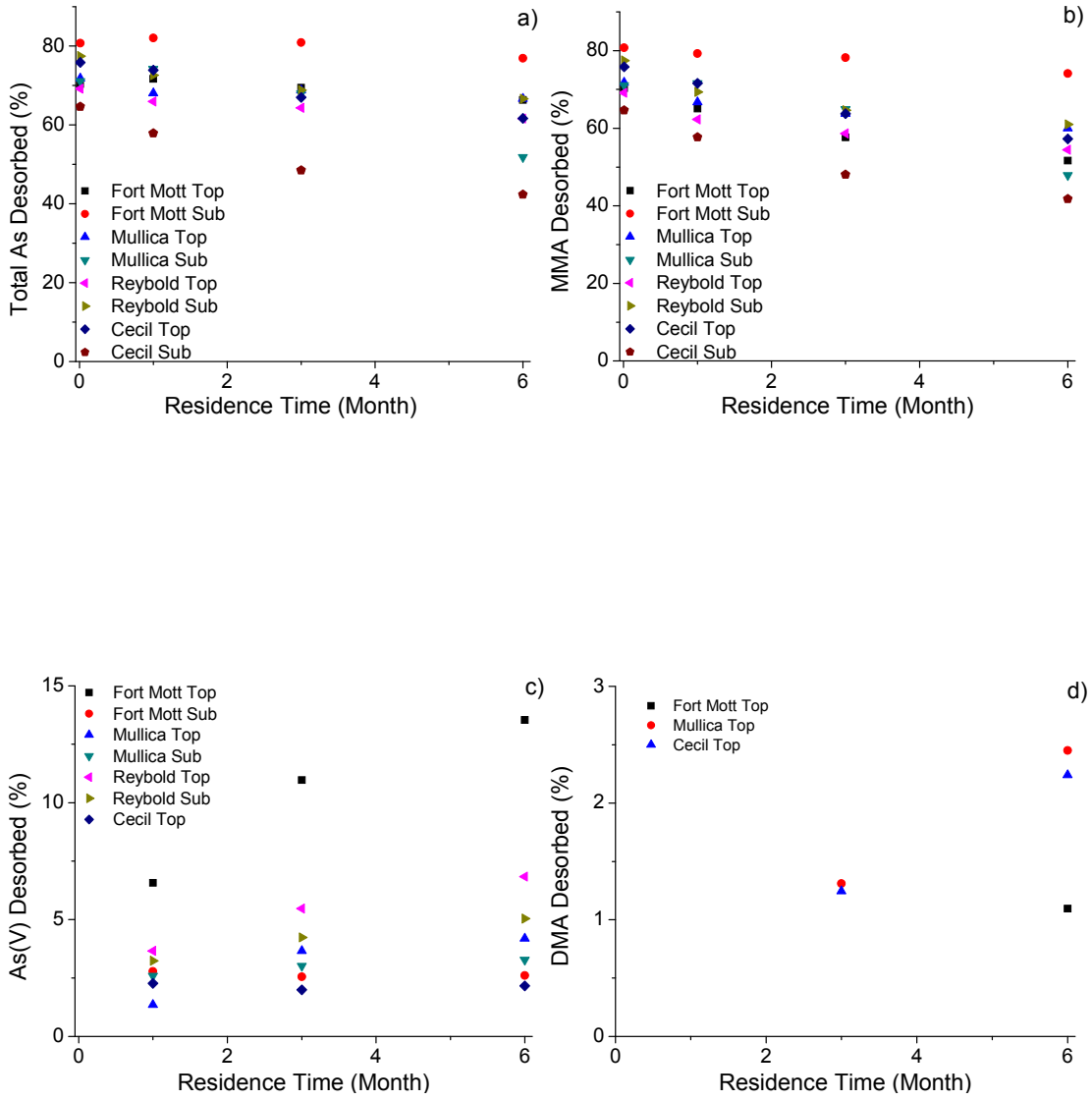
a)
Total As Desorbed (%)
Residence Time (Month)
Fort Mott Top
Fort Mott Sub
Mullica Top
Mullica Sub
Reybold Top
Reybold Sub
Cecil Top
Cecil Sub
b)
MMA Desorbed (%)
Residence Time (Month)
c)
As(V) Desorbed (%)
Residence Time (Month)
d)
DMA Desorbed (%)
Residence Time (Month)

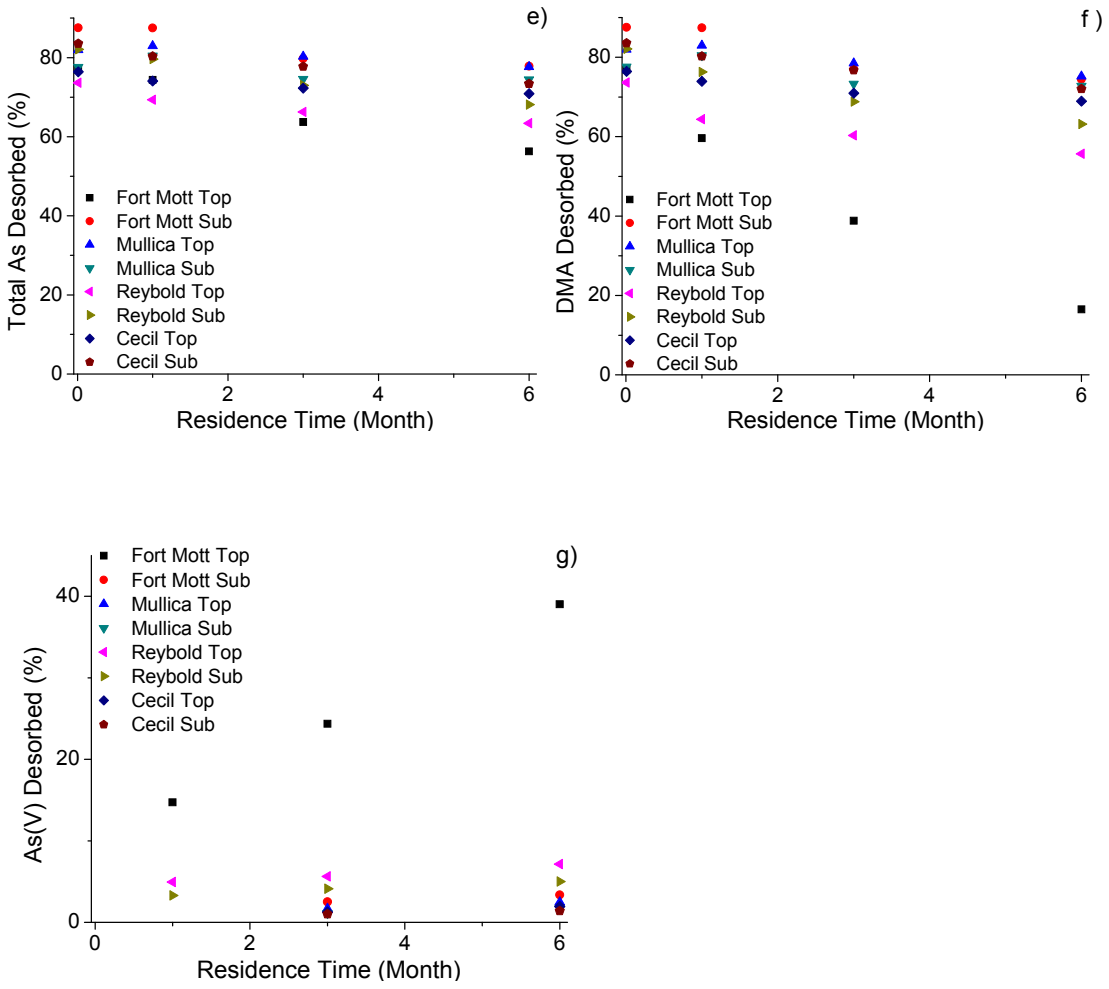

Figure 4.4 MMA and DMA desorption as affected by residence time a) total As desorption (the sum of MMA, AsV, and DMA) from MMA reacted samples, b) MMA desorption from MMA reacted samples, c) AsV desorption from MMA reacted samples, d) DMA desorption from MMA reacted samples, e) total As desorption (the sum of DMA and AsV) from DMA reacted samples, f) DMA desorption from DMA reacted samples, and g) AsV desorption from DMA reacted samples.

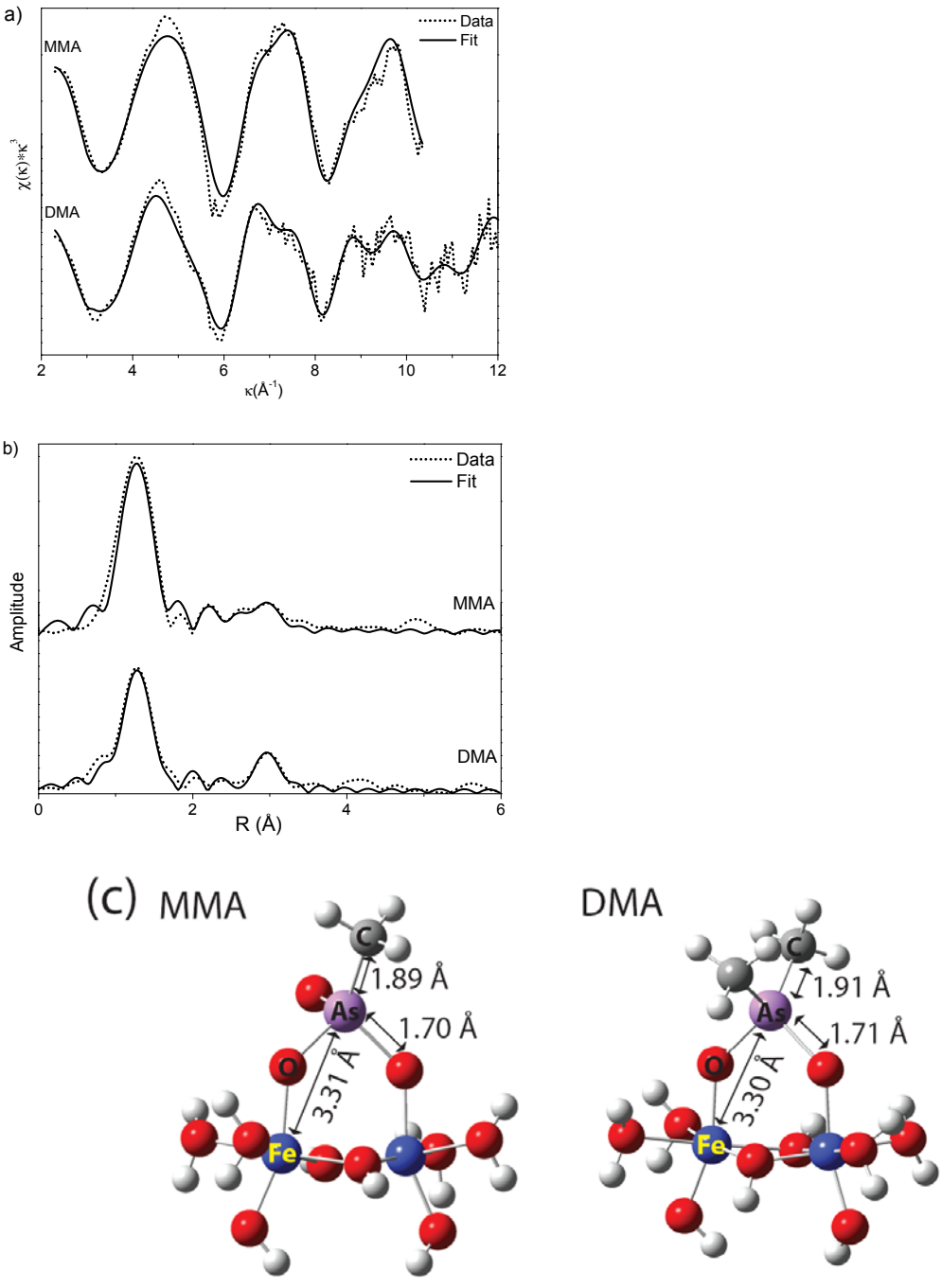

Figure 4.5 MMA and DMA XAS spectra in (a) κ space, (b) Fourier transformation of XAS spectra, (c) molecular configurations of MMA and DMA sorbed on goethite cluster.

Table 4.1 Soil Characteristics

	pH	OM (%)	CEC @ pH7 (meq/100 g)	Texture	Citrate-Dithionite Extracted (ppm)		Ammonium oxalate Extracted (ppm)		Metal Concentration by Microwave Digestion (PPM)											
					Al	Fe	Al	Fe	Al	Ca	Cu	Fe	K	Mg	Mn	Na	P	S	Zn	As	Ni
Fort Mott Top Soil	5.6	1.6	5.19	Loamy sand	821.16	956.45	795.17	716.28	4177.2	377.82	4.27	1869	205.55	306.37	19.48	10.34	113.35	70.88	6.89	0.79	3.64
Fort Mott Sub Soil	4.8	0.1	1.08	Sandy loam	757.17	1302.44	436.20	382.80	4184.8	45.18	4.16	2552.1	126.79	234.72	14.82	9.27	39.62	27.69	5	0.56	3.85
Mullica Top Soil	3.8	6.1	17.91	Loamy sand	1380.68	195.05	1154.00	160.43	2692.2	14.81	2.21	312.5	93.12	55.15	2.37	13.06	122.72	160.59	3	-	2.24
Mullica Sub Soil	4.8	0.2	1.69	Loamy sand	932.88	188.73	733.83	69.89	3043.5	13.6	1.14	460.4	86.68	94.15	3.12	3.71	22.25	27.47	2.13	-	3.68
Reybold Top Soil	5.2	1.4	6.16	Sandy loam	1797.60	4834.70	1384.33	533.70	8450	342.16	10.54	4936.3	346.82	678.3	234.36	28.17	369.25	93.46	16.23	0.43	7.38
Reybold Sub Soil	5.9	0.6	7.25	Loam	1912.83	6742.27	682.50	2397.71	13249	525.82	24.37	16400	636.34	1016.06	34.29	39.81	172.19	50.15	17.84	0.84	8.87
Cecil Top Soil	4.6	3.4	11.28	Loam	2693.17	9136.06	1255.20	3303.44	11001.6	221.41	43.16	19530.5	287.78	270.53	302.5	29.69	116.51	223.72	17.19	-	7.51
Cecil Sub Soil	5.3	2.3	8.09	Clay	5160.00	13634.51	1974.00	5358.33	36522	84.81	169.55	55414	388.17	586.31	239.77	39.18	302.09	157.98	40.4	-	21.11

Table 4.2 Structural parameters for XAS analysis of MMA and DMA sorbed on goethite.

		MMA-Fe	DMA-Fe	As^V-Fe [g]
As-O	CN [a] (Fixed)	3	2	
	R [b] (Å)	1.70 ± 0.008	1.71 ± 0.0056	
	Σ^2 [c] ($Å^2$)	0.0010 ± 0.0007	0.0011 ± 0.0005	
As-C	CN (Fixed)	1	2	
	R (Å)	1.89 ± 0.01	1.91 ± 0.009	
	Σ^2 ($Å^2$)	0.001 ± 0.001	0.0009 ± 0.0004	
As-O-O	CN (Fixed)	6	6	
	R (Å)	3.12 ±0.05	3.15 ±0.02	
	Σ^2 ($Å^2$)	0.0069 ± 0.004	0.0070 ± 0.003	
As-Fe	CN	1.8 ± 1.1	1.9 ± 0.5	1.3-2.9
	R (Å)	3.31 ± 0.03	3.30 ±0.08	3.23-3.37
	Σ^2 ($Å^2$)	0.008 ± 0.002	0.0069 ± 0.0008	0.0028-0.01
	E_0 [d] (eV)	4.13 ± 0.9	4.30 ± 0.86	
	S_0^2 [e] (Fixed)	0.98	0.98	

[a] Coordination number. [b] Interatomic distance. [c] Debye-Waller factor. [d] Energy shift. [e] Amplitude reduction factor. [f] Standard deviation. [g] Selected references of As^V sorbed on goethite analyzed by EXAFS [10, 12, 39-40].

Chapter 5

CONCLUSIONS AND FUTURE RESEARCHES

Conclusions

MMA and DMA are generally minor components of total As in the environment but can sometimes reach 10-50 % of total As [1-3]. Also, many organisms are capable of methylating As in their bodies. Those methylated As in the bodies are stable until they are excreted. The impacts of methylated As species, such as MMA and DMA, should not be underestimated. These studies have demonstrated that MMA and DMA are subject to various reactions and processes, such as sorption, desorption, reduction, oxidation, methylation, and demethylation. Thus, a better understanding of MMA and DMA behaviors and factors that impact MMA and DMA reactivity in the environment are crucial to predict global As cycling.

Results from this research have revealed that MMA and DMA sorption on AAO show similar trends to As^{V} sorption on AAO with slightly lower MMA sorption and much lower DMA sorption than As^{V} sorption. Also, MMA and DMA sorption is similar to MMA and DMA sorption to ferrihydrite and goethite. MMA and DMA sorption was higher at lower pH, and as the pH increased, the sorption decreased. FTIR and XAS studies have revealed that MMA and DMA mainly form bidentate binuclear complexes with AAO, similarly to As^{V} sorption on aluminum oxides. MMA and DMA also mainly form bidentate binuclear complexes with goethite.

μ-SXRF studies provided direct evidence for MMA and DMA association with the iron oxides in the Reybold soil, similar to As^V association with iron oxides in soils. Due to the strong sorption affinity of sorbed As species, extraction methods may alter As species on the surfaces of minerals. μ-SXRF and μ-XANES provided *in-situ* qualitative As speciation analysis on sorbed As species under aerobic or anaerobic conditions. Methylation was favored over demethylation under aerobic conditions, and demethylation was favored over methylation under anaerobic conditions. These studies also suggest that under anaerobic conditions, the presence of organoarsenicals, MMA and DMA, can be greater than previously thought.

This research also has shown that MMA and DMA are mainly sorbed to Al/Fe-oxides in soils, and the sorption rate and capacity depends on the Al/Fe concentration. Decreasing desorption of MMA and DMA over time suggests that As in soils, either as organic or inorganic species, could persist in soils during long term agricultural application of MMA and DMA. When these fields are used for further agricultural production, uptake of As by plants is possible. Accordingly, MMA and DMA sorption/desorption and biotransformation can play an important role in total arsenic cycling in the environment.

Future Research

These studies on MMA and DMA have successfully identified important sorption mechanisms and determined distribution, speciation, and biotransformation in soil systems, but additional questions remain and further research is needed. Inner-sphere bidentate binuclear complexes exist between MMA and DMA and Fe and Al oxides. These are the same types of surface complexes that As^V forms with Fe and Al

oxides. Despite similar types of surface complex formation, the sorption capacity, the amount of desorption, and the sorption affinity are largely different between As^V, MMA, and DMA. In addition to the molecular structural differences between these compounds, there are other factors that affecting the sorption capacity and affinity. One possible surface complex that may form is an outer-sphere complex, and the ratio of outer-sphere to inner-sphere complexes is different between As^V, MMA, and DMA. It is possible that DMA forms more outer-sphere complexes than As^V does. Resonant anomalous X-ray reflectivity (RAXR) would be an ideal technique to verify this hypothesis [4]. This technique can semi-quantify the amount of As atoms located at the distance that corresponds the bidentate binuclear complex formation and outer-sphere complex formation. However, this technique is relatively new to our research field, and few studies using RAXR have been reported. One drawback of the technique is that the studies can only be done on a single crystal, such as hematite or corundum surfaces. One could argue that the results for As reactions with single crystals do not mimic As sorption to Fe or Al oxides. There can be different sorption mechanisms at different crystal phases. Despite the potential drawbacks, this technique could still be useful.

Another approach to explain the different sorption capacity and affinity is the use of computational chemistry [5-6]. Such studies can be useful in calculating Gibbs free energies of As^V bidentate binuclear, monodentate mononuclear, or bidentate mononuclear complex formation and have successfully helped to identify that bidentate binuclear complex formation is thermodynamically the most stable. One can calculate Gibbs free energies for MMA and DMA sorption complex formation with Al/Fe oxide surfaces and compare the results. It is possible to see that As^V

bidentate binuclear complex formation is thermodynamically more stable than DMA bidentate binuclear complex formation. This can explain the weaker sorption capacity and affinity of DMA to Al/Fe oxide surfaces.

Studies from Chapter 3 have concluded that the redox potential is one factor that affects methylation/demethylation processes. Under anaerobic conditions, methylation is favored over demethylation, which means that MMA or DMA can be the more dominant species, and these studies showed that Fe oxides are the main sorbents in soils. We have not conducted any MMA and DMA sorption experiments to Fe oxide minerals under anaerobic conditions and do not know their sorption behavior under anaerobic conditions. One of the environmental concerns related to MMA and DMA is the accumulation of DMA in some U.S. grown rice, and rice is grown under flooded (reduced) environments. MMA and DMA sorption studies under anaerobic conditions are relevant to environment, and the results can be linked to the actual observations. One possible factor that can affect the MMA and DMA sorption is the reductive dissolution of Fe oxides. Dissolution will promote the formation of more crystalline Fe oxides mineral that have lower surface areas, and consequently sorption decreases [7]. Reduced Fe^{2+} species can reduce MMA and DMA so that sorption decreases. Finally, the dissolved Fe can form complexes or precipitate with MMA and DMA, and sorption decreases. The presence of carbonate species also can affect MMA and DMA sorption to Fe oxides. Preliminary experiments have shown that MMA and DMA sorption to AAO increases under anaerobic conditions, similar to As^{V} sorption on hematite due to dissolved carbonate species [8]. It is possible that MMA and DMA sorption also shows similar behavior. One could apply batch experimental and XAS techniques to address such questions.

REFERENCES

(1)Braman, R. S.; Foreback, C. C., Methylated forms of arsenic in environment. Science 1973, 182, (4118), 1247-1249.

(2)Bednar, A. J.; Garbarino, J. R.; Ranville, J. F.; Wildeman, T. R., Presence of organoarsenicals used in cotton production in agricultural water and soil of the southern United States. J. Agric. Food Chem. 2002, 50, (25), 7340-7344.

(3)Marin, A. R.; Pezeshki, S. R.; Masschelen, P. H.; Choi, H. S., Effect of dimethylarsenic acid (DMAA) on growth, tissue arsenic, and photosynthesis of rice plants. J. Plant Nutr. 1993, 16, (5), 865-880.

(4)Catalano, J. G.; Park, C.; Fenter, P.; Zhang, Z., Simultaneous inner- and outer-sphere arsenate adsorption on corundum and hematite. Geochim. Cosmochim. Acta 2008, 72, (8), 1986-2004.

(5)Kubicki, J. D.; Kwon, K. D.; Paul, K. W.; Sparks, D. L., Surface complex structures modelled with quantum chemical calculations: carbonate, phosphate, sulphate, arsenate and arsenite. European Journal of Soil Science 2007, 58, (4), 932-944.

(6)Kwon, K. D.; Kubicki, J. D., Molecular orbital theory study on surface complex structures of phosphates to iron hydroxides: Calculation of vibrational frequencies and adsorption energies. Langmuir 2004, 20, (21), 9249-9254.

(7)Kocar, B. D.; Herbel, M. J.; Tufano, K. J.; Fendorf, S., Contrasting effects of dissimilatory iron(III) and arsenic(V) reduction on arsenic retention and transport. Environ. Sci. Technol. 2006, 40, (21), 6715-6721.

(8)Arai, Y.; Sparks, D. L.; Davis, J. A., Effects of dissolved carbonate on arsenate adsorption and surface speciation at the hematite-water interface. Environ. Sci. Technol. 2004, 38, (3), 817-824.

Appendix

CHAPTER 2 COPYRIGHT PERMISSIONS